HOST-COMMENSAL-PATHOGEN INTERACTIONS

PROACTIVE IMMUNITY: COMMENSAL BACTERIA INTERACT WITH THE IMMUNE SYSTEM TO FIGHT *PSEUDOMONAS AERUGINOSA*

By OPHÉLIE QUILLIER, B. Sc.

A THESIS

SUBMITTED TO THE DEPARTMENT OF BIOCHEMISTRY AND BIOMEDICAL SCIENCES AND THE SCHOOL OF GRADUATE STUDIES

OF MCMASTER UNIVERSITY

IN PARTIAL FULFILLEMENT OF THE REQUIREMENTS

FOR THE DEGREE OF

MASTER OF SCIENCE

MASTER OF SCIENCE (2018) McMaster University

(Biochemistry and Biomedical Sciences) Hamilton, Ontario, CANADA

TITLE Proactive Immunity: Commensal Bacteria Interact with the Immune System to Fight *Pseudomonas aeruginosa*

AUTHOR Ophélie Quillier

B.Sc., Microbiology and Immunology

McGill University, Montréal, CANADA

SUPERVISOR Michael Surette, Ph.D

NUMBER OF PAGES xix, 158

Lay abstract

Antibiotics have for decades facilitated the cure of infections caused by pathogens of all kinds. Unfortunately, repeated exposure to antibiotics has rendered some pathogens highly resistant to traditional treatment. One notorious multi-drug resistant pathogen is *Pseudomonas aeruginosa*, now responsible for 10-15% of hospital-acquired respiratory infections. In this project we investigate the potential that lies in using commensal bacteria that exist in the microbiota of our respiratory tract to fight against pathogens that no longer respond to antibiotics. Stringent experiments with various models have revealed bacteria capable of killing *Pseudomonas aeruginosa* and helped us understand the mechanism of inhibition as well as the interactions of the bacteria with the immune system. Our results show that some bacteria of the microbiota are effective against *Pseudomonas aeruginosa* and that this line of study holds promise for the development of a new arsenal against a growing number of threatening pathogens.

Abstract

Multi-drug resistant *Pseudomonas aeruginosa* has become an increasing threat. A threat compounded by the fact that the pipeline of antimicrobial discovery continues to lose effectiveness. It is urgent that we identify new strategies to eliminate this and other multi-drug resistant pathogens. Meanwhile, we know that the resident bacteria of the respiratory tract interact with host cells to eliminate incoming threats.

The goal of this project is to understand the interactions at play in the microbiota of the respiratory tract and identify the specific commensal bacteria that inhibit *P. aeruginosa* in the presence of host cells.

Using a nasopharyngeal cell culture screen, we were able to identify several human commensals capable of inhibiting the growth of antibiotic-resistant *P. aeruginosa* in a host-dependent manner. It was also established that this phenotype can be reproduced in more complex systems, including a murine lung slice model, and that the elimination of the pathogen is dependent on the presence of living bacteria, mediated by a secreted factor.

We believe that the presence of these commensals has an immunomodulatory effect on the host. By characterizing the cytokines and chemokines produced by the host cells in response to the presence of these commensals, we have shown that these bacteria modify the immune response of the host to the pathogen.

Finally, having failed to develop a mouse model of infection, we have determined that the observed phenotype is not a direct action of the host cells, nor the result of

hydrogen peroxide secretion. We have further characterized the bacterial strains using genome assembly.

This study has confirmed that commensal bacteria create a unique immune environment that contributes to the clearance of pathogens. Identifying bacteria and bacterial products capable of stimulating host defenses and modulating inflammation could provide a new therapeutic approach to reducing infection susceptibility in high-risk patients.

Acknowledgements

I am deeply thankful for my time in the Surette Laboratory. Dr. Surette has been a tremendous supervisor who has given me both the guidance needed to fully develop my project and the independence to pursue my interests in both the fields of microbiology and immunology.

My supervisory committee members, Dr. Dawn Bowdish and Dr. Brian Coombes, have also participated in the success of this project through their helpful insights and their continued support.

This thesis would not be what it is today without the help and support from the members of the Surette Laboratory. I would like to acknowledge in particular Patrick Schenck for his valuable mentorship and guidance in the fields of immunology and model systems, as well as Daphnée Lamarche, Rachelle Szymkiewicz and Bryan Wu for sharing their expertise and their constant encouragements. Dr. Janine Strehmel from the Bowdish Laboratory has been of great assistance in learning techniques specific to immunology research.

Finally, my parents, as well as Gabriel, Linda, and Jean-Pierre deserve special thanks for going above and beyond to provide support and motivation throughout my degree, as well as for the hours of editing.

Doing my M.Sc. in the Surette Laboratory has been a rewarding experience that has shaped me as a scientist and is sure to influence my future endeavors. I wish continued success to Dr. Surette and all the members of his laboratory.

Table of Contents

List of Tables

List of Figures

List of Abbreviations and Symbols

AMR	antimicrobial resistance
BAL	bronchioalveolar lavage
BALF	bronchioalveolar lavage fluid
BHI	brain-heart infusion
BLAST	Basic Local Alignment Search Tool
CARD	the Comprehensive Antibiotic Resistance Database
CFU	colony forming unit
CNA	colistin, naladixic acid agar
CO_2	carbon dioxide
DMEM	Dulbecco's Modified Eagle Media
DNA	deoxyribonucleic acid
dNTP	deoxyribonucleotide triphosphate
EGF	epidermal growth factor
FBS	fetal bovine serum
FGF-2	fibroblast growth factor 2
Flt-3L	Fms-related tyrosine kinase 3 ligand
G-CSF	granulocyte colony stimulating factor
GM-CSF	granulocyte-macrophage colony stimulating factor
H_2	hydrogen
HBSS	Hank's Balanced Salt Solution

IFNα2	interferon α2
IFNγ	interferon γ
IL-1α	interleukin 1α
IL-1β	interleukin 1β
IL-1RA	interleukin 1 receptor antagonist
IL-2	interleukin 2
IL-3	interleukin 3
IL-4	interleukin 4
IL-5	interleukin 5
IL-6	interleukin 6
IL-7	interleukin 7
IL-8	interleukin 8
IL-9	interleukin 9
IL-10	interleukin 10
IL-12p40	interleukin 12 p40
IL-12p70	interleukin 12 p70
IL-13	interleukin 13
IL-15	interleukin 15
IL-17A	interleukin 17A
IL-18	interleukin 18
IP-10	interferon γ-induced protein 10

KC	keratinocyte chemoattractant
LIF	leukemia inhibition factor
LIX	lipopolysaccharide-induced CXC chemokine
LPS	lipopolysaccharide
LRT	lower respiratory tract
MCP-1	monocyte chemoattractant protein 1
MCP-3	monocyte chemoattractant protein 3
M-CSF	macrophage colony stimulating factor
MDC	macrophage-derived chemokine
MIG	monokine induced by γ interferon
MIP-1α	macrophage inflammatory protein 1α
MIP-1β	macrophage inflammatory protein 1β
N_2	nitrogen
O_2	oxygen
PATRIC	the Pathosystems Resource Integration Center
PBS	phosphate buffer saline
PCR	polymerase chain reaction
PCLS	precision-cut lung slice
PDGF-AA	platelet-derived growth factor AA
PDGF-AB/BB	platelet-derived growth factor AB/BB
PIA	*Pseudomonas* isolation agar

PRISM	Prediction Informatics for Secondary Metabolomes
PRR	pathogen recognition receptor
QUAST	Quality Assessment Tool for Genome Assemblies
RANTES	regulated on activation, normal T cell expressed and secreted
RAST	Rapid Annotation using Subsystems Technology
RNA	ribonucleic acid
rRNA	ribosomal ribonucleic acid
sCD40L	secreted cluster of differentiation 40 ligand
TGFα	transforming growth factor α
TLR	Toll-like receptor
TNFβ	tumour necrosis factor β
tRNA	transfer ribonucleic acid
URT	upper respiratory tract
VEGF	vascular endothelial growth factor
VF	virulence factor

Declaration of Academic Achievement

Ophélie Quillier contributed to the design and conception of the experiments in this study, performed all experiments, analyzed and interpreted data, and performed statistical analyses.

Dr. Steve Bernier developed the Detroit-562 cell culture model to isolate bacteria inhibiting specific pathogens, identified the bacterial strains having this effect (**Table A.1**) and provided the strains used in this study.

Dr. Janine Strehmel performed and analyzed the experiment verifying the viability of the murine precision-cut lung slices (**Figure 4.1**).

Dr. Surette provided advice and participated in the design and conception of all experiments. Dr. Bowdish also provided guidance in the design of several experiments.

Chapter 1 Introduction

1.1 The respiratory tract and respiratory infections

The respiratory tract is a complex organ system. It exchanges carbon dioxide for oxygen through a bidirectional flow of air. In all, the respiratory tract has a surface of 70 m^2, which is more than the skin (Hasleton, 1972). It is a mucosal barrier that is exposed to the ambient air and everything it contains, including microorganisms (France and Turner, 2017). In fact, we inhale between 1,500 and 14,000 organisms every hour (Thomson and Hewlett, 1896). To fight this constant exposure to potential pathogens**,** the respiratory tract possesses an arsenal defenses that prevent invading bacteria from colonizing. To start with, when bacteria enter the respiratory tract, they encounter nasal hair, which can trap particles. Then, for those that manage to get beyond the nasal hair, the airways are coated by a thin layer of mucus that traps any foreign particles, which are then removed by the cilia beating upwards (Hatch, 1961). Coughing is another mechanism that works to expulse the particles and microorganism inhaled (Munyard and Bush, 1996). Moreover, the cells lining the airway act as a physical barrier, using tight junctions to prevent microorganisms from penetrating the blood stream (Lloyd and Marsland, 2017). Finally, and most significantly for the purpose of this study, all of these barriers are assisted by the local immune system and the resident microbes. Unfortunately, it occurs that these systems fail and the invading pathogen is able to colonize and expand, causing the host to develop a respiratory infection.

Respiratory infections are the leading cause of morbidity and mortality worldwide (Ottomani *et al.,* 2004). These infections can be acute or chronic. In an acute infection, a pathogen is able to colonize the respiratory tract and cause an inflammatory response but in a healthy individual, it is then controlled by the immune system and eliminated (Taylor *et al.,* 2016). Chronic infections are more complex and often the result of an underlying immune dysregulation. In these cases, pathogenic bacteria manage to establish a stable population in the respiratory tract and the immune system is unable to clear it (Dickson *et al.,* 2016). Chronic infections rarely develop in healthy individuals but are often found in patients with cystic fibrosis, chronic obstructive pulmonary disorder, and other respiratory tract diseases (Stressman *et al.,* 2012). While there are some examples of chronic upper respiratory tract (URT) infections, it is more common that infections in the URT be acute and resolved quickly, contrasting with lower respiratory tract (LRT) infections that can be more severe. Most LRT infections originate in the URT and work their way down, either through microaspirations or direct dispersion along mucosal surfaces (Huxley *et al.,* 1978). A number of pathogens can cause acute infections in the respiratory tract, especially in children and the elderly. These include several viruses including the influenza virus and the respiratory syncytial virus as well as a number of bacteria including *Staphylococcus aureus*, *Streptococcus pneumoniae*, *Pseudomonas aeruginosa, Stenotrophomonas maltophilia, Moraxella* spp., *Klebsiella* spp. and *Burkoldheria cenocepacia.* These pathogens are also associated with chronic infections mostly in immunocompromised hosts.

1.2 The respiratory tract immune system

The immune system is the body's defense against infection. It recognizes and destroys anything harmful to the body, especially pathogenic microorganisms. It does this through two distinct arms. First is the innate immunity, a fast, short-lived response that initiates clearing of P. aeruginosa. It is also instrumental in priming and activating the second arm, the adaptive immune response. The adaptive immune response is slower but more specific to the microorganism causing the infection, and it usually leads to immunological memory (Murphy *et al*., 2008). The innate immune response involves many types of white blood cells, such as macrophages, neutrophils, eosinophils and dendritic cells. These cells are trained to recognize pathogens within a few minutes or hours after the infection, and work to contain or destroy them. They also recruit other immune cells of both the innate and adaptive immune responses (Murphy *et al*., 2008).

In the respiratory tract in particular, the immune system must handle the constant exposure to microorganisms to maintain proper function. However, inflammatory responses can be very damaging, especially in the lungs where edema can rapidly block an airway (Lloyd and Marsland, 2017). Therefore, the respiratory tract harbors a network of resident immune cells that recognize, sequester, and eliminate most threats we are exposed to without triggering a systemic and potentially damaging immune response (Segal *et al.,* 2013). There are several different types of cells involved in this local response including alveolar macrophages (Yona *et al.,* 2013), dendritic cells (Neyt and Lambrecht, 2013), and

innate lymphoid cells (Tait-Wojno and Artis, 2016). Epithelial cells, as well as some of these immune cells, can release a number of immune factors such as cytokines and chemokines, immunoglobulins, and host-defense peptides in the lumen of the respiratory tract to keep bacteria at bay (Iwasaki *et al.,* 2017).

1.3 The respiratory tract microbiota

The other population that contributes greatly to preventing pathogen colonization is the microbiota, the powerful significance of which we are only beginning to measure. The human microbiota consists of trillions of bacteria, archaebacteria, viruses, and small eukaryotes found in and on the body, including the skin, oral cavity, vaginal cavity, respiratory tract, and gastrointestinal tract (Costello *et al.*, 2009). In the respiratory tract, a complex population of microorganisms lives in the lumen and the mucus layer (Neish, 2014). These microorganisms are acquired from the mother at birth, with the dominating species reflecting the mother's vaginal microbiome in the case of natural birth or skin microbiome if the infant is born by cesarean section (Dominguez-Bello *et al.,* 2010). This population then evolves to closely resemble that of an adult during the first few years of life (Stearns *et al.,* 2015). While the respiratory tract has a lower biomass than other mucosal surfaces, such as the gastrointestinal tract, it is still stably colonized with a distinct microbial population (Bassis *et al.,* 2015). The dominating phyla are Bacteroidetes, Firmicutes, Proteobacteria, and Actinobacteria with

dominating species such as *Streptococcus, Prevotella, Actinomyces,* and *Veillonella* (Morris *et al.,* 2013).

It is known that the gut microbiota plays an essential role in health and disease. More recently, a small number of studies have indicated that the respiratory tract microbiota also impacts health. For example, germ-free mice have smaller lungs (Wostmann, 1981) and less alveoli (Yun *et al.,* 2014) than mice colonized with microbes, which suggests that the resident bacteria are involved in proper lung development. Other studies have shown that the composition of the microbiota in early life is correlated with microbiota stability and respiratory infection rates (Biesbroek *et al.,* 2014; Teo *et al.,* 2015). Of specific interest in the present paper, the microbiota is involved in colonization resistance.

1.4 Colonization resistance

To cause infection, pathogens must first colonize the respiratory tract to access nutrients and space in which to replicate (Bogaert *et al.,* 2004). Commensal bacteria prevent invading pathogens from colonizing mucosal surfaces through processes referred as "colonization resistance" (Baulmer and Sperandio, 2016). At its most basic level, colonization resistance is passive. The commensal bacteria do not necessarily target a specific pathogen but, simply by being there, occupying the available niches and consuming the nutrients present in the environment, they prevent other bacteria from having access to the necessary resources for

colonization (Kamada *et al.,* 2013). This holds especially true in the airways where the nutrients are limited.

Resident bacteria also have a more active role in colonization resistance. Indeed, since some species are in direct competition with each other, occupying the same niches and consuming similar nutrients, they have developed strategies and armed themselves against other specific bacteria. For instance, a study by Selva *et al.* (2009) showed that *Streptococcus pneumoniae* produces hydrogen peroxide, which induces lysogenic phages in *Staphylococcus aureus* and thereby lyses the cell. In another example, *Streptococcus epidermidis* produces a serine protease, Esp, which disrupts *S. aureus* biofilms and, by extension, its colonization (Iwase *et al.,* 2010). Bacteriocins, bacterially produced antimicrobial peptides, are commonly produced by bacteria of the respiratory tract to prevent colonization by other species (Bosch *et al.,* 2013).

1.5 Microbe-host interactions

The action of resident commensal species against colonization is not limited to direct interaction with invading bacteria. They are also known to cause interference by interacting indirectly with the immune system and boosting its effectiveness against infection. The resident microbiota contributes to the development of the local immune system. Several studies have shown that microbiota-derived signals, most importantly lipopolysaccharide (LPS), stimulate the development of these tissues and thereby optimize immune responses later in

life. In other words, the presence of tonic stimulation by pathobionts and other bacteria, mostly in early life, enables the immune cells to mount proper responses when they are faced with threats later in life (Lloyd and Marsland, 2017). This is evident in germ-free animals whose immune system is not fully functional.

Commensal bacteria can also communicate directly with immune cells, which are tasked precisely with eliminating pathogens. As demonstrated in a recent study by Kanmani *et al.* (2017) for instance, *Corynebacterium pseudodiphteriticum* improves the resistance of infant mice to respiratory syncytial virus and secondary *Streptococcus pneumoniae* infection through a TLR3-mediated antiviral response. In another example, peptidoglycan present on *Haemophilus influenzae* can prime neutrophils to better recognize and kill *Streptococcus pneumoniae* (Lysenko *et al.,* 2007).

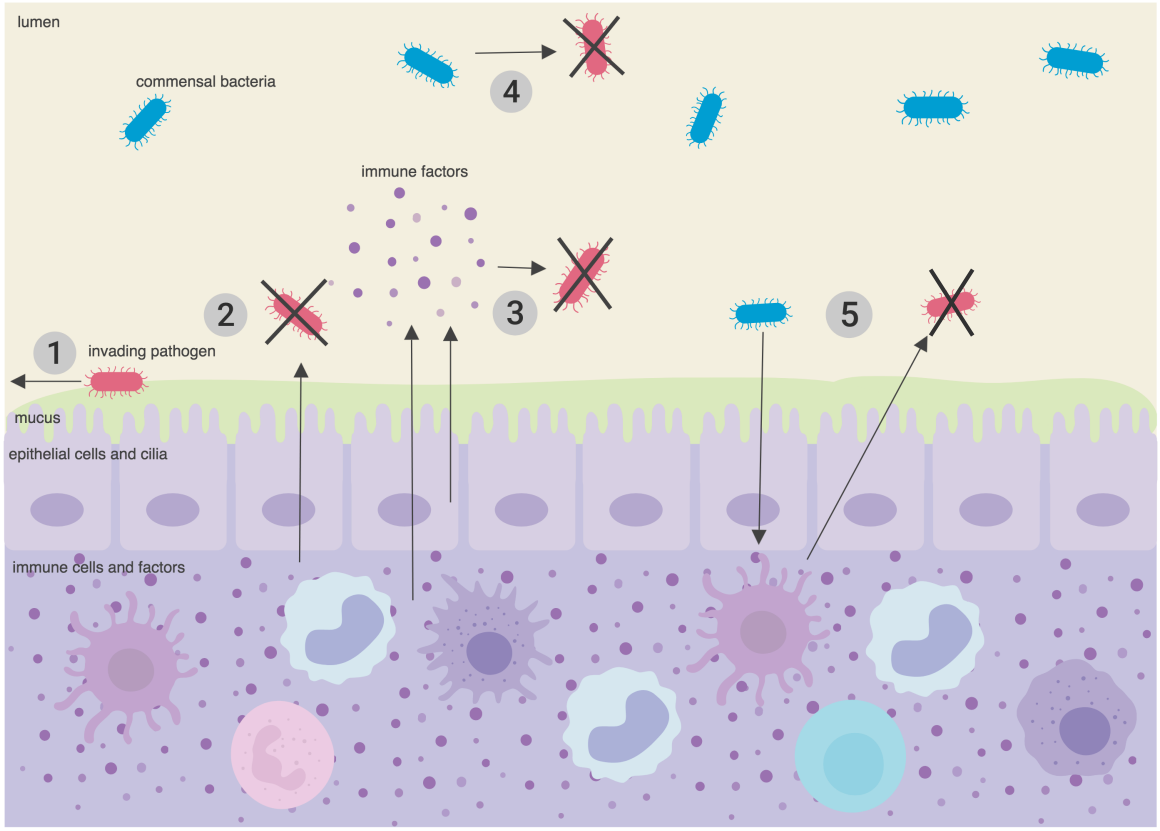

Figure 1.1 Different pathways work together to protect the respiratory tract. The respiratory tract is under constant exposure from invading microorganisms. It has developed a number of defense pathways in order to eliminate these threats. **1.** The airways are coated with a thin layer of mucus where the microorganisms get trapped. The beating cilia then remove bring the bacteria towards the mouth where they are either swallowed or expulsed. Coughing also helps in the removal of inhaled particles. **2.** Immune cells present in the tissue are capable of recognizing and eliminating most threats that present themselves in the respiratory tract. **3.** Immune cells, as well as epithelial cells, secrete various immune factors including cytokines, chemokines and host-defense peptides that are also capable of

eliminating specific microorganisms. **4.** Commensal bacteria from the microbiota remove threats through direct bacterial interference. **5.** Resident bacteria are also capable of helping the immune system to better eliminate pathogens.

1.6 Antibiotic resistance

To date, most treatments against bacterial infections have focused on reducing the pathogen burdens, usually through the use of antibiotics (Taylor *et al.,* 2016). Antibiotics are among the most important drugs ever developed. Since their discovery at the end of the 19th century, they have played a major role in reducing global mortality through the reduction of the spread and lethality of infectious diseases (Wright, 2007). However, soon after the discovery of antibiotics, it was found that bacteria can develop resistance to these compounds (Bellamy and Klimek, 1948) through various strategies, such as target modification, efflux pumps, and antibiotic inactivation (Alekshun and Levy, 2007). These resistance mechanisms have evolved alongside antibiotics as a means to survive in complex communities with other antibiotic producers as well as to protect the producers (Tenover, 2006). Through our extensive and often excessive use of antibiotics, we have exerted a selective pressure, resulting in the emergence of more antibiotic resistant pathogens, and even multi-drug resistant pathogens (Wright, 2007). These pathogens have become a global threat and finding solutions to this problem is one of the greatest medical challenges we face today (Schroeder *et al.*, 2017).

Antibiotics need to be better managed because the antibiotic discovery pipeline is no longer effective and the development and approval rates of antibiotics have rapidly decreased over the past 40 years (Wright, 2007). Indeed, after the accidental discovery of penicillin (Fleming, 1929), Selman Waksman developed an antibiotic discovery platform, which paved the way for the development of additional antibiotics over the following 20 years. Waksman's platform involved screening soil bacteria from the genera *Streptomycetes* or *Actinomycetes*, active producers of antimicrobials, to identify strains inhibiting the growth of pathogens (Schatz *et al*., 1944). Waksman's pioneer work led to the discovery of most antibiotic classes in use today; however, after twenty years of mining these bacteria, the platform's source of antimicrobial producers was depleted (Lewis, 2016). In response, the field switched to modifying existing antibiotics (Fischbach and Walsh, 2009) and creating synthetic antibiotics (Payne *et al*., 2007). Synthetic and modified antibiotics have seen some success but the process of drug discovery is slow and costly whereas bacteria are able to mutate and acquire new genes through horizontal transfer at a much faster pace. Only 5 in 5,000 compounds make it through the drug development pipeline and even fewer through the approval pipeline (Bush *et al*., 2011). Safety concerns remain the main reasons for withholding newly developed compounds from the market (Barton and Riley, 2016). Today, simply screening bacteria for the low-hanging fruit or creating analogs of existing compounds are no longer effective methods.

Since traditional pipelines are no longer effective against the rising threat of antimicrobial resistance, research is now focusing on developing alternative methods of engineering new antimicrobials or preventing infection (Vale *et al*., 2016). One possible avenue might be to find replacements or complements to traditional antibiotics. For example, monoclonal antibodies (DiGiandomenico and Sellman, 2015) or bacteriophages (Saha *et al*., 2016) can be used for targeted antibacterial action. There is also potential in the natural antimicrobial peptides that are produced by microorganisms to prevent the growth of competing bacteria. These can have an immunomodulatory effect or can also be produced by the host in response to some stimuli (Wang *et al*., 2016). Immunomodulatory compounds could be used to reduce susceptibility to infectious disease and/or act in conjunction with antibiotics. These compounds, and other antibacterial compounds, can be produced by commensal bacteria, as described previously.

1.7 Multidrug resistant *Pseudomonas aeruginosa*

One bacterial species in particular exemplifies the challenges of rising antibiotic resistance in airway pathogens. *Pseudomonas aeruginosa* is a Gram-negative bacterial pathogen that can tolerate a wide range of physical conditions, including low nutrients and temperatures higher than other bacteria (El Zowalaty *et al.,* 2015). It can be isolated from many different sources, from soil to medical equipment (Lister *et al.,* 2009; Walker *et al.,* 2004). It causes 10-15% of nosocomial infections worldwide (Blanc *et al.,* 1998). This pathogen is responsible for a number

of diseases. It can cause pneumonia and lower respiratory tract infections. These can be life-threatening for immunocompromised patients and can lead to the development of chronic infections in cystic fibrosis patients and others (Bodey *et al.,* 1983). *P. aeruginosa* infections are not limited to the respiratory tract. It can also cause skin infections in burn patients (Tredget *et al.,* 2004), ear infections (Keene *et al.,* 2004), as well as bloodstream infections, meningitis, brain abscesses (Al-Mulla *et al.,* 2014), and even endocarditis (El Zowalaty *et al.,* 2015). These wide-ranging infections are extremely hard to treat. Indeed, *P. aeruginosa* is not only naturally resistant to numerous antibiotics, notably through the expression of efflux pumps and the low permeability of its outer membrane (Mesaros *et al.,* 2007); it is also capable of developing further resistance mechanisms very rapidly and effectively (Stratena and Yordanov, 2009). Practically all known mechanisms of antimicrobial resistance are expressed by this pathogen (Pechere and Kohler, 1999), making it resistant to several drug classes, and therefore a notable threat.

1.8 Objectives and hypothesis

In the face of this threat and considering the lack of new antibiotics at our disposal, I consider that commensal bacteria can, through microbe-host-pathogen interactions, prevent colonization by specific invading pathogens, such as *Pseudomonas aeruginosa*. Investigating these interactions opens up new and promising avenues to explore in the effort to combat respiratory infections caused by this pathogen. Driven by this perspective, I hypothesize that ***we can identify and***

characterize commensal bacteria capable of inhibiting the growth of Pseudomonas aeruginosa.

I aim to do so through the following objectives:

1. **Develop model systems to identify bacteria inhibiting *P. aeruginosa* in a host-dependent manner.** As explored previously, resident bacteria of the respiratory tract can, through a number of different mechanisms, including host-dependent mechanisms, inhibit the growth and colonization of other bacterial species. I developed various models to investigate these specific host-interactions using human epithelial cells, murine lung slices, and an *in vivo* mouse model.
2. **Characterize the inhibitory activity of the bacteria.** After having identified bacteria inhibiting *P. aeruginosa*, I characterized this phenotype using heat-killed bacteria, filtered supernatant, and catalase. I also determined whether the inhibitory activity was mediated by the host cells themselves. Using genome assembly, I briefly examined the predicted genes present in the genomes of the bacteria to further understand their roles in the phenotype.
3. **Characterize the immunomodulatory effect of the bacteria.** By quantifying the cytokines and chemokines produced by the host in response to the bacteria, I determined the type of immune response triggered by the bacteria to explore the effect they would have *in vivo* and how the immune system could participate in the elimination of *P. aeruginosa.*

Chapter 2 Materials and methods

2.1 Bacteria and growth conditions

The bacterial strains used in this study excluding *Pseudomonas aeruginosa* PA14 (Rahme *et al.,* 1995), which was supplied by Dr. Steve Bernier, were obtained from the Surette Lab Human Isolates Library (**Table A.2**). All the aerobic strains were grown overnight in brain-heart infusion (BHI; Becton Dickinson, Ontario, Canada) broth with a neutral pH at 37°C in a 5% CO_2 atmosphere. Anaerobic strains used were grown overnight in BHI broth at 37°C in an anaerobic chamber (containing 5% CO_2, 5% H_2, and 90% N_2).

To generate heat-killed bacterial stocks, overnight cultures of the different bacterial strains were centrifuged 5 minutes at 4,000rpm and resuspended the pellet in phosphate buffer saline (PBS). They were then incubated at 80°C for 15 minutes. The heat-killed bacteria were washed by being centrifuged 5 minutes at 4,000rpm and resuspended in PBS. Viability was assessed by streaking the heat-killed stocks on BHI agar and incubated overnight.

To measure the bacterial load of the commensals, they were serially diluted and spotted on BHI and Colistin naladixic acid agar (CNA; Becton Dickinson, Ontario, Canada) supplemented with 5% (v/v) sheep's blood. *P. aeruginosa* was spotted on *Pseudomonas* Isolation Agar (PIA; Becton Dickinson, Ontario, Canada).

2.2 16S sequencing

To confirm the identity of the bacteria included in the study, the 16S rRNA gene of each strain was amplified and sequenced. Single colonies were picked with a sterile stick, resuspended in 50µL of 5% Chelex, and subsequently boiled for 15 minutes and centrifuged to remove debris. The supernatant was used as the template DNA.

A PCR mastermix was prepared with the following reagents: 5µL of 10X PCR buffer (Invitrogen, Ontario, Canada); 1.5mM of $MgCl_2$; 0.2mM of dNTPs; 0.2mM of forward and reverse primers (10µM); 0.25µL of Taq polymerase; and 35.25µL of water. The primers used were 16S_8f (MS7; AGAGTTTGATCCTGGCTCAG) for the forward primer and 16S_926r (MS14; CCGTCAATTCCTTTRAGTTT) for the reverse primer.

5µL of the template DNA was added to the mastermix and amplified on the thermocycler following this program: 2 minutes at 94°C; 30 cycles of: 30 seconds at 94°C, 30 seconds at 56°C, 1 minute at 72°C; 10 minutes at 72°C.

5µL of the amplification product was run on a 1% (w/v) agarose gel to verify the presence of the product. The product was sent for Sanger sequencing (Mobix Lab, Hamilton, Canada) in forward direction using the 16S_8f primer. The obtained sequences were run through BLAST (Altschul *et al.,* 1990).

2.3 Cell line

Detroit-562 cells (ATCC CCL-138), a human pharyngeal carcinoma cell line, were routinely cultured in Dulbecco's Modified Eagle Medium (DMEM; Thermo Fisher Scientific, Ontario, Canada) + supplements (10% fetal bovine serum (FBS; Thermo

Fisher Scientific, Ontario, Canada), 2 mM L-glutamine, 100 units/mL penicillin, and 100 µg/mL streptomycin) at 37°C and 5% CO_2.

2.4 Bacterial stimulation of Detroit-562 cells

Routinely grown Detroit-562 cells were seeded in 96-well plates (400,000 cells/well) and were grown overnight in 100µL of DMEM + supplements until a 90% confluence was reached. The medium was then replaced with 100µL of DMEM + supplements without any antibiotics. 1µL of an overnight culture or the heat-killed stock obtained from the commensal bacterial strains (i.e. *N. sicca, E. faecium, S. mitis,* and *B. vulgatus*) was added to the wells. After 24 hours, 1µL of an overnight culture of *P. aeruginosa* was added to the growth medium and incubated for 24 hours. The cell density of both the commensals and *P. aeruginosa* were measured at the start of the experiment, every hour for 4 hours, and at the end of the experiment through serial dilution and spotting on either BHI agar and CNA, or PIA.

2.5 Murine precision-cut lung slices (PCLS)

C57Bl/6 female mice between 1 and 3 months old were euthanized through isoflurane inhalation and bleeding. They were then perfused by slowly injecting 5 mL of PBS through the left ventricle of the heart to clear the blood from their circulation. The trachea of the mice was then exposed and suture silk was passed under the trachea. A small hole was punctured in the trachea and an 18-gage blunt-ended needle was inserted towards the lungs. The suture silk was tied around the

needle to keep it in place. 1.2 mL of a 1:1 Hank's Balanced Salt Solution (HBSS; Thermo Fisher Scientific, Ontario, Canada)/2% agarose solution was injected into the lungs of the mice and was pushed in with 0.3 mL of air. Gauze saturated with ice-cold HBSS was placed over the exposed lungs of the mice and the mice were placed on ice for 10 minutes to allow the agarose to solidify. The lungs were then recovered and stored in 10 mL of ice-cold HBSS and kept on ice until sliced.

The large lobe of the lung was cut into 1 cm sections. One section was glued to the cooling block of the vibrotome and was sliced into 250 microns thick slices. This was repeated for each of the sections. The PCLS were kept in ice-cold HBSS on ice during the slicing and were then transferred into 24-well plates containing 1 mL of DMEM + supplements with 250 ng/mL Amphotericin B, and incubated at 37°C, 5% CO_2. The medium was changed every hour for two to three hours and the slices were used for further testing after 24 hours.

2.6 PCLS viability assay

Two PCLS were pooled together and 300 µL of 0.1 mM Resazurin solution was added to the well. They were then incubated 4 hours at 37°C, 5% CO_2. DMEM and PCLS killed through a one hour treatment with 1% Triton in PBS were used as negative controls. After incubation, 150 µL of supernatant was transferred to a black 96-well plate and the fluorescence was measured with the following settings: excitation 560 nm (excitation bandwidth 9 nm) and emission 590 nm (emission

bandwidth 15 nm). The viability was measured every two days and the medium was changed every two to three days.

2.7 Bacterial stimulation of murine PCLS

The growth medium of the PCLS generated as described above was replaced with 1 mL of DMEM + supplements without any antibiotics. 10µL of an overnight culture and heat-killed stock of the different commensal bacterial strains were added to the growth medium and incubated at 37°C in aerobic or anaerobic conditions based on the bacterial cell's requirement. After 24 hours, 10µL of an overnight culture of *P. aeruginosa* was added to the growth medium and incubated for 24 hours at 37°C in 5% CO_2. Commensals' and *P. aeruginosa*'s colony forming units (CFUs) were quantified at the beginning of the experiment, every hour for four hours, and at the end of the experiment by serial dilution as previously described.

2.8 Detroit-562 and PCLS filtrates

Detroit-562 cells and PCLS were cultured and stimulated with bacteria as described above. The supernatant was collected following 24 hours of incubation and filtered using a 0.2µm filter. 1µL of *P. aeruginosa* was then added to 100µL of the supernatant and grown 24 hours at 37°C in 5% CO_2 atmosphere in the case of the Detroit-562 cells. In the case of the PCLS, 10µL of *P. aeruginosa* was then added to 1 mL of the supernatant. The bacterial load of *P. aeruginosa* was measured through serial dilution and spotting on PIA before and after incubation.

2.9 Cytokine and chemokine quantification

Detroit-562 cells and PCLS were stimulated with bacteria as described previously. 75µL of supernatant from the Detroit-562 cells or the PCLS was collected and filtered through a 0.2µm filter. Cytokine and chemokine measurements were obtained using the 42-plex Human Discovery Assay (Human Cytokine Array/Chemokine Array 42-plex with IL-18; Cat no: HD42; Eve Technologies, Alberta, Canada) in the case of the Detroit-562 cells and the 31-plex Mouse Discovery Assay (Mouse Cytokine Array/Chemokine Array 31-plex; Cat no: MD31; Eve Technologies, Alberta, Canada) in the case of the PCLS.

Eve technology uses 100 uniquely coloured bead sets with different concentrations of red and infrared fluorophore dyes. The beads are coupled to capture antibodies specific to the analyte of interest. They use Bio-Plex 200, a bead analyzer with a dual-laser system and a flow cytometry system to activate the fluorescent dye within the beads and identify and quantify the conjugated analyte.

The analytes with concentrations below the limit of detection were excluded from the analysis. The quantities were normalized based on the highest and lowest values. The obtained cytokine and chemokine measurements were analyzed using R version 3.3.2 (R Development Core Team, 2008). They were then hierarchically clustered and a heat-map was generated using the heatmap.2 function of the gplot package (Warnes *et al.,* 2005).

The following cytokines and chemokines were measured in the supernatant of the Detroit-562 cells: EGF, Eotaxin-1, FGF-2, Flt-3L, Fractalkine, G-CSF, GM-CSF, GRO-α, IFNα2, IFNγ, IL-1α, IL-1β, IL-1RA, IL-2, IL-3, IL-4, IL-5, IL-6, IL-7, IL-8, IL-9, IL-10, IL-12p40, IL-12p70, IL-13, IL-15, IL-17A, IL-18, IP-10, MCP-1, MCP-3, MDC, MIP-1α, MIP-1β, PDGF-AA, PDGF-AB/BB, RANTES, sCD40L, TNFα, TNFβ, VEGF-A.

The following cytokines and chemokines were measured in the supernatant of the PCLS: Eotaxin, G-CSF, GM-CSF, IFNγ, IL-1α, IL-1β, IL-2, IL-3, IL-4, IL-5, IL-6, IL-7, IL-9, IL-10, IL-12p40, IL-12p70, IL-13, IL-15, IL-17A, IP-10, KC, LIF, LIX, MCP-1, M-CSF, MIG, MIP-1α, MIP-1β, MIP-2, RANTES, TNFα, VEGF.

2.10 Mouse models of respiratory tract infection

To infect the lower respiratory tract, C57Bl/6 female mice between 1 and 3 months old were anesthetized through isoflurane inhalation. They were then infected intranasally with 40µL of a 5 x 10^8 CFUs/mL bacterial suspension of *P. aeruginosa* or *S. mitis* (final dose of 2 x 10^7 CFUs per mouse). To infect the upper respiratory tract, the mice were restrained in a nose cone. They were then infected intranasally with 10µL of a 5 x 10^8 CFUs/mL suspension of *P. aeruginosa* or *S. mitis* (final dose of 5 x 10^6 CFUs per mouse). The mice were monitored for three days and sacrificed if they reached endpoint (weight loss of 10%, moribund appearance) before the end of the assay period. Those that didn't reach endpoint were euthanized through isoflurane inhalation and bleeding. Nasal tissue, lungs, and spleen were collected and homogenized. CFUs were quantified as described above.

2.11 Bronchioalveolar lavage and nasal wash

C57Bl/6 female mice between 1 and 3 months old either uninfected or infected with *P. aeruginosa* were euthanized through isoflurane inhalation and bleeding. The trachea of the mice was then exposed and a small hole was punctured in the trachea. For bronchioalveolar lavages, an 18-gage blunt-ended needle was inserted towards the lungs. 800µL of PBS was injected into the lungs and aspirated back out three times. For nasal washes, a 26-gage needle fitted with a canula was inserted towards the head of the mice. 400µL of PBS was run through the nose of the mice and collected at the nostrils. The lavage fluid and nasal wash fluid were then centrifuged 5 minutes at 1,500rpm. The supernatant was serially diluted and plated on selective agar and the pellet was resuspended in 110µL of PBS and cytocentrifuged (Shandon Cytospin 4, Thermo Scientific, Ontario, Canada) 3 minutes at 3,000 rpm. The cells were then stained using the HEMA 3 stain set (Fisher Scientific, Ontario, Canada) and observed under a light microscope to quantify and identify the cells present in the sample.

2.12 PCLS washing

Murine PCLS were generated as previously described. The growth medium of the PCLS was replaced with 1 mL of DMEM + supplements without antibiotics. 10µL of *E. faecium* or *S. mitis* was added to the growth medium. After 24 hours, the growth medium was removed and the PCLS were washed 5 times with PBS. DMEM +

supplements and 250 ng/mL Amphotericin B was then added to the PCLS for 3 hours to kill any remaining commensal bacteria. The media was then replaced with DMEM + supplements without antibiotics and 10µL *P. aeruginosa* was added and incubated for 24 hours. The cell density of the commensals and *P. aeruginosa* was quantified as described previously.

2.13 PCLS immune priming

C57Bl/6 female mice between 1 and 3 months old were anesthetized through isoflurane inhalation. They were then infected with 40µL of a suspension of *S. mitis* in PBS at a bacterial load of approximately 5 x 10^8 cells/mL (for a final dose of 2 x 10^7 bacteria per mouse). The mice were then monitored for three days and sacrificed if they reached endpoint (weight loss of 10%, moribund appearance). Those that didn't reach endpoint were euthanized through isoflurane inhalation and bleeding and PCLS were collected. The PCLS were incubated overnight at 37°C, 5% CO_2 in DMEM + supplements and 250 ng/mL Amphotericin B. The growth medium of the PCLS was replaced with 1 mL of DMEM + supplements without antibiotics. 10µL of each commensal bacterial strain was added separately to the growth medium. After 24 hours, 10µL of *P. aeruginosa* was added and incubated for 24 hours. The cells density of the commensals and *P. aeruginosa* was quantified.

2.14 Bacterial genomic DNA extraction and genome assembly

The bacterial genomic DNA was extracted using the Wizard Genomic DNA Purification kit (Promega, A1125, USA) according to the manufacturer's instructions. Libraries were constructed using Nexterra reagents as per manufacturer's instructions, and sequenced on a MiSeq Illumina sequencer. Library generation and sequencing were carried out by the Farncombe Genomic Facility (McMaster University, Hamilton, Canada).

DNA sequences were processed using several tools. The A5-Miseq pipeline (Coil *et al.,* 2015) was used for assembly: it trimmed the adapters from the raw reads, filtered the low quality reads, proceeded to an error correction step, and assembled the remaining reads into contigs. Quality assessment of the raw and trimmed reads was performed using FastQC (Andrews, 2010) and Quast (Gurevich *et al.,* 2013) was used for the contig files. Prokka (Seemann, 2014) and RAST (Aziz *et al.,* 2008) were used in parallel for the genome annotations. Quast and A5_Miseq assembly statistics were used to comment the quality of the assembly. Prokka statistics were used to obtain the number of genes, tRNAs, and ribosomal RNAs in the genomes. The genomes annotated through RAST were uploaded to PATRIC (Wattam *et al.,* 2017) to predict virulence factor genes. The genomes annotated through Prokka were uploaded to CARD (Jia *et al.,* 2017) and PRISM (Skinnider *et al.,* 2017) to predict antimicrobial resistance genes and secondary metabolic pathways, respectively.

2.15 Statistical analyses

Statistics were performed by using GraphPad Prism (v.6.0), R (v.3.3.2), and Microsoft Excel (v.14.6.6). Unless noted otherwise, values are provided as mean with standard deviation (SD).

Chapter 3 Detroit-562 cell model

3.1 Rationale

Bacteria from the respiratory microbiota interact with the host to participate in the fight against invading pathogens; however, only a handful of such interactions have been characterized. It is therefore relevant to identify the specific interactions between resident bacteria and host cells that lead to the inhibition of pathogens. Moreover, it is advantageous to find ways to do so in a high throughput manner to screen large numbers of different bacterial isolates.

The first part of this chapter describes how a screen developed by Dr. Steve Bernier was used to identify human bacterial isolates inhibiting the growth of pathogens. In this screen, bacterial isolates were grown with Detroit-562 cells, a human nasopharyngeal cell line. A pathogen was then added to the supernatant and its growth was measured 24 hours later. Commensals were selected based on their ability to reduce the growth of *E. coli* in the presence of host cells. The inhibitory activity of these bacteria was confirmed against *P. aeruginosa.* Specific characteristics of the inhibitory phenotype were then investigated by introducing heat-killed bacteria and filtered supernatant and measuring the growth of *P. aeruginosa* over time.

The second part of this chapter relates how I characterized the immunological relationship between the host cells and the bacteria. While Detroit-562 cells are not immune cells, they secrete various cytokines and chemokines involved in activating, shaping, and maintaining an immune response. Measuring the levels of such proteins produced by the cells in the presence of different bacteria informs us on the type of immune response triggered, which enables us to better understand the relationship between the bacteria and the host.

3.2 Results

3.2.1 Human isolates inhibited the growth of *P. aeruginosa*

The objective of the initial screen was to identify commensal bacteria capable of killing or inhibiting the growth of airway pathogens with the help of the host. Detroit-562 cells were incubated with bacteria from the Human Isolates Library for 24 hours and then a pathogen was added. Bacterial growth was measured after 24 hours of co-culture. Using this screen Dr. Steve Bernier identified 111 bacterial strains inhibiting the growth of *Escherichia coli* in the presence of host cells (**Table A.1**). Of those bacterial strains, 30 also inhibited the growth of *Pseudomonas aeruginosa* and other airway pathogens, including *Stenotrophomonas maltophilia* and *Burkoldheria cenocepacia*. These bacterial strains included *Neisseria sicca, Enterococcus faecium, Streptococcus mitis,* and *Bacteroides vulgatus* (**Table A.2; Figure 3.1**).

These experiments showed the inhibition potential of these bacterial strains to be dependent on the presence of host cells since, in most cases, the effect was lost or diminished when the bacteria were grown with *P. aeruginosa* alone (**Figure 3.1b**). As shown, in the absence of a bacterial strain, *P. aeruginosa* grew to 2.0 ± 4.2 x 10^9 CFUs/mL in the presence of Detroit-562 cells (**Figure 3.1a**) and 1.1 ± 0.7 x 10^9 CFUs/mL in their absence (**Figure 3.1b**). When grown with *N. sicca* in the presence of host cells (**Figure 3.1a**), the growth of *P. aeruginosa* was decreased to 5.5 ± 5.6 x 10^5 CFUs/mL. The decrease was even more pronounced in absence of host cells (**Figure 3.1b**), reaching 6.7 ± 1.2 x 10^3 CFUs/mL. In the case of *E. faecium,* the growth of *P. aeruginosa* was significantly decreased to 7.6 ± 11.5 x 10^6 CFUs/mL in the presence of Detroit-562 cells (**Figure 3.1a**) but remained at 3.3 ± 2.3 x 10^9 CFUs/mL in the absence of host cells (**Figure 3.1b**). The presence of *S. mitis,* on the other hand, completely eliminated *P. aeruginosa,* both with and without host cells (**Figure 3.1**), as it was completely undetectable at the end of the experiment. Finally, the growth of P. aeruginosa was significantly reduced to 4.8 ± 12.3 x 10^6 CFUs/mL when grown with *B. vulgatus* in the presence of host cells (**Figure 3.1a**) but lost its significant decrease in the absence of host cells (**Figure 3.1b**), reaching 1.8 ± 1.9 x 10^8 CFUs/mL.

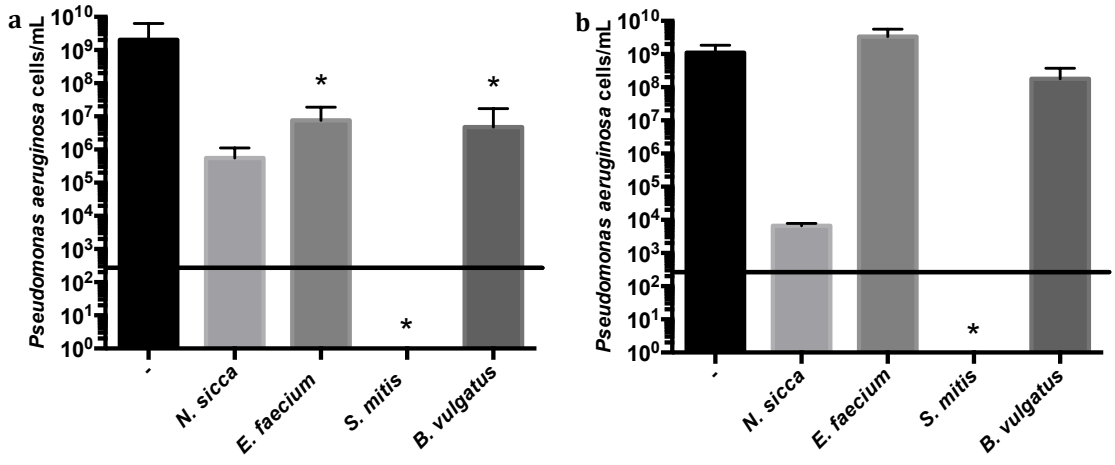

Figure 3.1 *N. sicca*, *E. faecium, S. mitis,* and *B. vulgatus* inhibited *P. aeruginosa* in the presence of Detroit-562 cells. *Neisseria sicca*, *Enterococcus faecium*, *Streptococcus mitis*, and *Bacteroides vulgatus* were incubated for 24 hours with (**a**) and without (**b**) Detroit-562 cells after which *Pseudomonas aeruginosa* was added and grown for an additional 24 hours. The bars represent the growth of *P. aeruginosa* in the presence of the four different commensals and alone (-) in presence (**a**) or absence (**b**) of the Detroit-562 cells after 24 hours of exposure. Error bars represent the SD. The black line represents the limit of detection. Results were pooled from 3 independent experiments (n = 3). * represents $p < 0.05$ (Kruskal-Wallis test) compared to *P. aeruginosa* (-).

3.2.2 *B. vulgatus* inhibited the growth of *P. aeruginosa*

The initial screen was performed in aerobic conditions using only oxygen-tolerant bacteria. However, considering that a majority of the bacteria composing our microbiota are anaerobic, it was important to test the effects of specific oxygen-

sensitive bacteria. I therefore incubated Detroit-562 cells with five randomly selected anaerobic commensals (**Table A.2**) in the absence of oxygen for 24 hours before incubating them with *P. aeruginosa* in aerobic conditions for another 24 hours (**Figure 3.2**).

Four of the five human isolates had very little effect on the growth of *P. aeruginosa,* whether in the presence of host cells (**Figure 3.2a**) or not (**Figure 3.2b**). A strain of *Bacteroides vulgatus,* though, had a considerable impact on *P. aeruginosa*, reducing its growth from 9.3 ± 4.1 x 10^7 CFUs/mL to 7.3 ± 3.0 x 10^4 CFUs/mL in presence of host cells (**Figure 3.2a**), with a p value < 0.05 (Kruskal-Wallis multiple comparison test). *B. vulgatus* had little effect in the absence of host cells (**Figure 3.2b**). Indeed, without Detroit-562 cells, *P. aeruginosa* grew to 9.3 ± 9.5 x 10^8 CFUs/mL alone and to 1.8 ± 1.9 x 10^8 CFUs/mL with *B. vulgatus*.

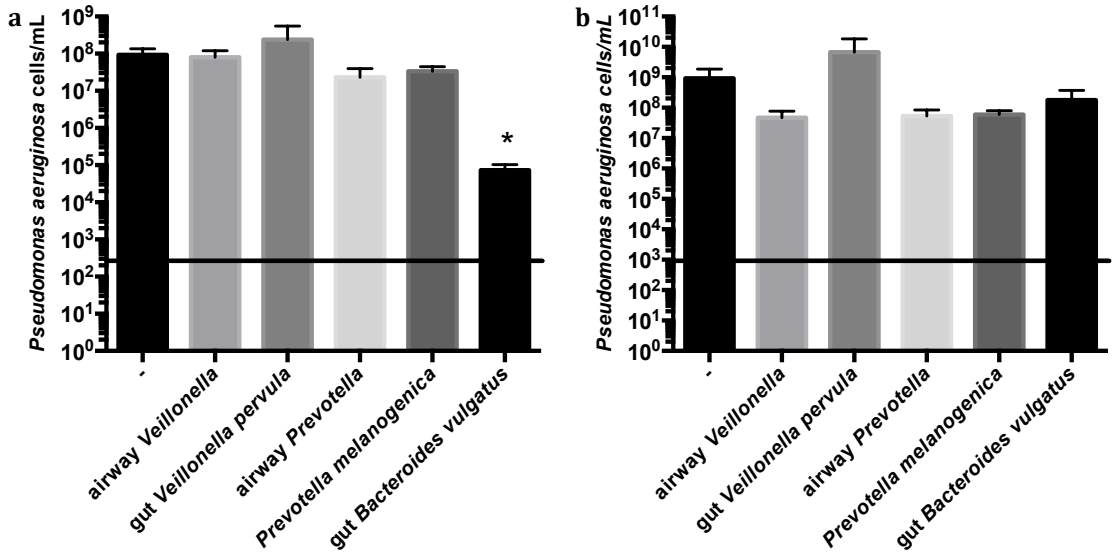

Figure 3.2 *B. vulgatus* inhibited the growth of *P. aeruginosa* in a host-dependent manner. Five randomly selected anaerobic commensal bacterial species, *Veillonella* spp., *Veillonella pervula, Prevotella* spp*., Prevotella melanogenica,* and *Bacteroides vulgatus*, were incubated for 24 hours with (**a**) and without (**b**) Detroit-562 cells in anaerobic conditions after which *Pseudomonas aeruginosa* was added and grown for 24 hours in aerobic conditions. The bars represent the growth of *P. aeruginosa* in presence of the five commensals and alone (-) in presence (**a**) or absence (**b**) of the Detroit-562 cells after 24 hours of exposure. Error bars represent the SD. The black line represents the limit of detection. Results were pooled from 2 independent experiments (n = 2). * represents $p < 0.05$ (Kruskal-Wallis test) compared to *P. aeruginosa* (-).

3.2.3 Characterization of commensal-induced killing of *P. aeruginosa*

A number of experiments were performed to better understand the interactions between the commensals, the host cells and *P. aeruginosa*. First, I performed a time course to determine the rate of killing activity, taking samples every hour for the first four hours of the assay (**Figure 3.3**). These tests revealed that when *P. aeruginosa* was grown without any other bacteria it grew steadily from a starting bacterial load of $1.4 \pm 2.8 \times 10^6$ CFUs/mL to $8.0 \pm 5.3 \times 10^9$ CFUs/mL within 24 hours in the presence of host cells and from $6.0 \pm 0.0 \times 10^5$ CFUs/mL to $1.3 \pm 0.6 \times 10^9$ CFUs/mL in the absence of host cells (**Figure 3.3**).

When grown with *N. sicca* in the presence of Detroit-562 cells, the growth of *P. aeruginosa* was reduced from 8.0 ± 8.5 x 10^5 CFUs/mL to 2.9 ± 0.4 x 10^5 CFUs/mL within four hours. After 24 hours, the culture reached a bacterial load of 5.5 ± 5.6 x 10^5 CFUs/mL. In the absence of host cells, the growth of *P. aeruginosa* followed a similar pattern, starting at 5.0 ± 1.4 x 10^5 CFUs/mL and reaching 2.1 ± 1.0 x 10^5 CFUs/mL within the first four hours. It then continued to decrease to reach 6.7 ± 1.2 x 10^3 CFUs/mL at hour 24 (**Figure 3.3a**).

In the case of *E. faecium,* the growth of *P. aeruginosa* followed the same pattern without Detroit-562 cells as *P. aeruginosa* grown without a commensal bacteria: it started at 9.0 ± 1.4 x 10^5 CFUs/mL and grew steadily to reach 3.3 ± 2.3 x 10^9 CFUs/mL after 24 hours of exposure. In the presence of host cells, however, the bacterial load of *P. aeruginosa* exposed to *E. faecium* dropped from 8.0 ± 2.8 x 10^5 CFUs/mL to 1.6 ± 0.6 x 10^5 CFUs/mL at hour 2. It then increased slightly and reached 1.7 ± 1.4 x 10^7 CFUs/mL within 24 hours (**Figure 3.3b**).

Finally, in the presence of *S. mitis,* the bacterial load of *P. aeruginosa* started at 1.3 ± 0.4 x 10^5 CFUs/mL and dropped rapidly until it was undetectable by hour 4, both with and without host cells (**Figure 3.3c**).

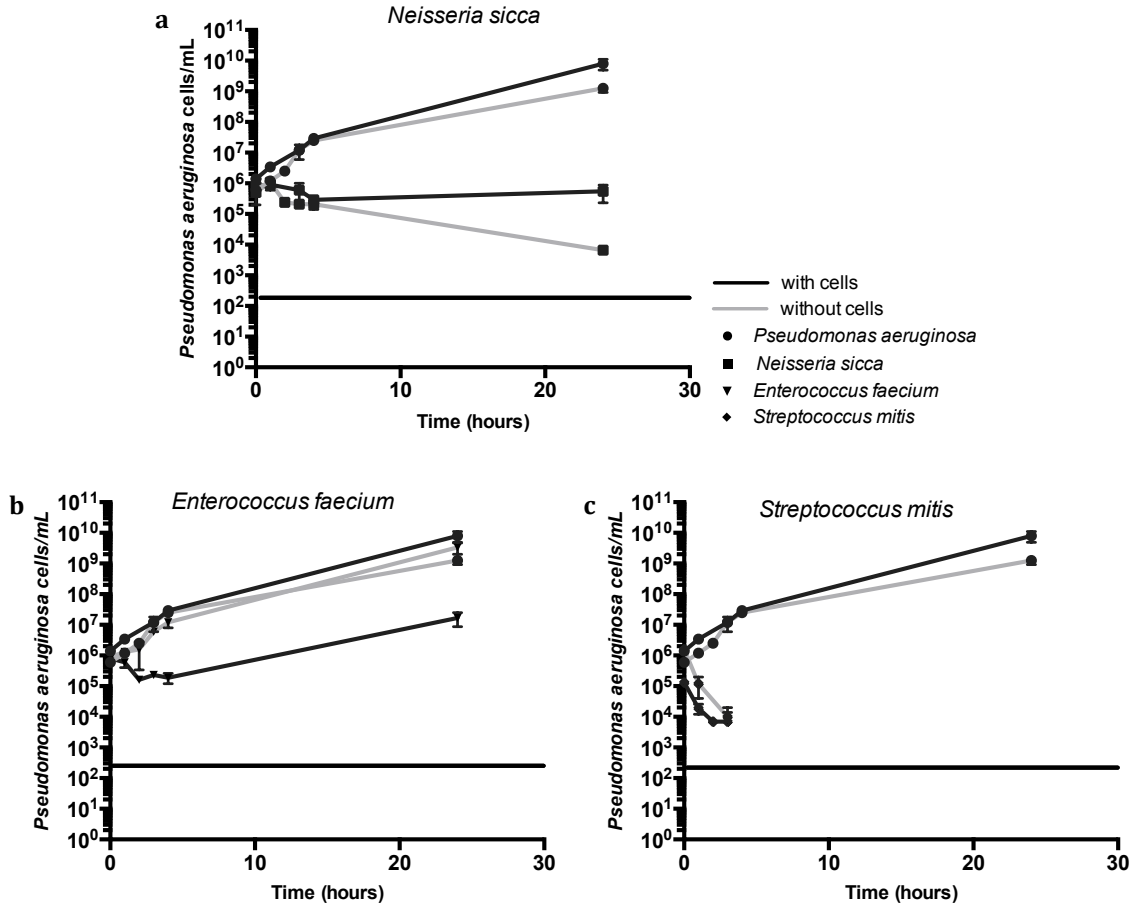

Figure 3.3 *P. aeruginosa* was inhibited within the first hours of exposure. *N. sicca*, *E. faecium*, and *S. mitis* were incubated for 24 hours with and without Detroit-562 cells after which *Pseudomonas aeruginosa* was added and grown for an additional 24 hours. The growth of *P. aeruginosa* was measured every hour for 4 hours and at the 24 hour point. The black line represents the limit of detection. Data is represented as mean with SD (n = 3 technical replicates).

I then sought to determine whether or not the presence of living bacteria was necessary to the killing effect. The commensal bacteria were incubated 15 minutes

at 80°C. The Detroit cells were then incubated with these heat-killed bacteria before the addition of *P. aeruginosa* (**Figure 3.4a**). Without any commensals, *P. aeruginosa* grew to 8.0 ± 0.0 x 10^9 CFUs/mL. With *N. sicca, E. faecium,* and *S. mitis,* the bacterial load of *P. aeruginosa* reached 1.5 ± 0.1 x 10^9 CFUs/mL, 1.4 ± 0.2 x 10^9 CFUs/mL, and 1.4 ± 0.2 x 10^9 CFUs/mL respectively.

Finally, to verify if the observed killing effect was caused by a soluble factor released by either the host cells or the commensals, I collected and filtered the supernatant of the Detroit cells which had been incubated with either *E. faecium* or *S. mitis* for 24 hours and exposed *P. aeruginosa* to these supernatants (**Figure 3.4b**). I found that *P. aeruginosa* grew to 4.1 ± 6.9 x 10^7 CFUs/mL when exposed to the supernatant from *E. faecium* and to 2.7 ± 4.6 x 10^6 CFUs/mL when exposed to the supernatant from *S. mitis, a*s opposed to its growth in isolation, which reached 8.0 ± 5.3 x 10^9 CFUs/mL.

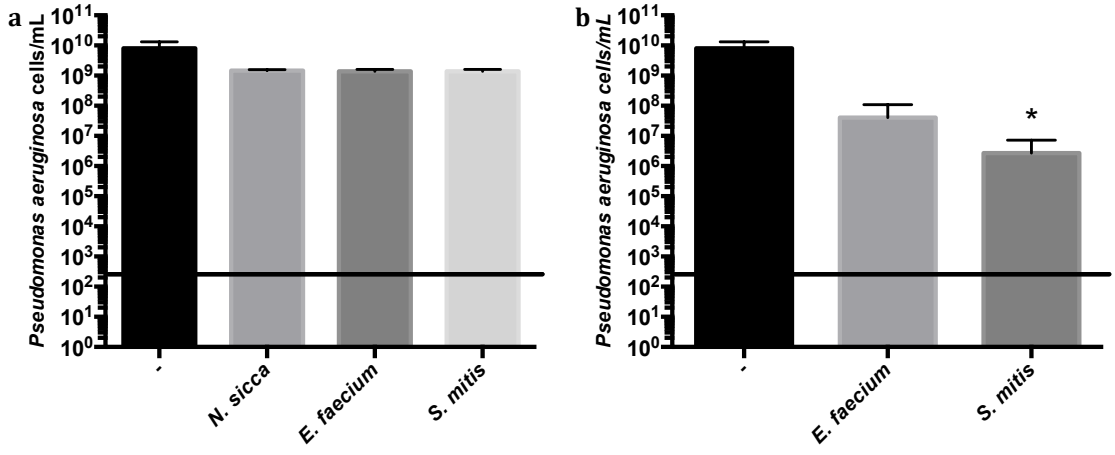

Figure 3.4 The killing effect was mediated by living bacteria secreting a soluble factor. (**a**) Heat-killed *Neisseria sicca*, *Enterococcus faecium*, and *Streptococcus mitis* were incubated for 24 hours with Detroit-562 cells after which *Pseudomonas aeruginosa* was added. The bars represent the growth of *P. aeruginosa* in presence of the four heat-killed commensals and alone (-) after 24 hours of exposure. (**b**) *Enterococcus faecium*, and *Streptococcus mitis* were incubated for 24 hours with Detroit-562 cells. The supernatant was then collected and filtered. *Pseudomonas aeruginosa* was then grown for 24 hours in the supernatants. The bars represent the growth of *P. aeruginosa* in the supernatant of the commensals and alone (-) after 24 hours of exposure. The black line represents the limit of detection. Error bars represent the SD (n = 3 technical replicates). * represents $p < 0.05$ (Kruskal-Wallis test) compared to *P. aeruginosa* (-).

3.2.4 Bacterial isolates altered *P. aeruginosa*-induced host cell cytokine profiles

As I hypothesize that the observed host-dependent bactericidal effect is driven by immune factors, I used a Luminex multiplex assay to measure the levels of cytokines and chemokines secreted by the Detroit cells in response to bacterial exposure (**Figure 3.5; Table A.3**). I performed this analysis on the Detroit cells under several conditions: a) unstimulated; b) exposed only to the commensal strains described above; c) exposed to both the commensal strains and *Pseudomonas aeruginosa*; and, d) exposed to *Pseudomonas aeruginosa* alone. I also

performed a hierarchical cluster analysis to determine how the different cytokine profiles compared to each other.

I found that unstimulated epithelial cells secreted both pro-inflammatory and anti-inflammatory cytokines and chemokines. Moreover, I observed that the pattern of cytokine clusters depended on the commensal to which the cells were exposed. For instance, the cytokine expression of the cells in response to *E. faecium* and in response to *S. mitis* were different but the response to *E. faecium* alone and *E. faecium* and *P. aeruginosa* were similar (**Figure 3.5**).

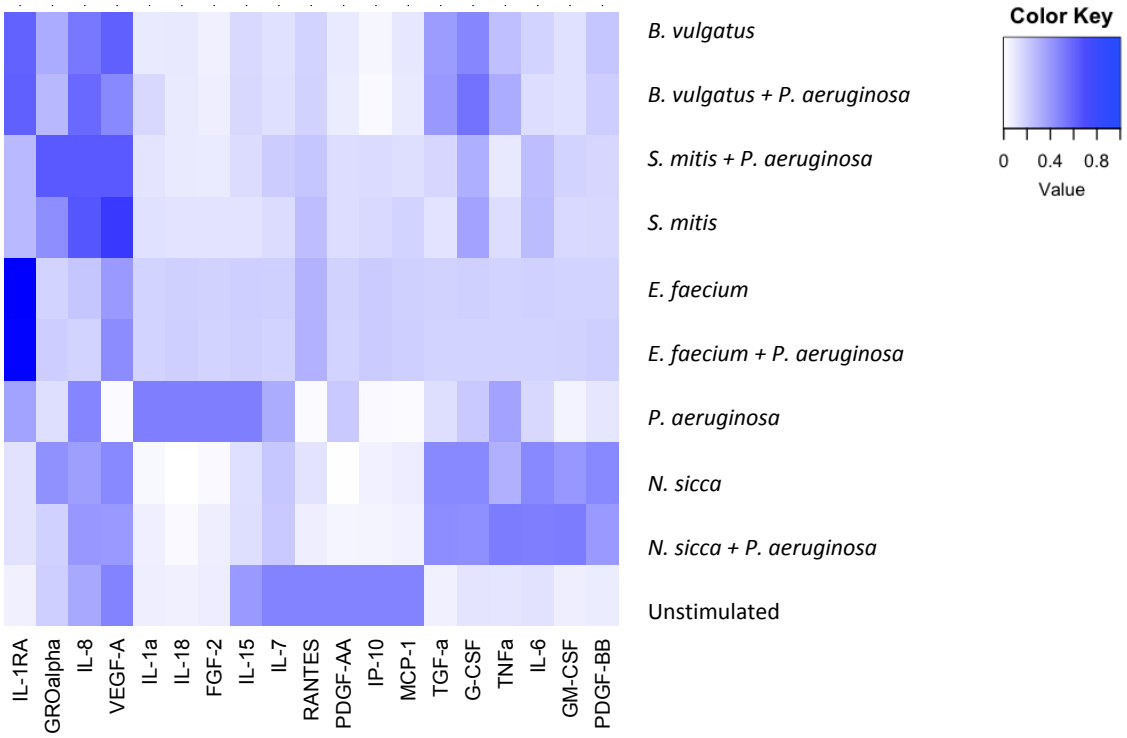

Figure 3.5 Epithelial cells produced different cytokines in response to the bacteria they were exposed to. *Neisseria sicca*, *Enterococcus faecium*,

Streptococcus mitis, and *Bacteroides vulgatus* were incubated for 24 hours with Detroit-562 cells after which *Pseudomonas aeruginosa* was added. After 24 hours of exposure, the cytokines and chemokines produced by the epithelial cells were measured using a Luminex multiplex assay (Eve technologies). The heatmap indicates the level of cytokines expressed by the cells exposed to the different bacteria or alone (unstimulated). The colour key shows the normalized cytokine and chemokine values.

As for the specific cytokines secreted, they varied depending on the bacteria present. The presence of *P. aeruginosa* alone led to the secretion of a number of pro-inflammatory cytokines, including IL-1α, which reached 18.5 pg/mL in unstimulated cells while the presence of *P. aeruginosa* led to a release of 365.1 pg/mL (**Figure 3.6a**). IL-18 was secreted to 189.5 pg/mL while it only reached 1.8 pg/mL in the presence of unstimulated cells (**Figure 3.6b**).

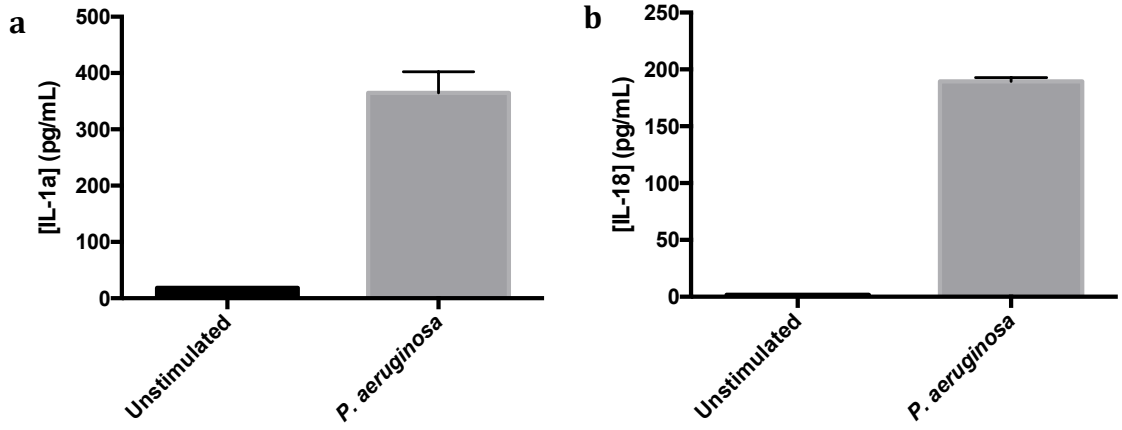

Figure 3.6 *P. aeruginosa* increased pro-inflammatory cytokines. Detroit-562 cells were incubated with *P. aeruginosa*. After 24 hours of exposure, the cytokines and chemokines produced by the epithelial cells were measured using a Luminex multiplex assay (Eve technologies). The bars represent the concentration of IL-1α (a) and IL-18 (b) produced by the Detroit-562 cells exposed to *P. aeruginosa* or alone (n = 2 technical replicates).

The presence of *N. sicca* kept the levels of these cytokines similar to unstimulated cells: 42.2 pg/mL for IL-1α (**Figure 3.7a**) and 7.1 pg/mL for IL-18 (**Figure 3.7b**).

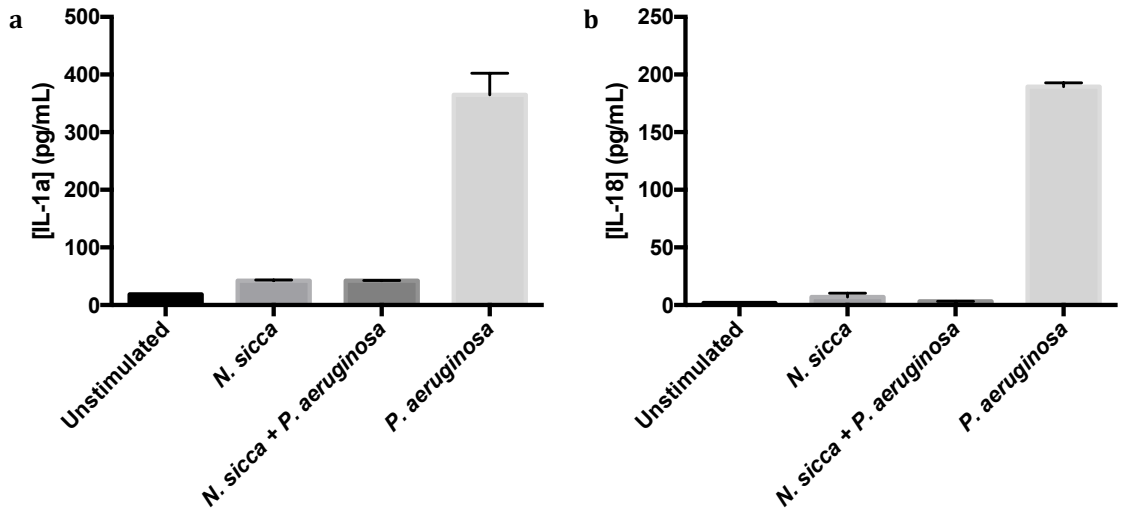

Figure 3.7 *N. sicca* did not increase pro-inflammatory cytokines. *Neisseria sicca* was incubated for 24 hours with Detroit-562 cells after which *Pseudomonas aeruginosa* was added. After 24 hours of exposure, the cytokines and chemokines produced by the epithelial cells were measured using a Luminex multiplex assay (Eve technologies). The bars represent the concentration of IL-1α (a) and IL-18 (b) produced by the Detroit-562 cells exposed to *Neisseria sicca, Neisseria sicca* + *P. aeruginosa, P. aeruginosa* or alone (n = 2 technical replicates).

Exposure to *E. faecium* led to very little expression of most cytokines with the exception of IL-1RA, which reached 95.1 pg/mL in the presence of *E. faecium* alone and 76.1 pg/mL in the presence of *E. faecium* + *P. aeruginosa,* as opposed to 3.3 pg/mL in the absence of any bacteria. By comparison, *P. aeruginosa* alone led to a concentration of IL-1RA of 68.4 pg/mL (**Figure 3.8**).

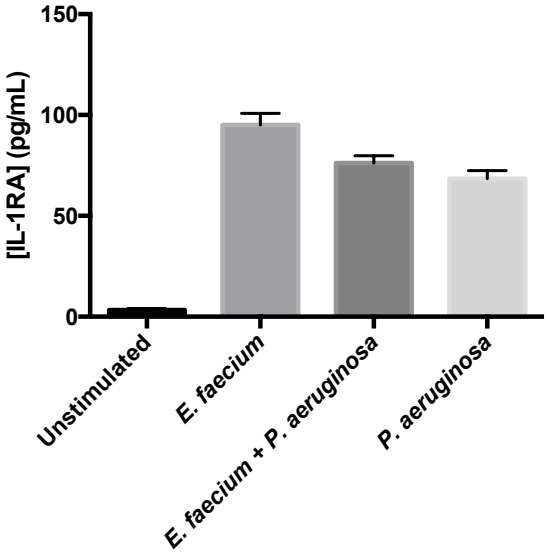

Figure 3.8 *E. faecium* increased an anti-inflammatory cytokine. *Enterococcus faecium* was incubated for 24 hours with Detroit-562 cells after which *Pseudomonas aeruginosa* was added. After 24 hours of exposure, the cytokines and chemokines produced by the epithelial cells were measured using a Luminex multiplex assay (Eve technologies). The bars represent the concentration of IL-1RA produced by the Detroit-562 cells exposed to *E. faecium, E. faecium* + *P. aeruginosa, P. aeruginosa* or alone (n = 2 technical replicates). * represents $p < 0.05$ (Kruskal-Wallis test).

In the presence of *S. mitis*, the epithelial cells released several neutrophil chemoattractants, including GROα and IL-8. Indeed, GROα was released from 8,267.1 pg/mL to 10,550.8 pg/mL (*S. mitis* alone) and 16,523.6 pg/mL (*S. mitis* + *P. aeruginosa)* while *P. aeruginosa* led to a release of this cytokine of 7,259.3 pg/mL (**Figure 3.9a**). *S. mitis* also led to an secretion of 5,582.9 pg/mL of GROα (**Figure 3.9b**) compared to unstimulated cells, which secreted 4,691.3 pg/mL.

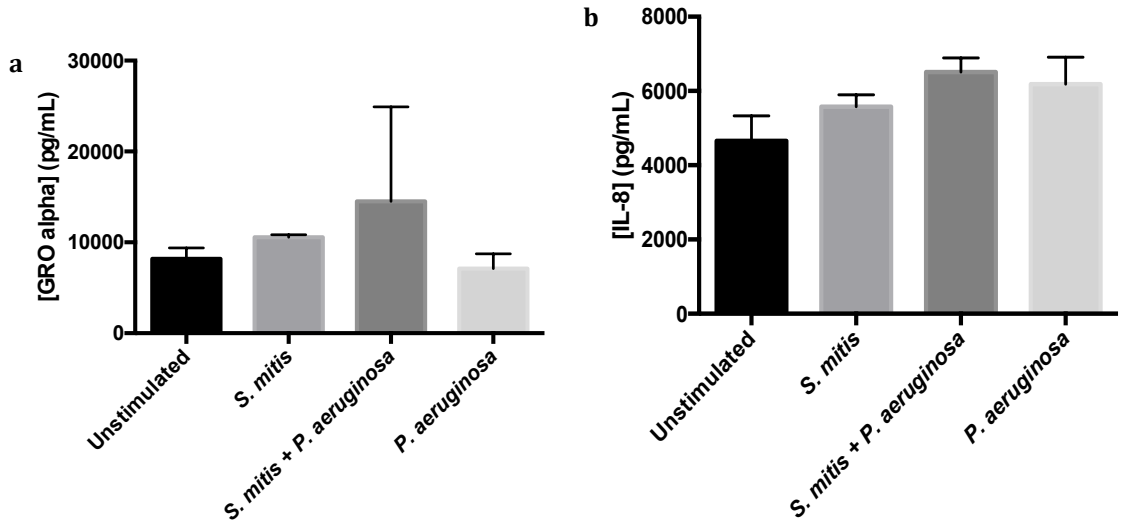

Figure 3.9 *S. mitis* increased neutrophil chemoattractants. *Streptococcus mitis* was incubated for 24 hours with Detroit-562 cells after which *Pseudomonas aeruginosa* was added. After 24 hours of exposure, the cytokines and chemokines produced by the epithelial cells were measured using a Luminex multiplex assay (Eve technologies). The bars represent the concentration of GROα (a) and IL-8 (b) produced by the Detroit-562 cells exposed to *S. mitis, S. mitis* + *P. aeruginosa, P. aeruginosa* or alone (n = 2 technical replicates). * represents $p < 0.05$ (Kruskal-Wallis test).

Finally, the presence of *B. vulgatus* led to a considerable upregulation of G-CSF by the Detroit-562 cells: from 22.5 pg/mL to 146.5 pg/mL in response to *B. vulgatus* alone and 152.0 pg/mL in response to *B. vulgatus* + *P. aeruginosa* in contrast to *P. aeruginosa,* which only increased this cytokine to 80.4 pg/mL (**Figure**

3.10a). The presence of *B. vulgatus* also kept VEGF-A (437.2 pg/mL and 307.9 pg/mL) at similar levels to unstimulated cells (447.6 pg/mL) while the presence of the *P. aeruginosa* downregulated this cytokine to 65.0 pg/mL (**Figure 3.10b**).

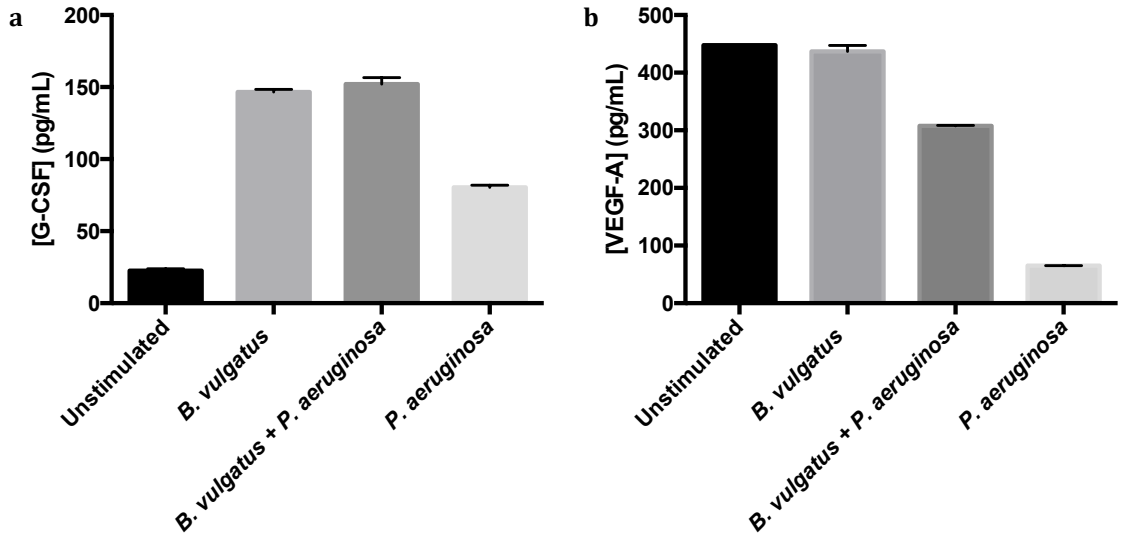

Figure 3.10 *B. vulgatus* increased specific cytokines. *Bacteroides vulgatus* was incubated for 24 hours in anaerobic conditions with Detroit-562 cells after which *Pseudomonas aeruginosa* was added. After 24 hours of exposure, the cytokines and chemokines produced by the epithelial cells were measured using a Luminex multiplex assay (Eve technologies). The bars represent the concentration of G-CSF (a) and VEGF-A (b) produced by the Detroit-562 cells exposed to *B. vulgatus, B. vulgatus* + *P. aeruginosa, P. aeruginosa* or alone (n = 2 technical replicates). * represents $p < 0.05$ (Kruskal-Wallis test).

3.3 Discussion

3.3.1 Human isolates inhibited the growth of *P. aeruginosa* through the active secretion of a soluble factor

Using a high-throughput screening method, Dr. Steve Bernier isolated over a hundred bacterial strains inhibiting the growth of *E. coli* (**Table A.1**). These hits proved to be host-dependent as, in the initial results, the inhibitory phenotype was lost in the absence of Detroit-562 cells. These bacteria were then tested against other airway pathogens. I chose *Neisseria sicca, Enterococcus faecium,* and *Streptococcus mitis* to do further studies as Dr. Bernier's work showed them to be effective against all the pathogens screened, especially *Pseudomonas aeruginosa*, the pathogen of interest (**Table A.2; Figure 3.1**). After repeating the experiment several times, however, I came up with variable results. In the case of *Neisseria sicca*, its presence led to a 1000x decrease in the growth of *P. aeruginosa*, both in presence and in absence of host cells. In fact, the inhibitory effect was more pronounced in absence of host cells. As for the presence of *E. faecium,* it also decreased the growth of *P. aeruginosa* 1000x but in a host-dependent manner, as the effect was lost in absence of Detroit-562 cells. The inhibitory activity of *S. mitis,* on the other hand, was not dependent on the host cells and its ability to completely inhibit *P. aeruginosa*, even in the absence of Detroit-562 cells, made it an interesting bacterium to study. These three bacteria were chosen from the initial screen. *B. vulgatus* was then added based on the results of the anaerobic screen (**Figure 3.2**). Indeed, as commensal bacteria are often anaerobic, I showed that this screen could be repeated in anaerobic conditions and tested the effects of five anaerobic bacteria.

Of these five, only *B. vulgatus* limited the growth of *P. aeruginosa* in a host dependent manner.

This is not the first instance in which bacteria modulating the growth and virulence of *P. aeruginosa* have been identified. In fact, *P. aeruginosa* is responsible for most of the morbidity and mortality associated with cystic fibrosis lung disease (Rajan and Saiman, 2002) where it exists in polymicrobial communities (Sibley *et al.,* 2008). Therefore, numerous studies investigate the impact of other bacterial species on the survival and pathogenicity of *P. aeruginosa.* These studies mostly focus on *Streptococcus* species, as they are frequently isolated from oral and respiratory samples (Filkins *et al.,* 2012). While many *Streptococcus* strains have been shown to either enhance the morbidity of cystic fibrosis or to potentiate the pathogenesis of *P. aeruginosa* (Sibley *et al.,* 2008), as is most notably the case of species from the *Streptococcus milleri* group (Sibley *et al.,* 2008), several studies focus on the protective role of these commensal bacteria. As such, Whiley *et al.* (2015) identified viridans streptococci, including *S. mitis,* inhibiting the growth of *P. aeruginosa* when inoculated as primary colonizers through the secretion of hydrogen peroxide. In another example, Scoffield and Wu (2015) used showed that *Streptococcus parasanguinis* could protect *Drosophila melanogaster* from killing by *P. aeruginosa* in a nitrite and hydrogen peroxide-dependent manner.

Removed from the context of cystic fibrosis lung infections, commensal bacteria have been shown to inhibit *P. aeruginosa.* For instance, *Corynebacterium*

mastitidis, an ocular commensal, protects mice from ocular surface disease mediated by *P. aeruginosa* (St Leger *et al.,* 2017).

Our next aim was to better understand the effects of our commensal bacteria of interest on the observed phenotype. I started by measuring the rate of killing of the different commensals by quantifying the growth of *P. aeruginosa* every hour for the first few hours of exposure to the commensals, with or without Detroit-562 cells (**Figure 3.3**). I found that, in every case, *P. aeruginosa* was inhibited during the first few hours. For all the commensals tested, there was a rapid decrease of the growth of *P. aeruginosa* by hour 2. It was then allowed to grow slightly in presence of both *N. sicca* and *E. faecium* but never reached the same level as when it grew alone. With *S. mitis, P. aeruginosa* was completely eliminated within the first four hours, both with and without host cells. These results clearly suggest that the presence of the commensals with the host cells created a hostile environment. Our study, therefore, could support the use of these bacteria as probiotics to prevent infections in susceptible populations.

It was also important to understand whether the inhibitory phenotype was simply the result of the Detroit-562 cells reacting to cell wall components of the bacteria, through TLR activation for instance or if the commensal bacteria had an active role in the phenotype. To do so, the bacteria were heat-killed and the assay was performed in the same way (**Figure 3.4a**). Here, the effect was lost and *P. aeruginosa* was able to grow in presence of the different commensals, indicating that

living bacteria were necessary for the inhibitory activity. It is safe to assume that the bacteria may be secreting specific factors in their environment, which could either directly inhibit *P. aeruginosa* or influence the host cells to do so.

While I believe that these bacteria could be used as probiotics, it would be more effective to isolate the molecule(s) exhibiting the inhibitory effect. The effect of filtered supernatant was tested against *P. aeruginosa* to verify whether the killing activity was mediated by a soluble factor released in the environment (**Figure 3.4b**). I found that the filtered supernatant of the Detroit-562 cells exposed to the different bacteria retained its inhibitory effect, albeit not to the same extent as when the bacteria were present. For instance, the growth of *P. aeruginosa* was decreased 1000x when exposed to the supernatant taken from the Detroit-562 cells incubated with *S. mitis,* while it was reduced to zero in presence of the living bacteria. This shows that the effect was catalyzed by a soluble factor released in the growth medium by either the commensal bacteria or the host cells and that this factor was probably constantly released while the bacteria were present, leading to a higher killing capacity.

3.3.2 Bacterial isolates altered *P. aeruginosa*-induced host cell cytokine profiles

Using a multiplex assay to quantify the cytokines produced by the Detroit-562 cells exposed to the different bacteria allowed us to gain a better understanding of the relationship between the host cells and the commensal bacteria. Each commensal strain created its own specific cytokine profile (**Figure 3.5**).

As expected, *P. aeruginosa* led to the secretion of a number of pro-inflammatory cytokines, such as IL-1α and IL-18 (**Figure 3.6**). Indeed, when cells are exposed to a pathogenic bacterium, they release inflammatory signals to initiate an inflammatory immune response and clear the threat (Murphy *et al.,* 2008). However, this inflammatory response can also be damaging to the surrounding tissue. It is therefore relevant that when the cells were exposed to the commensals, both in the presence or absence of *P. aeruginosa*, these pro-inflammatory cytokines and chemokines were not being upregulated to the same level (**Table A.3; Figure 3.7**). This suggests that the commensals did not rely on a pro-inflammatory immune response to help clear *P. aeruginosa* and that they prevented this pathogen from initiating the inflammatory response.

Moreover, *E. faecium* specifically upregulated an anti-inflammatory cytokine, IL-1RA (**Figure 3.8**), which is a receptor antagonist of IL-1 that blocks the action of this pro-inflammatory cytokine (Arend, 1990). This would further prevent the initiation of an inflammatory response and therefore protect the tissue.

S. mitis had a different effect (**Figure 3.9**). While it did prevent the upregulation of IL-1α and IL-18, it also led to the upregulation of GROα and IL-8, which are neutrophil chemoattractants and would lead to an influx of neutrophils to the site of infection. Neutrophils are one of the first lines of defense against infections; they recognize threats, then neutralize them and secrete various cytokines and chemokines to facilitate the elimination of the invading bacteria (Murphy *et al.,* 2008). This experimental model contained only epithelial cells so

neutrophils did not play a role. However, the upregulation of these chemokines suggests that in a more complete model involving different cell types, the presence of *S. mitis* should lead to the recruitment of neutrophils, thereby creating a hostile environment and facilitating the elimination of *P. aeruginosa*.

Finally, *B. vulgatus* also led to the upregulation of different cytokines, most notably G-CSF and VEGF-A (**Figure 3.10**). G-CSF is produced by cells to stimulate the production of granulocytes by the bone marrow. It is involved in neutrophil function (Nagata, 1989). In this regard, *B. vulgatus* could have effects similar to *S. mitis* and rely on neutrophils to help eliminate *P. aeruginosa*. VEGF-A is a marker of hypoxia (Hlatky *et al.,* 1996). As *B. vulgatus* is an anaerobic commensal, part of the experiment was performed in an anaerobic chamber. It was therefore logical that the Detroit-562 cells would release this factor and was most likely an effect of the environment rather than the presence of this specific pathogen.

P. aeruginosa is a complex pathogen that expresses numerous virulence factors and therefore activates immune responses through different pathways. It is recognized by TLR-2, TLR-4, and TLR-5 (Faure *et al.,* 2004; Morris *et al.,* 2009; Ramphal *et al.,* 2008; Skerrett *et al.,* 2007) and leads to the secretion of several pro-inflammatory cytokines, in particular IL-1, IL-6, IL-8, IL-17, IL-18 and GM-CSF (Epelman *et al.,* 2000; Joseph *et al.,* 2005, Kube *et al.,* 2001; Sawa *et al.,* 1997; Schultz *et al.,* 2002; Xu *et al.,* 2014). The eradication of *P. aeruginosa* is mostly mediated through the recruitment of professional phagocytic cells (Lovewell *et al.,* 2014). In the context of this epithelial cell model, these cells do not play a role as they are

absent from the model. However, upon stimulation with *P. aeruginosa,* airway epithelial cells release cytokines and chemokines such as IL-8, IL-6 and GM-CSF (Campodonico *et al.,* 2008; Lau *et al.,* 2005; Parker and Prince, 2011). These results are fairly consistent with our findings as I have demonstrated that stimulation of the Detroit-562 cells with *P. aeruginosa* led to the upregulation of pro-inflammatory cytokines, including IL-8, IL-1α, and IL-18 (**Figure 3.5**). Moreover, the response to *P. aeruginosa* can be hyper-inflammatory, which is the main driver of lung damage and therefore disease (Pierreakos *et al.,* 2012). Several studies have shows that reduced inflammation in the lungs leads to a better outcome for acute *P. aeruginosa* infections (Cohen and Prince, 2013; Sawa *et al.,* 1997; Veliz Rodriguez *et al.,* 2012). I have found that stimulation of the Detroit-562 with our commensal bacterial strains led to a reduction in pro-inflammatory cytokines (**Figure 3.5**), especially in the cases of *N. sicca* and *E. faecium*. This could indicate that, *in vivo,* these commensals could ameliorate the outcomes of a *P. aeruginosa* infection.

Overall, these results seem consistent with the studies investigating the airway epithelial cell response to *P. aeruginosa* and support the potentially protective effect of the commensal strains. However, it is important to emphasize that these studies are preliminary and only represent one biological replicate. It is therefore difficult to differentiate between differences of biological importance and difference due to sample variation. Despite this, I do provide an interesting starting point into the study of the immunomodulatory effects of the bacteria in the context

of a *P. aeruginosa* infection. Further studies are necessary to confirm and deepen our investigation into the roles of these cytokines.

3.4 Conclusions

Overall, I have identified and further characterized four different human bacterial isolates whose presence with human airway cells led to a reduction in growth of *P. aeruginosa*, a common airway pathogen. These commensals created a hostile environment for *P. aeruginosa* through the active secretion of a soluble factor, resulting in a rapid decrease in bacterial load of *P. aeruginosa*.

The elimination of pathogens *in vivo* involves the immune system. To understand the type of immune response the different bacteria of interest would trigger, I analyzed the cytokines released by the Detroit-562 cells in their presence. While *P. aeruginosa* led to the release of pro-inflammatory cytokines, none of the commensals did so, indicating that they would not cause harm to a living organism. Moreover, they each released specific factors leading either to a reduction in inflammation or the creation of a hostile environment through the recruitment and activation of specific innate immune cells.

These results suggest that the commensals of interest, *N. sicca, E. faecium, S. mitis,* and *B. vulgatus,* have immunomodulatory properties that could be exploited through their use as probiotics. However, it is important to better characterize these immunomodulatory properties, as well as their inhibitory potential against *P. aeruginosa* through the use of more complex *in vitro* and *in vivo* models.

Chapter 4 PCLS model

4.1 Rationale

The initial antimicrobial screen was performed in cell culture using pharyngeal epithelial carcinoma cells, Detroit-562 cells, all of which were of the same type and of cancerous origin. This cell culture provided an adequate model for determining whether or not the presence of host epithelial cells could influence bacterial killing but could not account for the diversity of cells that compose organs and the immune system. Precision-cut lung slices (PCLS) are a culture model using thin, viable slices containing alveoli tissue as well as intrapulmonary airway and blood vessels. This method allows for the preservation of the morphology and the different cell types present *in vivo* while providing access to individual cells (Sanderson, 2011). PCLS are different from cell cultures in that they contain different viable cell types including epithelial cells but also resident innate immune cells such as alveolar macrophages or neutrophils. This model allows for the simplicity of a bacterial monocolonization; however, it does not involve more complicated factors such as the adaptive immune system (Sanderson, 2011).

4.2 Results

4.2.1 PCLS remained viable and did not influence the growth of the bacteria

I verified that the PCLS remained viable for the duration of the experiment using a resazurin viability assay. Using DMEM and PCLS killed with 1% Triton as

controls, I found that the level of fluorescence produced by the viable PCLS was ten-fold higher than both negative controls and stayed at the same level for up to 8 days (**Figure 4.1**).

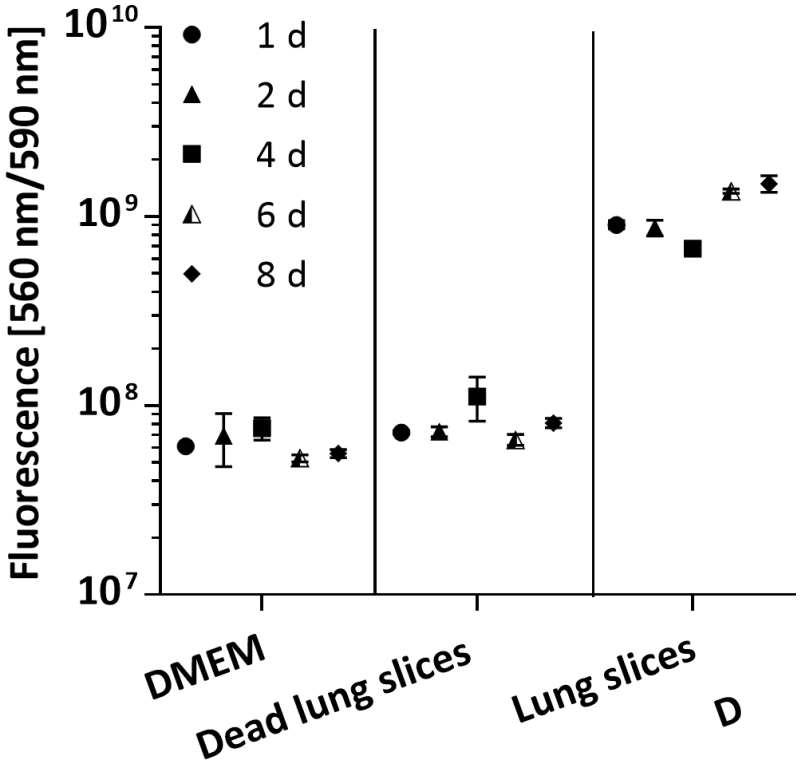

Figure 4.1 PCLS remained viable for the duration of the experiment. The PCLS at different time points were incubated for 4 hours at 37°C, 5% CO_2 with a 0.5 mM Resazurin solution. The 560 nm/590 nm fluorescence was then measured in a black 96-well plate. The negative controls are DMEM with no PCLS and PCLS treated with 1% Triton in PBS for 1 hour. Each symbol represents the mean of four PCLS with SD. Data obtained from Dr. Janine Strehmel.

To better understand the influence of the PCLS on the growth of our commensals of interest, I measured the bacterial load of *N. sicca* (**Figure 4.2a**)*, E. faecium* (**Figure 4.2b**)*, S. mitis* (**Figure 4.2c**)*,* and *B. vulgatus* (**Figure 4.2d**) grown in the presence or absence of PCLS at different time points. I found that, in the presence of PCLS, the bacterial loads *N. sicca* increased steadily: it started at 1.4 ± 1.1 x 10^5 CFUs/mL, reaching 1.6 ± 0.5 x 10^8 CFUs/mL after 24 hours and 6.2 ± 15.8 x 10^9 CFUs/mL after 48 hours. The growth of *N. sicca* was similar in the absence of PCLS during the first 24 hours but the bacterial load remained the same afterwards. To be more precise, this commensal started at a bacterial load of 1.3 ± 0.6 x 10^5 CFUs/mL, grew to 1.5 ± 0.4 x 10^8 CFUs/mL after 24 hours and remained at a similar level, 1.2 ± 1.0 x 10^8 CFUs/mL, for the following 24 hours (**Figure 4.2a**).

In the case of *E. faecium,* the pattern was similar in the presence or absence of PCLS but the final bacterial loads were slightly lower in the absence of host cells. In the presence of Detroit-562 cells, *E. faecium* started at 1.3 ± 0.9 x 10^5 CFUs/mL, grew to 1.6 ± 0.5 x 10^7 CFUs/mL within 24 hours to finally reach 1.0 ± 2.4 x 10^8 CFUs/mL at the end of the experiment. In the absence of host cells, the cell density of this commensal was slightly lower, starting at 6.7 ± 3.1 x 10^4 CFUs/mL, growing to 8.0 ± 0.0 x 10^6 CFUs/mL, and reaching 1.1 ± 0.4 x 10^7 CFUs/mL at the end of the experiment (**Figure 4.2b**).

S. mitis started at a bacterial load of 2.2 ± 1.4 x 10^5 CFUs/mL with PCLS and grew to 9.3 ± 5.1 x 10^6 CFUs/mL during the first 24 hours. However, it was below

the limit of detection after the 48 hours of incubation. This was also the case in the absence of PCLS, where *S. mitis* grew from 2.1 ± 0.8 x 10^5 CFUs/mL to 3.1 ± 3.0 x 10^6 CFUs/mL in 24 hours before falling under the limit of detection at the end of the experiment (**Figure 4.2c**).

Finally, for *B. vulgatus* I only have results of its growth in presence of PCLS. This bacterial strain was grown in anaerobic conditions for the first 24 hours and in aerobic conditions for the following 24 hours. Accordingly, I found that this bacterium started at 5.7 ± 7.1 x 10^5 CFUs/mL, reached 1.1 ± 0.5 x 10^7 CFUs/mL after 24 hours, and was undetectable after 48 hours (**Figure 4.2d**).

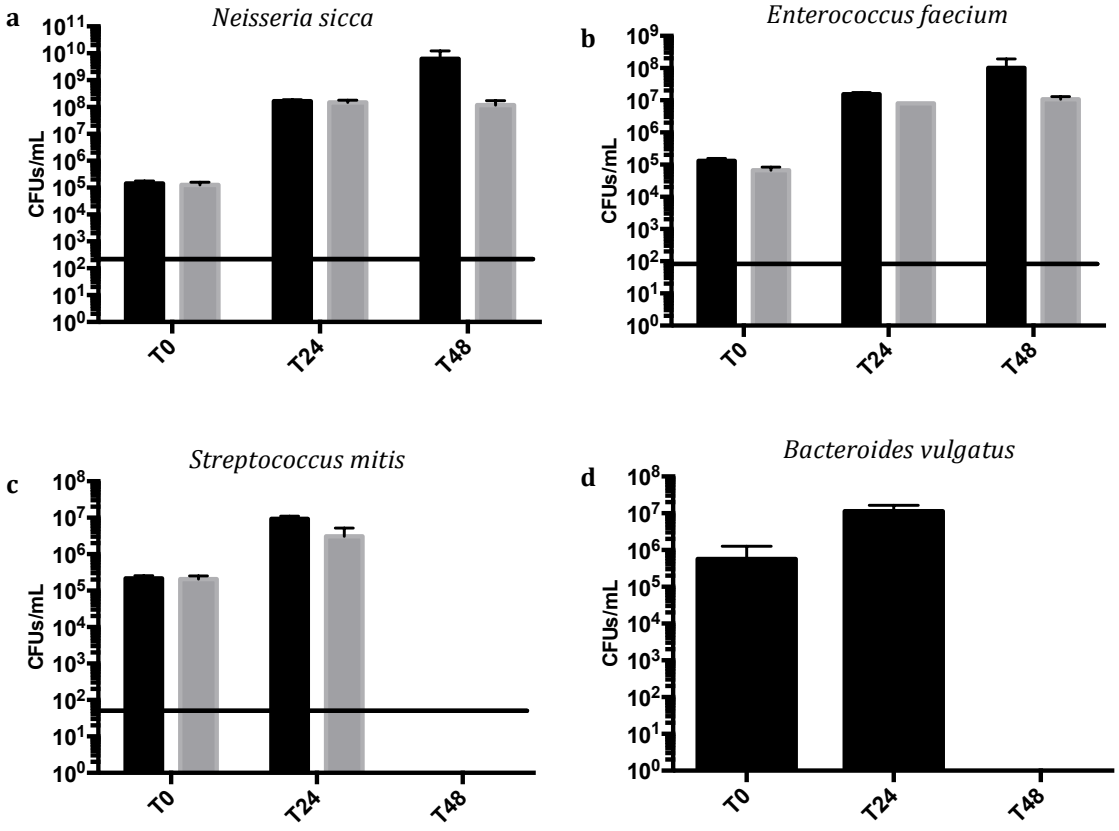

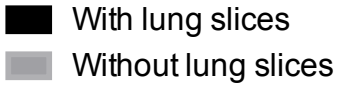

Figure 4.2 *S. mitis* and *B. vulgatus* did not survive the full experiment. *Neisseria sicca* (**a**), *Enterococcus faecium* (**b**), and *Streptococcus mitis* (**c**) were incubated for 48 hours in the presence (black bars) or absence (grey bars) of PCLS in aerobic conditions. *Bacteroides vulgatus* (**d**) was incubated with PCLS for 24 hours in anaerobic conditions and for an additional 24 hours in aerobic conditions. The bars represent the growth of the four commensals at the start of the experiment (T0), after 24 hours (T24), and at the end of the experiment (T48). Error bars represent the SD. The black line represents the limit of detection. Results were pooled from 5 independent experiments (n = 3/experiment).

4.2.2 *E. faecium* and *S. mitis* inhibited the growth of *P. aeruginosa*

In the previous chapter, I found that our four commensals of interest, *N. sicca, E. faecium, S. mitis,* and *B. vulgatus* had an effect on the growth of *P. aeruginosa* in presence of Detroit-562 cells. The same assay was repeated with the PCLS to verify whether or not the commensals retained their inhibitory capacity in the presence of different cell types (**Figure 4.3**). In the cases of *N. sicca, E. faecium,* and *S. mitis,* the PCLS model results were similar to those obtained in the Detroit-562 model. Without commensals, *P. aeruginosa* grew to an average of 3.3 ± 7.1 x 10^9 CFUs/mL in presence of PCLS (**Figure 4.3a**) and to 3.0 ± 3.8 x 10^8 CFUs/mL in absence of PCLS

(**Figure 4.3b**). With PCLS, the presence of *N. sicca* had little effect on the bacterial load of *P. aeruginosa,* which reached 2.7 ± 8.4 x 10^9 CFUs/mL (**Figure 4.3a**). However, in absence of PCLS, the presence of *N. sicca* led to a decrease to 2.8 ± 3.9 x 10^7 CFUs/mL (**Figure 4.3b**). With *E. faecium,* the cell density of *P. aeruginosa* was significantly reduced to 2.5 ± 8.7 x 10^5 CFUs/mL in the presence of PCLS (**Figure 4.3a**) while it reached 3.8 ± 8.0 x 10^5 CFUs/mL in the absence of PCLS (**Figure 4.3b**). In the case of *S. mitis, P. aeruginosa* was significantly reduced in both conditions: it grew to 1.9 ± 6.7 x 10^2 CFUs/mL with the PCLS (**Figure 4.3a**) and was below the limit of detection in the absence of PCLS (**Figure 4.3b**). Finally, *B. vulgatus* lost its inhibitory activity and allowed *P. aeruginosa* to grow to 1.1 ± 1.8 x 10^9 CFUs/mL in the presence of PCLS (**Figure 4.3a**) and to 6.7 ± 7.0 x 10^7 CFUs/mL in the absence of PCLS (**Figure 4.3b**).

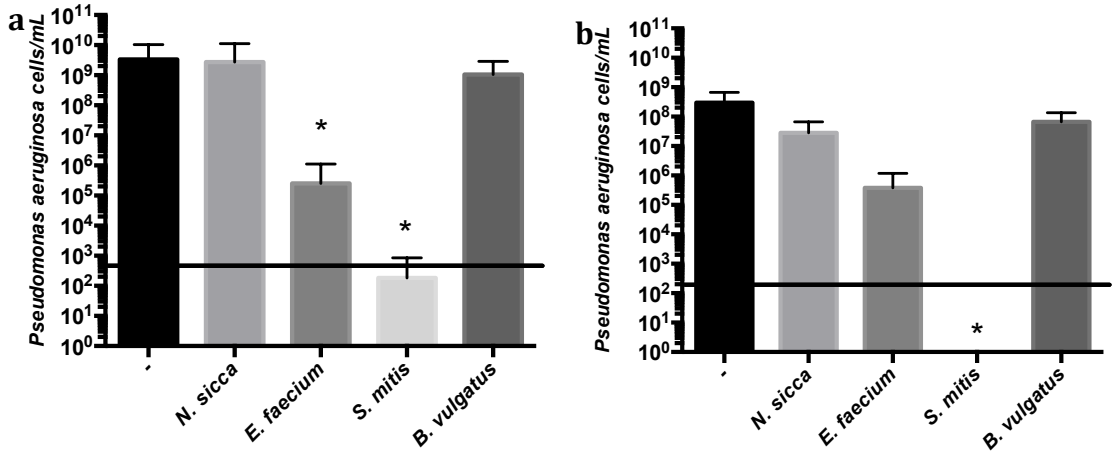

Figure 4.3 *E. faecium* and *S. mitis* inhibited *P. aeruginosa* in the presence of PCLS. *Neisseria sicca*, *Enterococcus faecium*, *Streptococcus mitis*, and *Bacteroides vulgatus* were incubated for 24 hours in DMEM with (**a**) and without (**b**) PCLS after

which *Pseudomonas aeruginosa* was added and grown for an additional 24 hours. The bars represent the growth of *P. aeruginosa* in the presence of the four different commensals and alone (-) in presence (**a**) or absence (**b**) of the PCLS after 24 hours of exposure. Error bars represent the SD. The black line represents the limit of detection. Results were pooled from 5 independent experiments (n = 3/experiment). * represents $p < 0.05$ (Kruskal-Wallis test) compared to *P. aeruginosa.*

4.2.3 Characterization of the commensal-induced killing of *P. aeruginosa*

As in the Detroit-562 cell assay, a number of experiments were performed to better understand the interactions between the commensals, the PCLS, and the pathogen. I started with a time course to determine the rate of killing activity. Samples of the supernatant of the PCLS exposed to the different bacteria were taken every hour for the first four hours of the assay (**Figure 4.4**). The growth of *P. aeruginosa* fluctuated slightly in the first few hours. With a starting bacterial load of $1.4 \pm 0.3 \times 10^5$ CFUs/mL, the bacterial load of *P. aeruginosa* went to $8.3 \pm 10.2 \times 10^5$ CFUs/mL in the presence of PCLS and to $1.1 \pm 1.3 \times 10^7$ CFUs/mL in the absence of PCLS during the first hour. It then reached $8.0 \pm 3.0 \times 10^5$ CFUs/mL with PCLS and $1.0 \pm 1.2 \times 10^7$ CFUs/mL without PCLS after two hours. At hour 3, the bacterial load of *P. aeruginosa* in the presence of the PCLS was $1.1 \pm 0.2 \times 10^6$ CFUs/mL and it reached $1.0 \pm 0.4 \times 10^7$ CFUs/mL in the absence of PCLS. It then grew to $6.7 \pm 1.2 \times 10^5$ CFUs/mL with PCLS and $1.9 \pm 1.1 \times 10^6$ CFUs/mL without PCLS within the next

hour. Finally, after 24 hours, the bacterial load of *P. aeruginosa* had reached 1.9 ± 0.3 x 10^8 CFUs/mL in the presence of PCLS and 2.7 ± 1.2 x 10^7 CFUs/mL in the absence of PCLS (**Figure 4.4**).

In presence of *N. sicca,* the pattern of growth of *P. aeruginosa* was similar both with and without PCLS during the first four hours. However, while the bacterial load of *P. aeruginosa* continued to increase to reach 1.1 ± 1.5 x 10^8 CFUs/mL after 24 hours in the presence of PCLS, in the absence of PCLS, the bacterial load of *P. aeruginosa* remained low and only reached 1.1 ± 0.2 x 10^5 CFUs/mL at the end of the incubation period (**Figure 4.4a**).

In the case of *E. faecium*, the growth of *P. aeruginosa* also fluctuated slightly in the same range during the first 4 hours. However, during the remaining period of incubation, the bacterial load of *P. aeruginosa* alone steadily increased while it decreased to 3.9 ± 0.5 x 10^3 CFUs/mL in the presence of PCLS and to 7.3 ± 4.2 x 10^3 CFUs/mL in the absence of PCLS when grown with *E. faecium* (**Figure 4.4b**).

With *S. mitis*, interestingly, the bacterial load of *P. aeruginosa* rapidly decreased within the first 4 hours, reaching 1.3 ± 1.0 x 10^4 CFUs/mL with PCLS and 1.7 ± 2.0 x 10^3 CFUs/mL without PCLS within the first 4 hours until it was undetectable by the end of the 24 hours of incubation (**Figure 4.4c**).

Finally, in the presence of *B. vulgatus,* the bacterial load of *P. aeruginosa* over time mirrored the bacterial load of *P. aeruginosa* grown alone. It fluctuated in the same range over the first four hours and reached similar bacterial loads of 1.6 ± 0.7

x 10^8 CFUs/mL with PCLS and 6.7 ± 7.0 x 10^7 CFUs/mL without PCLS at the end of the experiment (**Figure 4.4d**).

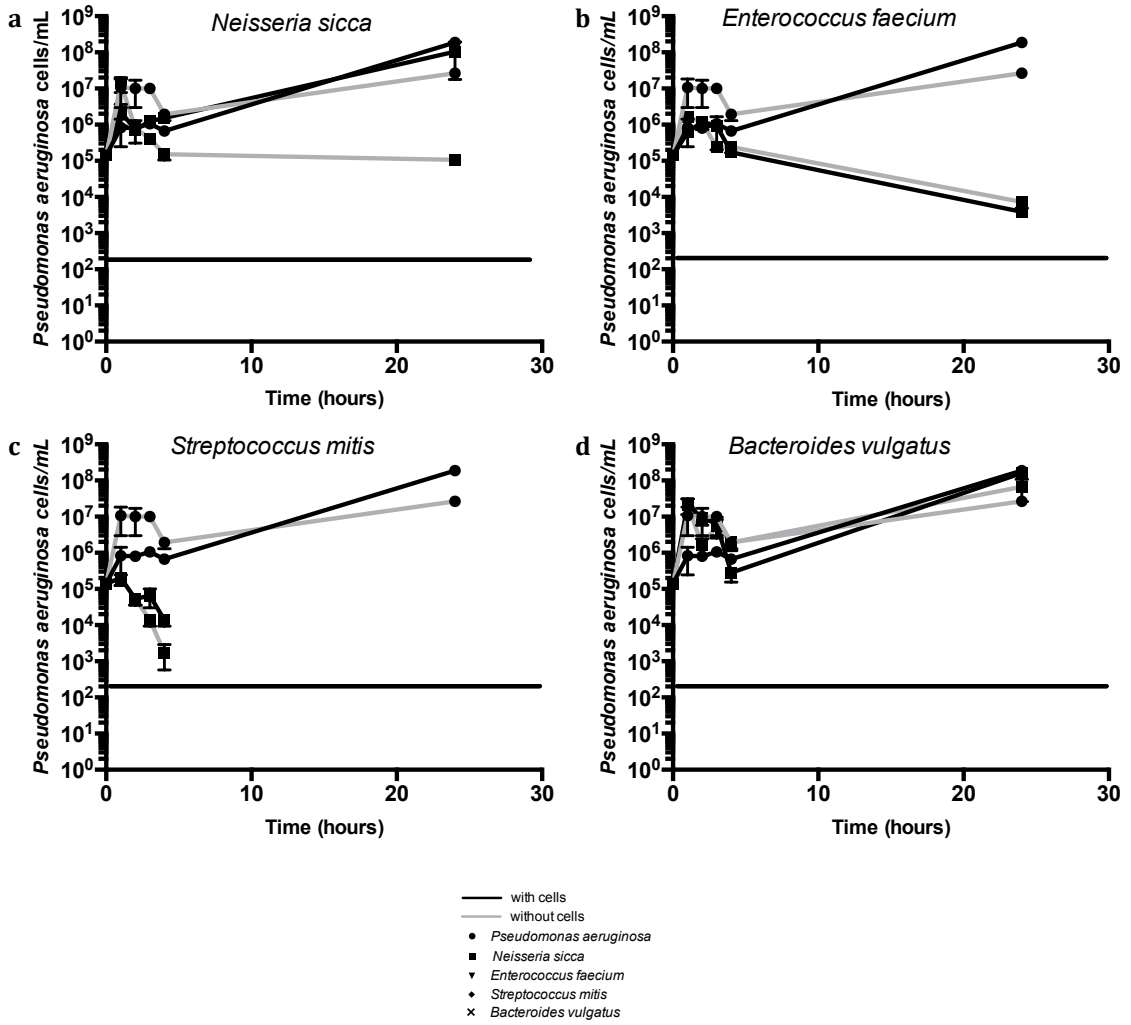

Figure 4.4 *P. aeruginosa* was inhibited within the first hours of exposure. *Neisseria sicca*, *Enterococcus faecium*, *Streptococcus mitis,* and *Bacteroides vulgatus* were incubated for 24 hours with or without PCLS after which *Pseudomonas aeruginosa* was added and grown for an additional 24 hours. The growth of *P.*

aeruginosa was measured every hour for 4 hours and at the 24 hour time point. The black line represents the limit of detection. Data is represented as mean with SD (n = 3 technical replicates).

To explore the mechanism of *P. aeruginosa* killing, the same assay was completed with heat-killed commensals (**Figure 4.5a**). I found that all the heat-killed commensals allowed *P. aeruginosa* to grow to the same level as when it grows alone, 2.1 ± 0.8 x 10^8 CFUs/mL. Indeed, in presence of *N. sicca, P. aeruginosa* grew to 2.6 ± 2.1 x 10^8 CFUs/mL. In presence of *E. faecium,* it reached 5.9 ± 8.0 x 10^8 CFUs/mL. Finally, when exposed to *S. mitis*, *P. aeruginosa* grew to 4.6 ± 5.4 x 10^8 CFUs/mL.

I also collected and filtered the supernatant of the PCLS incubated with the commensals. The killing activity of these supernatants was tested against *P. aeruginosa* to verify whether it was due to a direct interaction with the commensals or the release of a soluble factor (**Figure 4.5b**). When grown alone, *P. aeruginosa* grew to 3.3 ± 7.1 x 10^9 CFUs/mL. As seen in the first assay, *N. sicca* allowed *P. aeruginosa* to reach similar levels, 4.0 ± 2.8 x 10^8 CFUs/mL. By contrast, the bacterial load of *P. aeruginosa* was significantly reduced to 7.9 ± 7.3 x 10^3 CFUs/mL in presence of *E. faecium* and undetectable in presence of *S. mitis.*

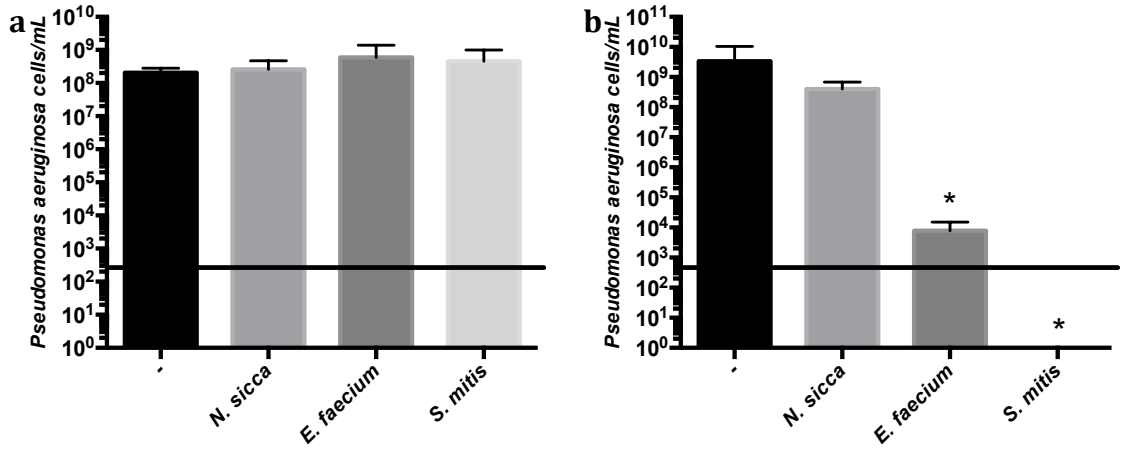

Figure 4.5 The killing effect was mediated by living bacteria secreting a soluble factor. (**a**) Heat-killed *Neisseria sicca*, *Enterococcus faecium*, and *Streptococcus mitis* were incubated for 24 hours with PCLS after which *Pseudomonas aeruginosa* was added. The bars represent the growth of *P. aeruginosa* in presence of the three heat-killed commensals and alone (-) after 24 hours of exposure. (**b**) *Neisseria sicca, Enterococcus faecium*, and *Streptococcus mitis* were incubated for 24 hours with PCLS. The supernatant was then collected and filtered. *Pseudomonas aeruginosa* was then grown for 24 hours in the supernatants. The bars represent the growth of *P. aeruginosa* in the supernatant of the commensals and alone (-) after 24 hours of exposure. Error bars represent the SD. The black line represents the limit of detection. Results were pooled from 3 independent experiments (n = 2 technical replicates). * represents $p < 0.05$ (Kruskal-Wallis test) compared to *P. aeruginosa* (-).

4.2.4 Bacterial isolates altered *P. aeruginosa*-induced PCLS cytokine profiles

As shown in the Detroit-562 cell model, bacterial isolates have immunomodulatory activity and lead to the secretion of various cytokines and chemokines by the host cells. To verify whether the cytokine profiles were similar between the Detroit-562 cell model and the PCLS model, I performed a Luminex assay on the supernatant of the PCLS in the following conditions: a) unstimulated; b) exposed only to the commensal strains described above; c) exposed to both the commensal strains and *Pseudomonas aeruginosa*; and, d) exposed to *Pseudomonas aeruginosa* alone (**Figure 4.6; Table A.4**).

Based on the cluster analysis, the pattern of cytokine expression mostly clustered based on the commensal present. Indeed, the profiles of the PCLS exposed to *S. mitis* or *S. mitis + P. aeruginosa* are similar and cluster together. The same is true for *E. faecium* and *E. faecium + P. aeruginosa.* However, the cytokines secreted in presence of *N. sicca + P. aeruginosa* and *B. vulgatus + P. aeruginosa* are more similar to the cytokines secreted in presence of *P. aeruginosa* alone rather than those secreted in presence of *N. sicca* and *B. vulgatus* respectively.

I also looked at the cytokines produced by the PCLS incubated in anaerobic conditions for 24 hours, either exposed to *P. aeruginosa* or unstimulated to verify that these incubations do not affect the cytokine profile of the PCLS (**Figure 4.6**). I found that the cytokine profiles clustered with aerobic incubations of *P. aeruginosa* and unstimulated PCLS respectively.

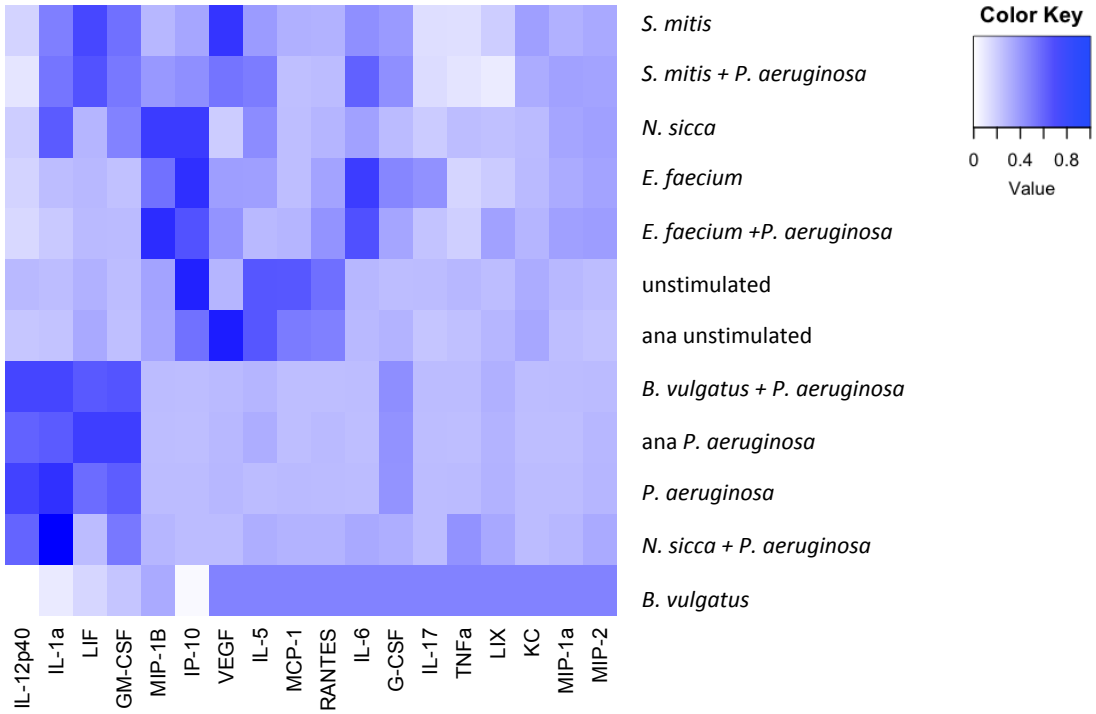

Figure 4.6 PCLS produced different cytokines in response to the bacteria they were exposed to. *Neisseria sicca*, *Enterococcus faecium*, *Streptococcus mitis*, and *Bacteroides vulgatus* were incubated for 24 hours with PCLS after which *Pseudomonas aeruginosa* was added. After 24 hours of exposure, the cytokines and chemokines secreted by the PCLS were measured using a Luminex multiplex assay (Eve technologies). The heatmap indicates the level of cytokines secreted by the PCLS exposed to the different bacteria or alone (unstimulated). "ana" indicates that the PCLS were incubated in the anaerobic chamber for 24 hours during the assay. The colour key indicates the normalized cytokine and chemokine values.

Of interest, IP-10 (**Figure 4.7**) was reduced by the presence of *P. aeruginosa*; alone as well as with *N. sicca* and *B. vulgatus.* Indeed, IP-10 was expressed to 290.4 pg/mL in unstimulated PCLS. The presence of *N. sicca* led to an upregulation of this chemokine to 410.4 pg/mL. In presence of *E. faecium* and *S. mitis* it reached 149.3 pg/mL, and 132.3 pg/mL respectively. The presence of *B. vulgatus* reduced IP-10 to 28 pg/mL. By contrast, the bacterial load of this cytokine dropped to zero when *P. aeruginosa* was present, whether alone or with *N. sicca* or *B. vulgatus.* In the presence of *E. faecium + B. vulgatus*, the cytokine was reduced to 73.3 pg/mL. Finally, with *S. mitis + P. aeruginosa,* the bacterial load reached 158 pg/mL.

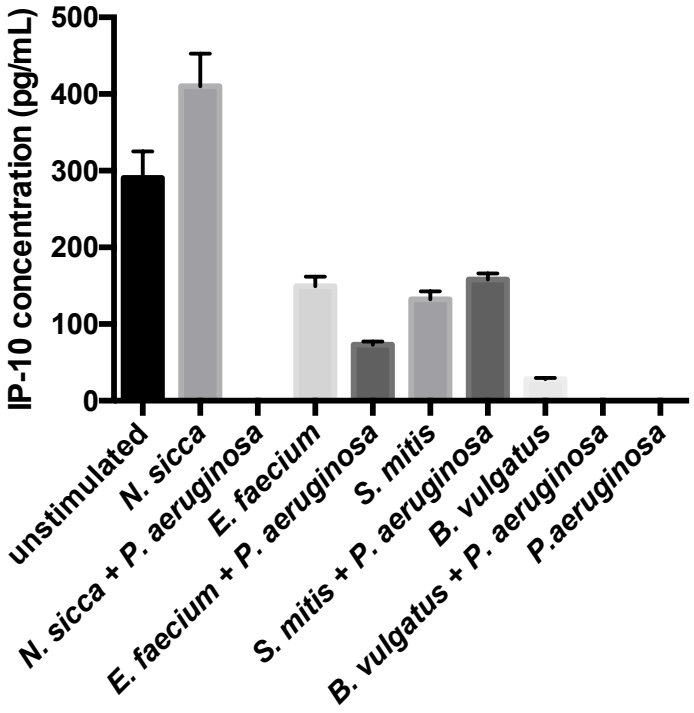

Figure 4.7 IP-10 was reduced in presence of *P. aeruginosa.* *Neisseria sicca*, *Enterococcus faecium*, *Streptococcus mitis*, and *Bacteroides vulgatus* were incubated for 24 hours with PCLS after which *Pseudomonas aeruginosa* was added. After 24 hours of exposure, the cytokines and chemokines produced by the PCLS were measured using a Luminex multiplex assay (Eve technologies). The bars represent the concentration of IP-10 produced by the PCLS exposed to the different bacteria or alone (n = 2 technical replicates).

The presence of the pathogen *P. aeruginosa* alone led to the upregulation of a number of cytokines (**Figure 4.8**). As in the Detroit-562 cell model, the concentration of IL-1α (**Figure 4.8a**) was upregulated from 1.2 pg/mL to 60.7 pg/mL. GM-CSF (**Figure 4.8b**) was upregulated from 7 pg/mL to 274.2 pg/mL. Finally, the concentration of G-CSF (**Figure 4.8c**) reached 226 pg/mL instead of 8.9 pg/mL.

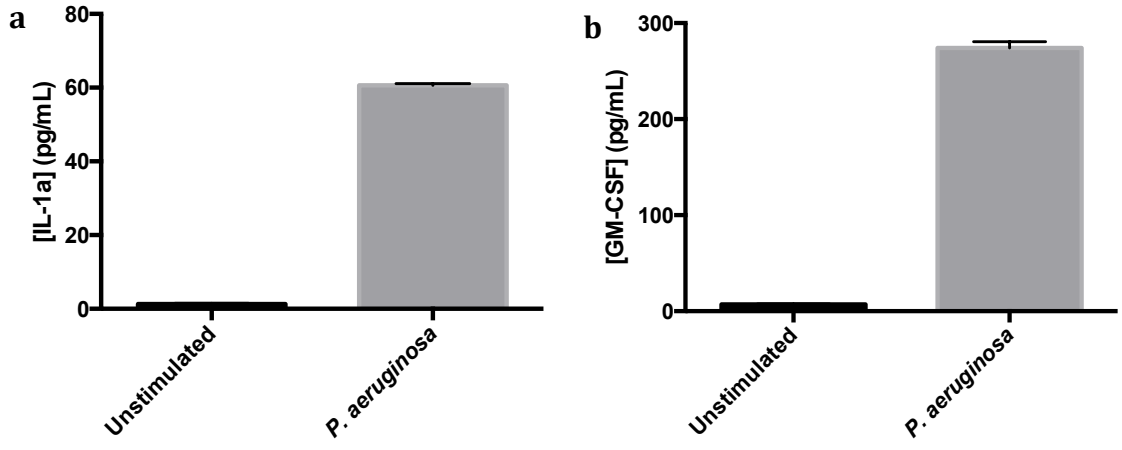

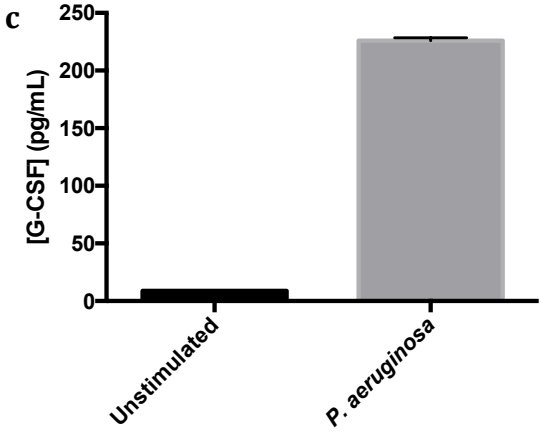

Figure 4.8 *P. aeruginosa* increased pro-inflammatory cytokines. PCLS were incubated with *P. aeruginosa*. After 24 hours of exposure, the cytokines and chemokines produced by the PCLS were measured using a Luminex multiplex assay (Eve technologies). The bars represent the concentration of IL-1α, GM-CSF, and G-CSF produced by the PCLS exposed to *P. aeruginosa* or alone (n = 2 technical replicates).

The presence of *E. faecium* on the other hand, prevented this upregulation (**Figure 4.9**). This is particularly notable in the case of IL-1α, which was upregulated from 1.2 pg/mL to 60.7 pg/mL by *P. aeruginosa* while the presence of *E. faecium* kept it at 6.4 pg/mL by itself and at 2.9 pg/mL with *P. aeruginosa.*

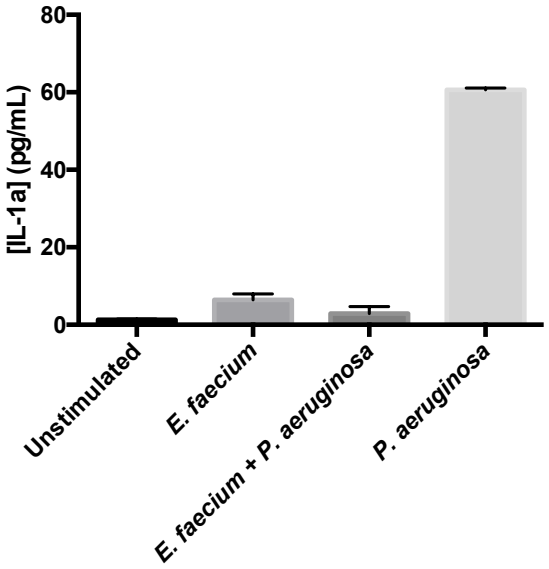

Figure 4.9 *E. faecium* did not increase pro-inflammatory cytokines. *Enterococcus faecium* was incubated for 24 hours with PCLS after which *Pseudomonas aeruginosa* was added. After 24 hours of exposure, the cytokines and chemokines produced by the PCLS were measured using a Luminex multiplex assay (Eve technologies). The bars represent the concentration of IL-1α produced by the PCLS exposed to *E. faecium, E. faecium* + *P. aeruginosa, P. aeruginosa* or alone (n = 2 technical replicates).

The presence of *S. mitis* led to the upregulation of a couple of chemokines that were downregulated by the PCLS exposed to *P. aeruginosa* (**Figure 4.10**). For instance, KC (**Figure 4.10a**) was expressed at a concentration of 764.6 pg/mL by unstimulated PCLS, and became undetectable after incubation with *P. aeruginosa*. KC increased to 3,506.9 pg/mL with *S. mitis* and to 2,641.7 pg/mL with *S. mitis + P.*

aeruginosa. Finally, the concentration of MIP-1β (**Figure 4.10b**) was increased from 35.8 pg/mL to 71.7 pg/mL in presence of *S. mitis* alone and to 105.5 pg/mL in presence of *S. mitis + P. aeruginosa* while it was not detectable in the presence of *P. aeruginosa* alone.

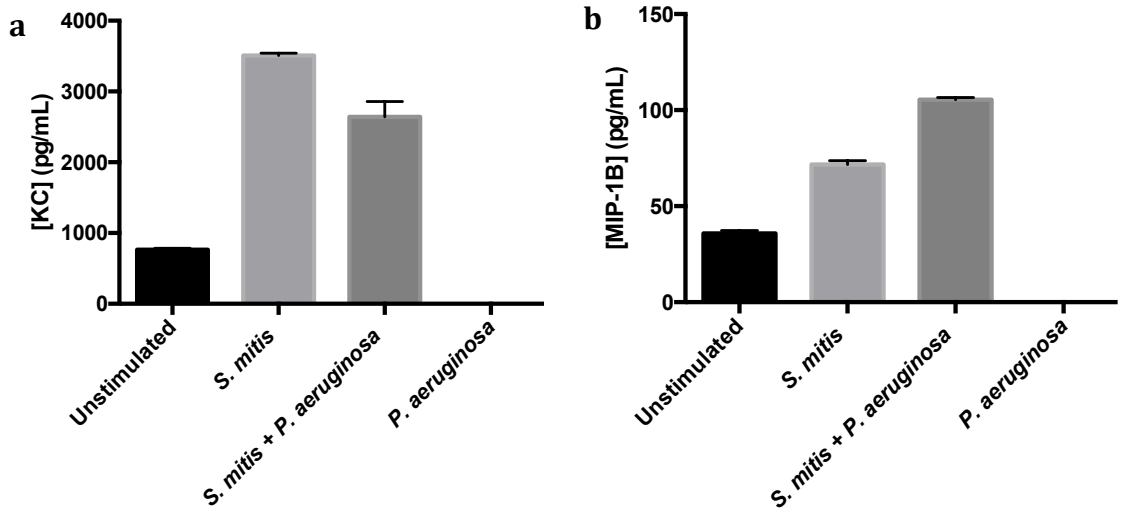

Figure 4.10 *S. mitis* increased innate immune cells chemoattractants. *Streptococcus mitis* was incubated for 24 hours with PCLS after which *Pseudomonas aeruginosa* was added. After 24 hours of exposure, the cytokines and chemokines produced by the PCLS were measured using a Luminex multiplex assay (Eve technologies). The bars represent the concentration of KC and MIP-1β produced by the Detroit-562 exposed to *S. mitis, S. mitis* + *P. aeruginosa, P. aeruginosa* or alone (n = 2 technical replicates).

4.3 Discussion

4.3.1 PCLS remained viable and did not influence the growth of the bacteria

In our assay, the PCLS were exposed to bacteria for 48 hours. Since I was looking for host-bacteria interactions, it was important that the cells composing the PCLS remain viable for the duration of the experiment. Therefore, I used a viability assay over 8 days to verify that the PCLS survived (**Figure 4.1**). Based on the results of this assay, I can assert that the PCLS were still viable eight days after slicing. This assured us that the bacteria could interact with host cells composing the PCLS and that these murine cells are metabolically active and capable of secreting immune factors for the duration of the experiment.

I also verified whether the PCLS affected the growth of the commensals (**Figure 4.2**). I found that *N. sicca* reached similar bacterial loads within 24 hours in the presence or absence of PCLS. However, it reached a higher bacterial load in the presence of PCLS within 48 hours. In the case of *E. faecium,* its bacterial load was ten-fold higher at both time points in the presence of PCLS. These two commensals grew better with the PCLS. It is possible that the PCLS provide nutrients for these bacteria, which would explain this increased growth.

S. mitis reached similar bacterial loads during the first 24 hours of growth in the presence or absence of the PCLS. However, it was undetectable in both conditions by the end of the experiment. This might be due to a lack of nutrients or the secretion of an autolysin molecule.

B. vulgatus is able to grow 24 hours with the PCLS but it was also undetectable by the end of the experiment. The reason was clear in this case however: *B. vulgatus* is an anaerobe and the second half of the experiment took place in aerobic conditions, an environment in which this bacterium was unable to survive.

4.3.2 *E. faecium* and *S. mitis* inhibited the growth of *P. aeruginosa* through the active secretion of a soluble factor

When completing similar assays to the Detroit-562 cells, I found consistent results (**Figure 4.3**). *N. sicca* showed very little inhibitory activity against *P. aeruginosa* in the presence of PCLS, but did reduce *P. aeruginosa* growth in the absence of PCLS. In this case, it seems that the presence of the host cells is reducing the inhibitory capacity of the commensal. In this case, the PCLS could have an effect on the environment that reduces the efficacy of this commensal against *P. aeruginosa.* But the main finding, where this commensal is concerned, is that its effects were negligible and tended to vary from experiment to experiment, be it in the Detroit-562 cell model or the PCLS model.

In the cases of both *E. faecium* and *S. mitis,* on the other hand, I got rather promising results when compared to the Detroit-562 cell model. Indeed, *E. faecium* led to a 4-fold reduction in the bacterial load of *P. aeruginosa* at the 24 hour mark, both in the presence and the absence of PCLS. *S. mitis* had the most dramatic effect,

completely killing off *P. aeruginosa* until it was mostly undetectable by the end of the experiment.

The last commensal, *B. vulgatus* had shown some effects in the Detroit-562 model. However, these effects were lost in this PCLS model. The presence of *B. vulgatus* did not prevent the growth of *P. aeruginosa* for the duration of the experiment. This might be due to the PCLS not surviving the incubation period in anaerobic conditions. However, considering that the PCLS still secreted cytokines and chemokines at the end of the experiment, as shown with the Luminex multiplex assay, I concluded that the PCLS were still viable but that *B. vulgatus* didn't show any effect against *P. aeruginosa* in this model.

I measured the bacterial load of *P. aeruginosa* within the first four hours of exposure to the commensals and the PCLS to determine the dynamics between the different bacteria (**Figure 4.4**). I found that, in the presence of *N. sicca, E. faecium,* and *B. vulgatus, P. aeruginosa* growth during the first four hours of exposure was similar to that of *P. aeruginosa* alone. *N. sicca* and *B. vulgatus* had no effect on the growth of *P. aeruginosa* throughout the experiment, which reached bacterial loads similar to the bacterial load of *P. aeruginosa* alone. In the case of *E. faecium,* while it had no effect during the first four hours, there was then a decrease in the bacterial load *P. aeruginosa* during the following 20 hours. *S. mitis* inhibited *P. aeruginosa* from the beginning, which continued to decrease until it was undetectable at the end of the experiment.

To rule out a simple interaction of the Pattern Recognition Receptors (PRRs) expressed by the different cells composing the PCLS with the outer membrane of the bacteria, I determined that heat-killed bacteria had the same effect as live bacteria. The assay was repeated in the same way as with the live bacteria (**Figure 4.5a**). I found that the inhibitory phenotype was lost and *P. aeruginosa* grew to similar levels, whether alone or in presence of the different heat-killed commensals. From this, I can conclude that the bacteria are active participants in the phenotype and that it is not simply their presence in the cell culture medium that leads to the inhibition of *P. aeruginosa*.

Once this was established, it was important to verify if the observed phenotype was the result of a direct interaction of *P. aeruginosa* with either the commensals or the PCLS. To do so, filtered supernatant of the PCLS exposed to the different commensals was used as growth medium for *P. aeruginosa* (**Figure 4.5b**). *N. sicca* filtrates didn't have an effect on the bacterial load of *P. aeruginosa* while *E. faecium* filtrates prevented *P. aeruginosa* from growing, and *S. mitis* filtrates completely killed *P. aeruginosa*. The phenotype was therefore surely driven by one or several soluble factors released by either the PCLS or the commensal bacteria.

4.3.3 Bacterial isolates altered *P. aeruginosa*-induced PCLS cytokine profiles

PCLS contain a number of different cell types, including epithelial cells as well as immune cells. As such, there is greater potential for cytokine production compared to Detroit-562 cells in response to bacterial challenge. While a number of

cytokines released by the precision-cut lung cells was more or less similar to those released by the Detroit-562 cells, it is not relevant to compare the two because Detroit-562 cells are of human origin while the PCLS are obtained from mice.

Cluster analysis revealed that cytokine profiles from PCLS incubated with commensals that induce killing of *P. aeruginosa* clustered separately from commensals that did not (**Figure 4.6**). *E. faecium* and *S. mitis* induced cytokine expression that clustered together, whether or not *P. aeruginosa* was present in the sample. These commensals blocked the growth of *P. aeruginosa* within the first few hours of exposure, it is therefore understandable that *P. aeruginosa* did not influence the cytokines released by the PCLS and the profile was dominated by the cytokines released in response to the commensal bacteria. *N. sicca* and *B. vulgatus,* which did not inhibit *P. aeruginosa,* showed similar clustering to *P. aeruginosa* alone. This suggests that *P. aeruginosa* took over the system rapidly and dominated the cytokine response.

Additionally, I assessed the cytokines released by the PCLS that had been exposed to anaerobic conditions for 24 hours. I found that the patterns of cytokine expression of unstimulated PCLS and unstimulated anaerobic PCLS clustered together and the only notable difference was an increased expression of VEGF in the anaerobic PCLS. Since VEGF is induced by hypoxia (Hlatky *et al.,* 1996), this result is understandable. The same is true for anaerobic PCLS exposed to *P. aeruginosa,* which had an almost identical cytokine profile as the PCLS that never experienced hypoxia.

One analyte was of particular interest (**Figure 4.7**). IP-10 is a chemokine that has been shown to have direct antibacterial activity against specific pathogens such as *Escherichia coli* and *Listeria monocytogenes* (Yung and Murphy, 2012; Cole *et al.,* 2001). Of interest, IP-10 is involved in the innate defense against *P. aeruginosa* in the cornea, which is influenced by the ocular microbiota (Yoon *et al.,* 2013). It was expressed at high levels in unstimulated PCLS while the presence of *P. aeruginosa* led to a decrease of this chemokine to the point where it was undetectable. IP-10 was expressed in presence of all the commensals. However, the presence of *P. aeruginosa* with *N. sicca* and *B. vulgatus* completely abrogated IP-10 expression. With *E. faecium,* the expression of this chemokine was slightly decreased when *P. aeruginosa* was present, whereas, *S. mitis* maintained IP-10 to similar levels whether or not *P. aeruginosa* was there. These observations matched the inhibitory activity of the commensals, where *P. aeruginosa* was not inhibited by the first two, while *E. faecium* decreased the bacterial load of *P. aeruginosa* and *S. mitis* completely inhibited it. Of interest for future studies is the fact that the presence of *P. aeruginosa* prevents the secretion of IP-10 in the first two cases, i.e. incubations with *N. sicca* and *B. vulgatus*. The results of our study hint at the possibility that *P. aeruginosa* has developed strategies to prevent the secretion of IP-10 precisely because this chemokine plays a role in its inhibition. Although, more experiments are needed to assess the exact activity of IP-10 against *P. aeruginosa* before any such assertion could be made.

In terms of the specific cytokines and chemokines released in response to the different bacteria, the results are fairly similar to the Detroit-562 cell model. Alone, *P. aeruginosa* triggered the release of pro-inflammatory cytokines, such as IL-1α, as well as the release of cytokines involved in innate immune cell initiation and amplification, such as G-CSF and GM-CSF (Metcalf, 1985) (**Figure 4.8**). This shows that the system was getting ready to fight against this invading pathogen and was mounting an inflammatory immune response, as well as priming innate immune cells.

When *E. faecium* was introduced, I had more of an anti-inflammatory effect (**Figure 4.9**). In the presence of this pathogen, none of the pro-inflammatory cytokines released by *P. aeruginosa* were upregulated. As explored in the Detroit-562 cell model, the presence of this commensal could protect the host from a damaging hyper-inflammatory response.

Similarly, the presence of *S. mitis*, as in the Detroit-562 cell model, generates the upregulation of a number of cytokines and chemokines, including KC and MIP-1β (**Figure 4.10**). These chemokines are involved in the recruitment of innate immune cells, in particular neutrophils, to the site of infection (Kobayashi, 2006; Wolpe and Cerami, 1989). The presence of *S. mitis* in the respiratory tract could lead to an influx of neutrophils and other innate immune cells, which would be able to inhibit *P. aeruginosa* when it is introduced.

As stated in the previous chapter, the immune response to *P. aeruginosa* is dependent on the secretion of pro-inflammatory cytokines, such as IL-1 and GM-CSF

(Kube *et al.,* 2001), which I also observed both in the Detroit-562 cell model and the PCLS model. Moreover, the hyper-inflammatory response to *P. aeruginosa* in susceptible individuals causes lung damage (Pierrakos *et al.,* 2012; Wolbeling *et al.,* 2011). Therefore, the anti-inflammatory effects of *E. faecium* are of great interest and could be exploited to prevent the development of symptoms. Finally, the clearance of *P. aeruginosa* both in mice and in humans is highly dependent on innate immune cells and phagocytosis. I have shown here that stimulation of PCLS by *S. mitis* led to the secretion of chemokines involved in innate immune cell recruitment. This commensal could therefore also be beneficial *in vivo.* This interaction has been observed elsewhere. In a 2017 study, Song *et al.* showed that co-infecting mice with *P. aeruginosa* and *S. mitis* led to decreased lung inflammation, possibly via the TLR-4 signaling pathway.

4.4 Conclusions

In this chapter I established a murine PCLS model, which served as a proxy for an *in vivo* model. I found that *E. faecium* and *S. mitis* had similar effects as in the Detroit-562 cell model, preventing the growth of *P. aeruginosa* and completely killing it, respectively. The other two commensals, *N. sicca* and *B. vulgatus,* showed very little inhibitory activity.

The characteristics of the observed phenotype reflected those found in the Detroit-562 cell model, with the inhibitory activity being dependent on the presence of living bacteria during the priming period while a direct interaction with bacteria

and the tissue is not essential to inhibit *P. aeruginosa*. The time frame of inhibition was also similar, with *E. faecium* and *S. mitis* showing inhibitory activity within the first few hours of exposure.

Finally, the patterns of cytokine expression reflected the inhibitory phenotype. That is, they were dominated by the cytokine response to a commensal when the latter was able to inhibit *P. aeruginosa* or the cytokine response was dominated by *P. aeruginosa* when the latter survived in the presence of the commensal. A few products of potential interest emerge from these assays: IP-10 might be released by the cells and exercise direct bactericidal activity against *P. aeruginosa*. Neutrophil chemoattractants are released by *S. mitis*, potentially creating a hostile environment and thereby inhibiting the growth of *P. aeruginosa*.

While some of these results further clarify the interactions between the host cells, the commensal bacteria, and the pathogen, the exact mechanism of inhibition of *P. aeruginosa* remains unclear. Further experiments need to be done to better understand how *P. aeruginosa* is being killed in these models.

Chapter 5 Mouse models and mechanistic studies

5.1 Rationale

The two models developed during this project, the Detroit-562 cell model and the murine PCLS model, provide insights into the colonization resistance and the immunomodulatory activities of the commensals of interest. However, they are still simplified models and do not provide the complexity of a complete living organism. Indeed, an *in vivo* model integrates the many different systems necessary to keep the animal alive as well as a complete and functional immune system and a diverse microbiome. All these systems can not be accounted for in the *in vitro* tissue culture models. I, therefore, attempted to develop an *in vivo* model of mouse infection with our bacteria of interest. To do so, I tested the effects of both the pathogen, *P. aeruginosa*, and the most promising commensal, *S. mitis*, in separate models of upper and lower respiratory tract infections. I monitored the mice for signs of infection, measured the bacteria load in different organs, and observed the innate immune cell recruitment to the lungs and nasal tissue.

The *in vivo* model did not yield any satisfactory results. I therefore focused on only the first two models in attempting to characterize the potential mechanism behind the observed inhibitory activity. To differentiate whether the killing of *P. aeruginosa* was mediated by the bacteria or the host cells, I primed the PCLS both *in vitro* and *in vivo*, and measured their inhibitory potential. Moreover, bearing in mind that *Streptococcus* species release hydrogen peroxide as an antibacterial

mechanism, notably against *P. aeruginosa* (Whiley *et al.,* 2015), I determined whether the inhibitory potential of *S. mitis* had something to do with this chemical.

Finally, bacteria identified in the screen as potentially immunomodulatory were further characterized by whole genome sequencing. These genomes were examined for genes encoding antibiotic resistance, potential virulence factors and pathways involved in secondary metabolite production.

5.2 Results

5.2.1 Mice tolerated and cleared *S. mitis* in the respiratory tract

In the initial design of the experiment, *S. mitis* was to be used as a potential protective probiotic for respiratory infections. For this reason, *S. mitis* was tested to ensure this commensal would not contribute to illness or systemic infection to the mice. I therefore infected mice with 2.0 x 10^7 CFUs/mL of *S. mitis* in the lungs and monitored them for three days. The mice did not show any signs of infection, maintained constant weight over the period of infection (**Figure 5.1a**), and the bacterial strain was undetectable in the nose, lungs, or spleen of the mice at the end of the experiment.

I repeated a similar experiment with an intranasal infection using a dose of 6.0 x 10^8 CFUs/mL of *S. mitis.* The mice showed minimal weight loss (**Figure 5.1b**) over the two days of infection. Their weight went from 19.8 grams to 18.9 grams for the first mouse, or a loss of 4.5% of the body weight, and from 18.8 grams to 18.0 grams for the second mouse, or a loss of 4.3% of the body weight. However, the mice

did not appear moribund and *S. mitis* was undetectable in the lungs, nose, and spleen of the mice.

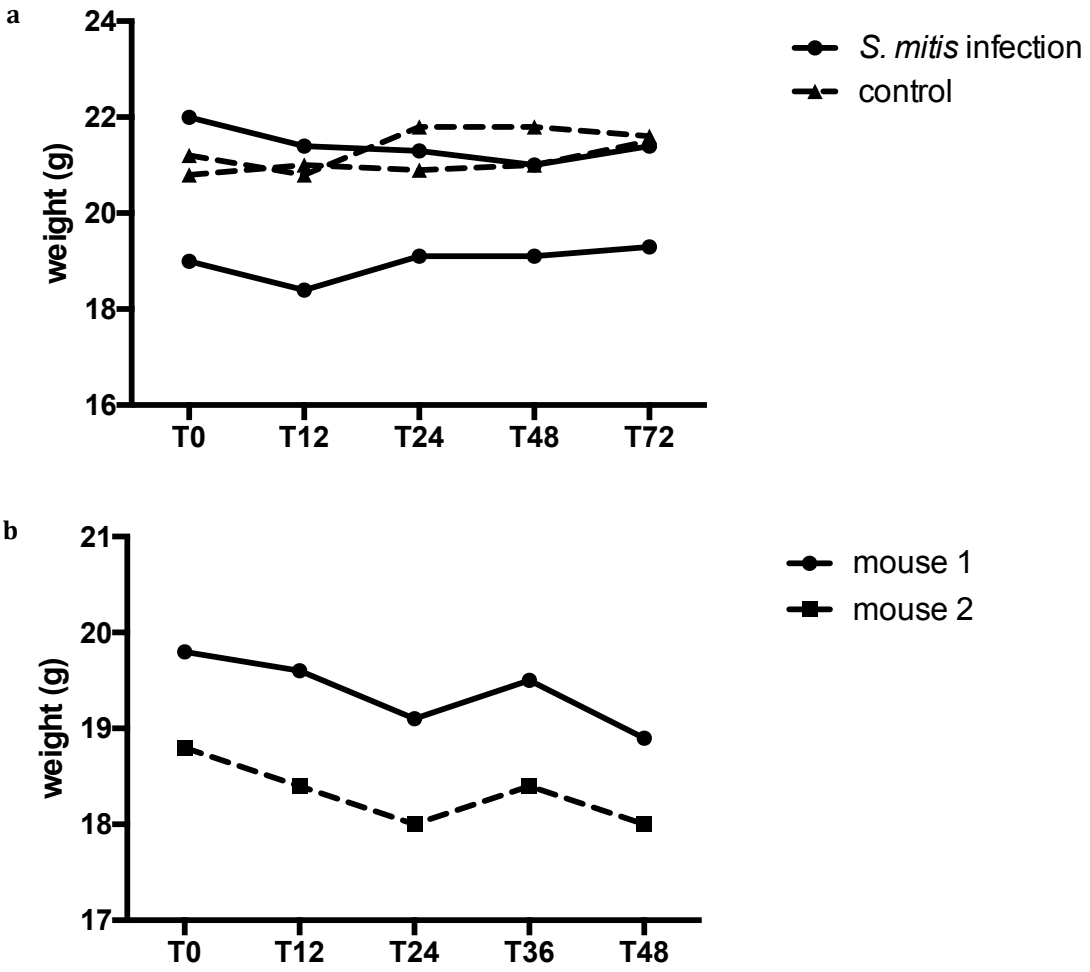

Figure 5.1 Mice infected with *S. mitis* maintained a constant weight. (**a**) Two SPF mice were infected in the lower respiratory tract with 2.0 x 10^7 CFUs/mL of *S. mitis*. Two other SPF mice were used as controls and not infected. (**b**) Two SPF mice were infected in the upper respiratory tract with 6.0 x 10^8 CFUs/mL of *S. mitis*. The mice were weighed every 12 hours for 2 to 3 days. They were then sacrificed and

the spleen, lungs, and nasal tissue were collected. No *S. mitis* was detected in any of the tissues. Each dot represents the weight of a mouse at the indicated time point.

5.2.2 Upper and lower respiratory tract *P. aeruginosa* infections had disparate effects

To develop a mouse model of infection, it was necessary to verify the impact of a *P. aeruginosa* infection either in the upper respiratory tract or the lower respiratory tract. *P. aeruginosa* is not a pathogen known to infect mice, as it is either rapidly cleared or causes acute sepsis and death, depending on the strain and dosage (Bragonzi, 2010). Consequently, there has been some limited success in developing mouse models of infection using different strains of this pathogen (Bragonzi, 2010; Fothergill *et al.,* 2014). Still, I tested whether our strain of interest, *P. aeruginosa* PA14, would cause mice to develop symptoms of infection. I obtained disparate results depending on whether *P. aeruginosa* was introduced in the lower or the upper respiratory tract (**Figures 5.2**). Indeed, mice receiving a 2.0 x 10^7 CFUs/mL dose of *P. aeruginosa* directly in the lungs very developed symptoms at a rapid rate. In less than 24 hours, four of the five mice within the experiment were moribund and had lost significant weight, while the fifth had already died. On average, the mice weighed 20.28 grams at the beginning of the experiment and 18.80 grams before they were sacrificed, representing a significant 7.3% loss in body weight (**Figure 5.2a**). When the mice were euthanized, their lungs were found to contain blood. The lungs, nasal tissue, and spleens of these mice were collected. *P.*

aeruginosa was found at elevated levels in all these tissues, most importantly in the spleen where it was found at a bacterial load of 9.4 ± 13.8 x 10^5 CFUs/mL. Moreover, the bacterial load of *P. aeruginosa* in both the lungs and the nasal tissue was increased compared to the inoculum, reaching 1.1 ± 1.9 x 10^8 CFUs/mL in the lungs and 6.3 ± 3.8 x 10^8 CFUs/mL in the nose (**Figure 5.2b**).

By contrast, when the mice were exposed to the same pathogen, 2.0 x 10^7 CFUs/mL of *Pseudomonas aeruginosa*, in the upper respiratory tract, they did not show any signs of infection. All mice within the experiment maintained a constant weight (**Figure 5.2c**). In addition, *P. aeruginosa* was undetectable in all of the tissues collected after three days of infection.

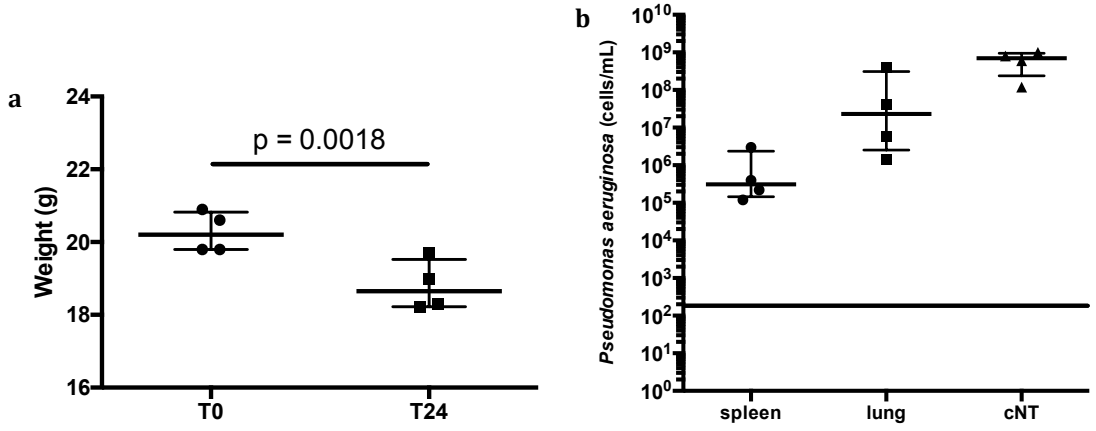

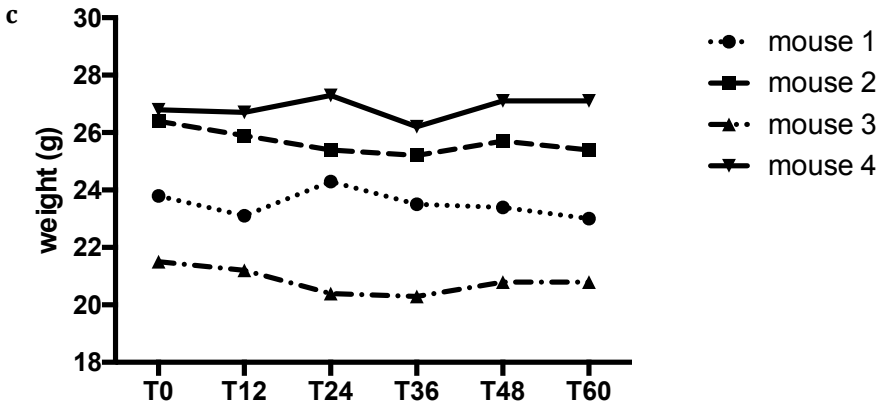

Figure 5.2 Mice infected with *P. aeruginosa* displayed disparate symptoms. (**a** and **b**) Five SPF mice were infected with 2.0 x 10^7 CFUs/mL of *Pseudomonas aeruginosa* in the lungs. After 24 hours, one mouse had died (data excluded) and the four other were moribund. Therefore, the mice were weighed, sacrificed and the spleen, lungs, and nasal tissue were collected, homogenized, and plated on PIA. (**a**) Each dot represents the weight of a mouse (n = 4) with the mean and quartiles. The p value was obtained through an unpaired t test. (**b**) Each dot represents the cell density of *P. aeruginosa* in each mouse (n = 4) at the specified site with the mean and quartiles. The black line represents the inoculum. (**c**) Four SPF mice were infected intranasally with 2.0 x 10^7 CFUs/mL of *Pseudomonas aeruginosa*. The mice were weighed every 12 hours for 3 days. They were then sacrificed and the spleen, lungs, and nasal tissue were collected. No *P. aeruginosa* was detected in any of the tissues. Each dot represents the weight of a mouse (n = 4) at the indicated time point.

5.2.3 No innate immune cell influx was detected in the lungs of mice with an upper respiratory tract *P. aeruginosa* infection

To tease apart the effects of the bacteria on the innate immune response in the lungs and nasal tissue of the mice, bronchioalveolar lavages and nasal washed were collected from healthy mice as well as the mice infected intranasally with 2.0 x 10^7 CFUs/mL of *Pseudomonas aeruginosa.* Microscope slides of the cells present in these lavages were then prepared using a cytospin and HEMA stained (**Figures 5.3**). I found that there were similar levels of innate immune cells present in the lungs of healthy mice (**Figure 5.3a**) and mice infected with *P. aeruginosa* (**Figure 5.3b**). Moreover, the majority of the cells present were mononuclear. Very few immune cells were identified in the nasal wash cytospins (**data not shown**).

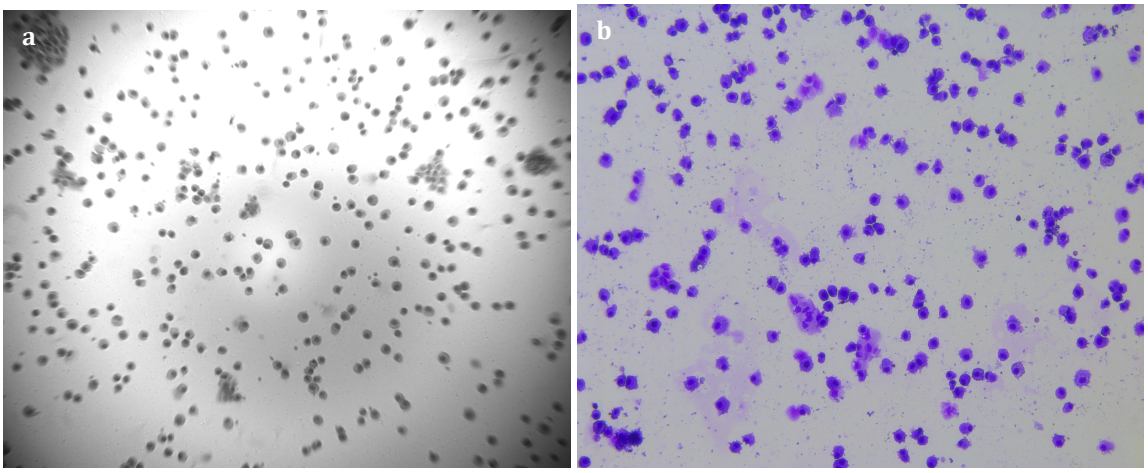

Figure 5.3 Mice infected with *P. aeruginosa* did not display an influx of innate immune cells. A bronchioalveolar lavage was obtained from a healthy mouse (**a**) and from a mouse after a 3-day *P. aeruginosa* infection (**b**). The cells were then

spotted on a microscope slide using a cytospin. The cells were then HEMA stained and observed under a bright-light microscope (x100).

5.2.4 The PCLS did not directly inhibit *P. aeruginosa*

Based on the results from the two *in vitro* models, I hypothesized that the inhibition of *P. aeruginosa* was either mediated by the commensal bacteria with assistance from the host cells, or by the host cells after being primed by the presence of the different commensals. To test these alternatives, I used two different methods to prime the PCLS, one *in vitro* (**Figure 5.4a**) and one *in vivo* (**Figure 5.4b**). I then measured whether the inhibitory potential of these PCLS had been increased by the priming.

To start with, I incubated the PCLS with *E. faecium* or *S. mitis*, washed and then incubated the PCLS with antibiotics. An additional washing step was performed followed by the measurement of the killing activity of these washed PCLS against *P. aeruginosa* (**Figure 5.4a**). I found that the washed PCLS did not retain the inhibitory phenotype imparted by the commensals. Indeed, whereas in the previous assay, the presence of *E. faecium* had reduced the bacterial load of *P. aeruginosa* from 1.9 ± 0.3 x 10^8 CFUs/mL to 3.9 ± 0.5 x 10^3 CFUs/mL, with the washed PCLS, the *E. faecium* had no effect on *P. aeruginosa*, which remained at 6.0 ± 2.0 x 10^7 CFUs/mL. Similarly, with *S. mitis*, while in the previous assay *P. aeruginosa* had been undetectable in the presence of the commensal, it grew to 3.4 ± 5.4 x 10^8 CFUs/mL when the PCLS were washed.

I also primed the PCLS *in vivo* by inoculating mice with *S. mitis* and obtaining PCLS from these mice three days later (**Figure 5.4b**). The full assay with all the commensals was repeated with these primed PCLS. Minimal differences were detectable between the primed and normal PCLS. The bacterial load of *P. aeruginosa* reached 1.9 ± 0.3 x 10^8 CFUs/mL in the presence of normal PCLS and 7.3 ± 1.2 x 10^7 CFUs/mL in the presence of primed PCLS. With *N. sicca, P. aeruginosa* grew to 1.1 ± 1.5 x 10^8 CFUs/mL in the presence of normal PCLS while it was decreased to 3.8 ± 3.6 x 10^6 CFUs/mL in the presence of primed PCLS. The bacterial load of *P. aeruginosa* was 3.9 ± 0.5 x 10^3 CFUs/mL in the presence of *E. faecium* and normal PCLS and maintained approximately the same bacterial load in the presence of primed PCLS, reaching 2.5 ± 0.3 x 10^3 CFUs/mL. With *S. mitis, P. aeruginosa* was undetectable in both conditions. Finally, in the presence of *B. vulgatus,* the bacterial load of *P. aeruginosa* was 1.6 ± 0.7 x 10^8 CFUs/mL and 9.3 ± 4.1 x 10^7 CFUs/mL in presence of normal and primed PCLS respectively.

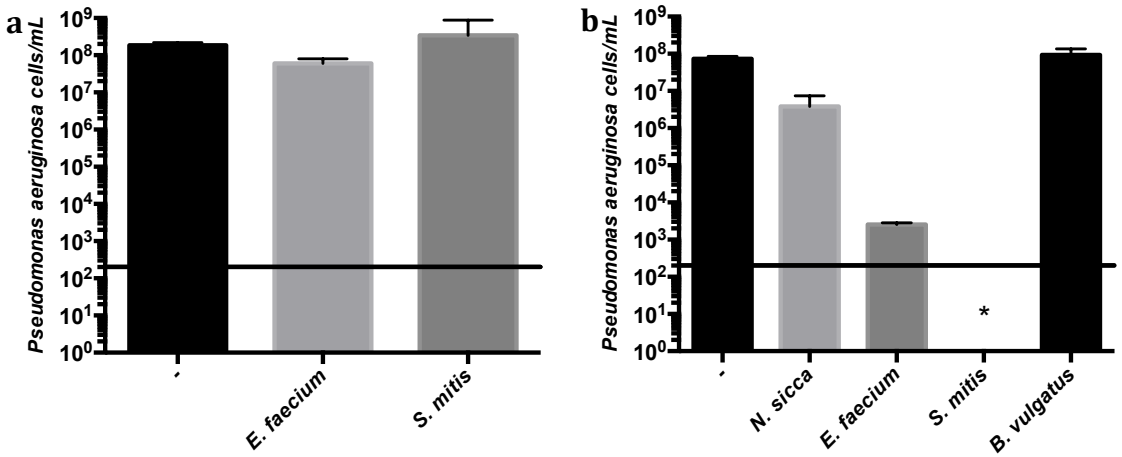

Figure 5.4 PCLS were not sufficient to mediate the inhibitory activity. (**a**) Two commensal bacteria, *Enterococcus faecium*, and *Streptococcus mitis* were incubated for 24 hours with murine PCLS. The supernatant was then removed and the PCLS were washed five times with PBS. They were then incubated for three hours with DMEM containing Penicillin and Streptomycin to kill any remaining bacteria. The media was removed, the PCLS were washed five times, and the media was replaced with DMEM containing no antibiotics. *Pseudomonas aeruginosa* was added to the supernatant. (**b**) Two SPF mice were infected intranasally with 2.0 x 10^7 of *S. mitis*. After three days, they were euthanized and PCLS were generated from these mice. Four commensal bacteria, *Neisseria sicca*, *Enterococcus faecium*, *Streptococcus mitis*, and *Bacteroides vulgatus* were incubated for 24 hours with these primed murine PCLS after which *Pseudomonas aeruginosa* was added. The bars represent the cell density of *P. aeruginosa* in presence of the washed slices previously exposed to the two commensals (**a**) or of the primed PCLS previously exposed *in vivo* to *S. mitis* and the commensals (**b**). The black line represents the limit of detection. Error bars represent the SD. (n = 3). * represents $p < 0.05$ (Kruskal-Wallis test) compared to *P. aeruginosa* (-).

5.2.5 Hydrogen peroxide participated in the elimination of *P. aeruginosa*

One of the potential mechanisms of the inhibitory activity of *S. mitis* against *P. aeruginosa* is the release of hydrogen peroxide (Whiley *et al.,* 2015). Catalase transforms hydrogen peroxide into oxygen and water (Chelikani *et al.,* 2004).

Therefore, the addition of catalase to the medium removes the hydrogen peroxide present. I repeated the assay with different concentrations of catalase added to the growth medium between the incubation with *S. mitis* and the addition of *P. aeruginosa* (**Figure 5.5**). I found that ten units/mL of catalase had no impact on the inhibitory activity of *S. mitis,* as *P. aeruginosa* remained undetectable. The addition of 20, 50, and 100 units/mL, however, allowed *P. aeruginosa* to grow to 1.6 ± 0.5 x 10^3 CFUs/mL, 1.5 ± 0.6 x 10^3 CFUs/mL, and 2.5 ± 1.2 x 10^3 CFUs/mL respectively.

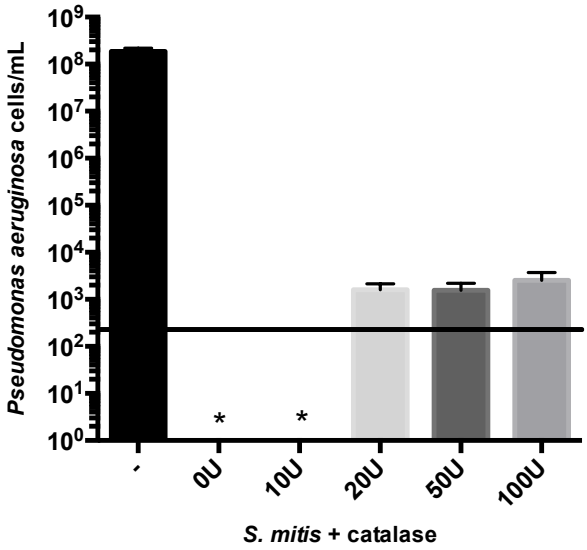

Figure 5.5 Catalase reduced but did not inhibit the killing capacity of *S. mitis.* *Streptococcus mitis* was incubated for 24 hours with murine PCLS after which different concentrations of catalase were added to the medium. *Pseudomonas aeruginosa* was then added. The bars represent the growth of *P. aeruginosa* in the presence of *S. mitis* and catalase, and alone (-). The black line represents the limit of detection. Error bars represent the SD. (n = 3). * represents $p < 0.05$ (Kruskal-Wallis test) compared to *P. aeruginosa* (-).

5.2.6 The genomes of the bacteria revealed antimicrobial resistance genes, virulence factor genes, and secondary metabolite pathways

Analyzing the genome of bacterial strains can aid in understanding their potential antimicrobial activity against *P. aeruginosa*. With this in mind, the genomes of *N. sicca, E. faecium, S. mitis, B. vulgatus,* and *P. aeruginosa* were extracted. These genomes were sequenced using Next Generation Sequencing Technology specifically Illumina Sequencing. I followed a series of steps to assess the quality of the raw reads and draft genomes after assembly. Trimming of low quality bases and adapter sequences were performed to develop high quality genome assemblies. To do this, a5_Miseq (Coil *et al.,* 2015) was used, as it is a software tool that combines quality trimming and assembly. The quality of the raw reads was assessed before and after trimming using a common quality assessment tool known as FastQC (Andrews, 2010). This also verified that the adapter sequences were successfully removed. The overall quality of the sequence reads was assessed by comparing the total number of raw reads to the total number of trimmed reads. Draft genome assembly was assessed for quality using the software tool QUAST (Gurevich *et al.,* 2013). Both QUAST and a5_Miseq assembly statistics were used to investigate the assembly capability (**Table 5.1**). For instance, the genome size of *Streptococcus mitis* is 2.15Mb with a GC content of 40% (Petrosyan *et al.,* 2016). By comparison, the genome of the strain of *Streptococcus mitis* used in this study was 2.03Mb with a GC content of 39.7% (**Table 5.1**). The same

verification was performed for all the isolates. Once the quality of the draft genome was determined, genome annotation was performed on all genome sequences. Prokka (Seemann, 2014) was the software tool used to annotate the genomes. The statistics obtained from Prokka revealed the numbers of genes, tRNAs, and ribosomal RNAs present in our genomes (**Table 5.1**). Another popular genomic annotation tool called RAST (Aziz *et al.,* 2008) was also used to annotate these genome sequences. Post-assembly, there are many downstream processes which can be used to understand the various features of the sequenced and annotated genomes.

Table 5.1 Summary of assembly and annotation data. Whole genome sequencing data were obtained for the different bacterial strains used in the study. These genomes were assembled with A5_MiSeq and annotated with Prokka.

	Streptococcus mitis	*Enterococcus faecium*	*Pseudomonas aeruginosa*	*Neisseria sicca*	*Bacteroides vulgatus*
Number of contigs	72	232	84	175	124
Genome size	2031560	3039384	7083848	2655258	5268607
Longest scaffold	204611	95951	559514	120667	228110
GC content	39.7	37.8	65.9	51.1	42.2
Coverage	216	268	168	234	123
N50	150150	33449	191650	41695	103528
Number of genes	1965	3006	6762	2468	4477
Number of tRNAs	58	62	67	54	68
Number of ribosomal RNAs	4	7	6	3	11

The assembled sequences were uploaded to PATRIC (Wattam *et al.,* 2017), which uses RAST (Aziz *et al.,* 2008) for annotation (**Table A.6**). Focusing on virulence genes, I found that the genome of *N. sicca* contained 40 different predicted virulence factors. The genome of *E. faecium* contained 11 virulence factor genes. While I predicted that the genome of *S. mitis* contained very few antimicrobial resistance genes, it contained 140 virulence factor genes. In the case of *B. vulgatus,* I found only one virulence gene. Finally, the genome of *P. aeruginosa* contained 344 virulence factors.

CARD (Jia *et al.,* 2017) was used on the assembled sequences to predict antimicrobial resistance (AMR) genes (**Table A.5**). Overall, the tool found 4 AMR genes in the genome of *N. sicca,* mostly involved in antibiotic inactivation. There were 22 hits for *E. faecium.* The main resistance mechanism found for this isolate was antibiotic target alteration. The genome of *S. mitis* contained only two AMR genes, both antibiotic efflux genes. The same was true for *B. vulgatus,* which had four hits, two of which were antibiotic efflux genes. Finally, the genome of *P. aeruginosa* contained a large number of AMR genes. The majority of these were efflux genes (41/50 genes), which were excluded from this analysis. The remaining genes were involved in antibiotic inactivation and antibiotic target alteration.

The assembled and annotated sequences were also run through PRISM (Skinnider *et al.,* 2017) (**Table A.7**) to identify secondary metabolite pathways present in the genomes of our bacteria. Overall, PRISM yielded very little result. No gene clusters were identified for *N. sicca* and *B. vulgatus.* In the case of *E. faecium* and *S. mitis,* one gene cluster was identified for each species, both being polyketide clusters. Finally, several sequences of secondary metabolite pathways were identified in the genome of *P. aeruginosa.* The majority were non-ribosomal peptide clusters with one polyketide cluster and one unknown thiotemplated cluster type.

5.3 Discussion

5.3.1 Mice tolerated and cleared *S. mitis* in the respiratory tract

Towards the development of the mouse model of infection, I verified that *S. mitis,* the commensal showing the most promising results, could be tolerated by the mice. Indeed, if *S. mitis* caused disease in the mice, it would not be useful as a potential protective probiotic. I also established whether *S. mitis* could colonize the upper or lower respiratory tract of the mice. If the commensal could establish itself as a commensal in the mice, it could affect the long-term resistance to *P. aeruginosa*. However, even if it did not colonize the nose or lungs of the mice, the commensal could still impact the immune system of the host and therefore contribute to protecting the mice against an infection. In fact, while the impact of probiotics has not been fully elucidated, it is known that colonization is not necessary for them to exert their effects. In fact, probiotics often impact host health by stimulating the immune system (Isolauri *et al.,* 2001). As such, a double-blind, randomized, controlled, prospective trial has shown that immune stimulation with a mixture of probiotic strains, *Lactobacillus paracasei, Lactobacillus casei* 431, and *Lactobacillus fermentium* PCC, significantly reduced the incidence of upper respiratory infections in susceptible populations (Zhang *et al.,* 2018).

Overall, the mice tolerated the presence of *S. mitis* both in the nose and the lungs and were able to clear this bacterium within a few days (**Figures 5.1**). This commensal is therefore safe to use in an infection model.

5.3.2 Upper and lower respiratory tract *P. aeruginosa* infections had disparate effects

The development of a mouse model of infection would have allowed for the testing of the effects of the commensals of interest *in vivo* and see whether or not these commensals could protect living animals from an infection. This would have brought us one step closer to knowing if these commensals could have applications as probiotics given in prevention of infection in susceptible population. Moreover, such a model could have furthered our understanding of the immune response involved in the inhibitory phenotype. As such, I could have measured the cytokine response triggered in the different tissues as well as quantified the recruitment of innate immune cells to the site of infection.

However, *P. aeruginosa* does not easily infect mice. A few model of acute pneumonia caused by *P. aeruginosa* have been developed. These are dependent on the strain used and the cell density inoculated, and result in either rapid clearance or rapid sepsis and death. In order to establish a model of *P. aeruginosa* colonization, an immobilizing agent must be used (Bragonzi, 2010). In spite of this background knowledge, I attempted to infect mice with our strain of *P. aeruginosa*. When P. aeruginosa was infiltrated in the lungs of mice, they developed symptoms of infection very rapidly and started dying (**Figure 5.2a**). Upon collection of tissues, I saw that *P. aeruginosa* had spread throughout the whole organism, probably through the blood stream, as it was present in the spleen (**Figure 5.2b**), indicating that the mice had developed sepsis. This was an extreme form of disease and I judged that it was unethical to submit the mice to this infection. Therefore, this experiment was only conducted once.

An intranasal infection prevents such a direct exposure to the lungs of mice. Based on the results of the lung infection, I expected a nasal infection to cause milder symptoms and potentially lead to short-term colonization. However, the mice did not display any symptoms of infection and were able to clear *P. aeruginosa* in a few days (**Figure 5.2c**). As the aim of this experiment was to demonstrate a protective phenotype with the commensal bacteria, this model was not useful as there was no infection to protect the mice from and no colonization to block.

5.3.3 No innate immune cell influx was detected in the lungs of mice with an upper respiratory tract *P. aeruginosa* infection

As described above, the model of infection I attempted to develop was not a success. It would be difficult to show the effects of the commensal of interest in mice that were either too sick or not sick enough. However, it remained possible to show that the presence of the commensal could reduce the inflammatory response triggered by *P. aeruginosa*. *In vivo,* detection of flagellin by TLR5 results in the secretion of IL-8, a neutrophil chemoattractant, leading to a massive influx of neutrophils to the site of *P. aeruginosa* infection (Kim *et al.,* 2014). Therefore, I expected to detect a quantifiable inflammatory response in the respiratory tract of mice infected with *P. aeruginosa.* I collected bronchioalveolar lavages and nasal washes from healthy mice (**Figure 5.3a**) and from mice infected intranasally with *P. aeruginosa* (**Figure 5.3b**). I expected to see a greater infiltration of innate immune cells, in particular neutrophils, in the lungs of infected mice. During preliminary

assays, I found that there were no visible differences in the number of cells in the lungs of mice infected intranasally with *P. aeruginosa.* However, these results were not quantified. It is possible that the lung infection led to a significant influx of immune cells to the site of infection. However, the lungs of these mice were too damaged for bronchioalveolar lavages. Moreover, very few immune cells were detected in nasal washes. It would therefore be impossible to tell if the presence of *S. mitis* in this system would lead to decreased inflammation.

Overall, our limited experiments to develop an *in vitro* mouse model of *P. aeruginosa* infection did not yield any promising results. However, it would be interesting to repeat some of these experiments to verify the reproducibility of our preliminary results. It would be of interest to explore different models of *P. aeruginosa* infection. For instance, Sibley *et al.* (2008) developed a *Drosophila* model to investigate polymicrobial infections and showed that *P. aeruginosa* could infect this insect. Moreover, there are other ways to assess the immune response triggered by the presence of *P. aeruginosa*. Measuring the cytokines and chemokines produced in the site of infection and quantifying the immune cells present could reveal the protective potential of the commensals.

5.3.4 The PCLS did not directly inhibit *P. aeruginosa*

In the absence of an *in vitro* model, I sought to better understand the mechanism behind the inhibitory activity of the commensals. Since the commensals

of interest also showed activity in a host-independent manner, I hypothesized that the killing activity was most probably a direct action of the bacteria themselves, potentially influenced by the host cells. However, I wanted to establish whether or not the cells composing the PCLS also had a direct effect. In which case, the model would consist of PCLS primed by the bacteria to increase their inhibitory activity against *P. aeruginosa*. Using two different methods, priming the PCLS *in vitro* (**Figure 5.4a**) and *in vivo* (**Figure 5.4b**), I found that the PCLS had no inherent inhibitory effect of their own. PCLS primed *in vivo* did show a slight increase in the killing activity against *P. aeruginosa*, most notably in presence of *N. sicca*. However, I concluded that the PCLS alone were not sufficient to mediate this phenotype.

5.3.5 Hydrogen peroxide participated in the elimination of *P. aeruginosa*

Having established that the observed phenotype was directly mediated by the commensal bacteria, I examined different possibilities for the mechanism of action. In the case of *S. mitis*, it was a possibility that its inhibitory effect against *P. aeruginosa* was through the release of hydrogen peroxide. Indeed, many *Streptococcus* species use this mechanism as an antibacterial defense and *P. aeruginosa* has been shown to be susceptible to this chemical (Whiley *et al.,* 2015). Using different concentrations of catalase, I examined the effect of *S. mitis* in the absence of hydrogen peroxide (**Figure 5.5**). I found that the cell density of *P. aeruginosa* was increased starting at 20 units/mL of catalase. However, the increase was not proportional to the concentration of catalase in the medium and the

bacterial load of *P. aeruginosa* was still lower than when it grew alone. This indicates *S. mitis* probably released hydrogen peroxide, which participated in the elimination of *P. aeruginosa*. As I did not measure whether the concentrations of catalase used removed all the hydrogen peroxide from the environment, it is impossible to exclude that the catalase was saturated or had a short half-life and that hydrogen peroxide was still the mediator of the effect. However, considering that the increase in *P. aeruginosa* CFUs was not proportional to the concentration of catalase, it is safe to assume that the release of hydrogen peroxide alone was not sufficient to explain the phenotype.

Hydrogen peroxide is only one potential mechanism of action in this assay. Several experiments could be performed to further pinpoint how the commensal bacteria are inhibiting the growth of or eliminating *P. aeruginosa.* For instance, it would be relevant to further characterize the factors secreted in the supernatant by heat-inactivating it or by using mass spectrometry or related methods. I could also investigate the antimicrobial peptides released by either the bacteria themselves or the host cells to determine whether these molecules play a role in the system.

5.3.6 The genomes of the bacteria revealed antimicrobial resistance genes, virulence factor genes, and secondary metabolite pathways

Genome analysis is a powerful tool that can reveal specific genes present in the genomes of and potentially expressed by the bacteria of interest. The presence of certain genes could explain how the bacteria contribute to the elimination of *P.*

aeruginosa as well as their immunomodulatory effects. I used several tools to gain a broad understanding of the different AMR genes (**Table A.5**), virulence factor genes (**Table A.6**), and secondary metabolite pathways (**Table A.7**) that may be expressed in our bacteria of interest in attempt to shed light on the inhibitory activity against *P. aeruginosa* exhibited by these bacteria.

Overall, with the exception of *E. faecium,* the commensal bacteria possessed very few antimicrobial resistance genes (**Table A.5**). This is reassuring for their potential use as probiotics as they would not be able to grow unchecked. The genome of *Enterococcus faecium*, however, contained 22 antibiotic resistance genes.

Unsurprisingly, as this study involves a multidrug resistant strain of *P. aeruginosa*, 50 AMR genes were predicted in the genome of this pathogen (**Table A.5**). However, the majority of these genes were antibiotic efflux genes. It is known that *P. aeruginosa* expresses a large number of efflux pumps. These pumps are not only involved in the efflux of antibiotics but also in the efflux of any xenobiotic the bacterium encounters. Moreover, these efflux pumps are only involved in antibiotic resistance when they are over expressed (Strateva and Yordanov, 2009). While I can conclude from our results that the identified genes are present in the genome of the bacteria, I have no indication of their level of expression and whether or not they are expressed at all.

I also used another tool, PATRIC (Wattam *et al.,* 2017), to identify virulence factor genes contained in the genomes of the bacterial strains (**Table A.6**). Virulence

factors are molecules produced by bacteria and other microorganisms, which makes them more effective in colonizing and persisting in a host (Bergan, 1981). I expected *P. aeruginosa* to contain high numbers of these genes while the other bacteria would not. Indeed, as a pathogen, *P. aeruginosa* uses virulence genes to colonize the host, escape immune detection, and therefore, establish a better infection. In contrast, the other bacteria are commensal organisms, with the potential exception of *E. faecium,* which is an opportunistic pathogen, and would not require as many virulence factors.

As expected, the genome of *P. aeruginosa* contained a very large number of virulence factor genes (**Table A.6**). Most of these genes were involved in secretion systems (also reflected in AMR efflux pumps identified), adherence, and acquisition of nutrients. The commensal isolates did not contain as many virulence genes. *E. faecium* expressed 11 and *B. vulgatus* only one. The genome of *N. sicca* contained 40 genes and the genome of *S. mitis* contained 140 genes. While these numbers are higher than expected, I bear in mind that virulence factors are involved in adherence and immune evasion, which are also traits beneficial to commensal species.

My last step was to use PRISM (Skinnider *et al.,* 2017) to identify secondary metabolite pathways in the genomes of our bacteria (**Table A.7**). Overall, PRISM yielded very little results. Only the pathogen, *P. aeruginosa,* contained several secondary metabolite pathway gene clusters in its genome.

While genome analysis allows us to visualize the genomes of the different bacteria and can provide a lot of information as to how they would behave *in vivo*

and their potential effects on the host and other bacteria, it has its limits. As mentioned above, I can conclude that genes are present in the genome of the bacteria but there is no indication as to whether or not these genes are expressed and to what level they are expressed. For instance, I couldn't rely simply on the antimicrobial gene predictions to deduce which antibiotics the bacteria are resistant to; I would have to physically test the different antibiotics. In fact, the genes identified are simply predictions based on incomplete databases. They can therefore be used for general assessment and potentially hypothesis generation but further testing is necessary to validate these results.

Nonetheless, these results undeniably provide insight into the functioning of the bacteria of interest and will undoubtedly prove useful in the pursuit of specifics on the various mechanisms at play.

5.4 Conclusions

An *in vivo* mouse model of infection was a logical third step to envisage after developing increasingly complex *in vitro* models, but I encountered a number of roadblocks that prevented the full development of such a model. Still, I was able to demonstrate that *S. mitis* was safe for the mice and its specific effects could eventually be assessed in this model. I also developed several methods that could be used to quantify the immunomodulatory effects of the different commensals *in vivo.* Some of these experiments could be repeated and further developed to better understand the mechanisms involved in the observed inhibitory phenotype.

Several other methods can also be used to elucidate the mechanisms of action. Here, I ruled out the effects of immune priming and hydrogen peroxide as the main drivers of the phenotype.

Using sequencing and genome assembly and annotation, I confirmed the identity of our bacteria and identified specific genes encoding for antimicrobial resistance, virulence factors, and secondary metabolite pathways. The genes identified confirm the multidrug resistance status of our pathogen but also showed that some of the commensal strains have the potential to virulent and/or resistant to a number of antibiotics. These results can be used for further studies to deepen our understanding of the mechanism at play in the inhibitory phenotype identified in these bacteria.

On the whole, even though I have not been able to define just how the commensals inhibit *P. aeruginosa* yet, I have made progress in identifying various factors that play a role in this phenotype and ruling out others who do not.

Chapter 6 Conclusion and future directions

Antimicrobial resistance is one of the biggest threats that we face today. It is already responsible for 23,000 deaths in the United States alone (CDC) and this number will only continue to increase. It is now imperative that we find new ways of treating infections caused by resistant microbes or, better still, preventing the development of these infections. A number of strategies are used to do so, from using bioinformatics to identify new targets for antibiotics to engineering phages that target specific pathogens. Here, I focus on the role and potential of the respiratory tract microbiota in the prevention of airway infections. I are motivated to pursue this by studies that have shown commensal bacteria from the microbiota to be effective in inhibiting the colonization of pathogens and other bacteria in the respiratory tract. The defense strategies known to the commensals include: occupying the available space and consuming the nutrients; exercising direct antagonistic commensal-pathogen interactions; and/or, interacting with the host. Based on this knowledge, specific commensal bacterial species could be developed into probiotics to help the host fight against respiratory tract infections. More precisely, I focus on infections caused by *Pseudomonas aeruginosa,* a pathogen responsible for a number of different infections, mostly in immunocompromised patients. *P. aeruginosa* is of great interest as it is intrinsically resistant to numerous antibiotics and can acquire new antimicrobial resistance genes easily. It is one of the

bacteria that are considered serious threats (CDC), as very few therapeutic options remain available against this pathogen.

To identify bacterial isolates inhibiting the growth of *P. aeruginosa,* bacteria from the Human isolates library were grown with or without Detroit-562 cells after which *P. aeruginosa* was added. The bacterial load of *P. aeruginosa* was measured at the end of the experiment and bacterial strains participating in a reduction in the presence of host cells four were selected for further study. From the 30 isolates found to inhibit the growth of *P. aeruginosa*, I selected four: *Neisseria sicca, Enterococcus faecium, Streptococcus mitis,* and *Bacteroides vulgatus.* All of these bacteria inhibited the growth of *P. aeruginosa* in the initial screen. In the cases of *E. faecium* and *B. vulgatus*, the effect was host-dependent. *S. mitis* did not exhibit a host-dependent phenotype; however, it completely eliminated *P. aeruginosa,* which was undetectable by the end of the experiment. I also found that the inhibitory effect occurred during the first few hours of exposure, that it was dependent on the presence of living bacteria, and that it was most likely the result of a secreted factor.

Despite the either host-dependent or independent effects of these bacteria, I believe the interaction with the host cells to be instrumental. The host typically relies on its immune system to eliminate bacterial threats. I therefore characterized the immune response of the Detroit-562 cells to the different bacterial strains by quantifying the cytokines and chemokines released by the cells by the end of the experiment. In doing this, I found that, while the presence of *P. aeruginosa* led to the release of pro-inflammatory cytokines, the commensal strains maintained an anti-

inflammatory environment. *E. faecium* in particular led to the secretion of an anti-inflammatory cytokine. *S. mitis* had a different effect, upregulating neutrophil chemoattractants. The presence of these different bacteria could create an immune environment *in vivo* that would be detrimental to the growth of *P. aeruginosa.*

Considering the potential use of these bacteria as probiotics in living organisms, I verified whether they would survive and have similar effects in a model containing most of the cell types they would be exposed to in the respiratory tract of mice. PCLS remained viable in culture for at least a week and they did not dramatically affect the growth of the commensal bacteria. This model also afforded us the advantage that it maintained the simplicity of cell culture while providing the complexity of cells and factors present in an *in vivo* model. I repeated the same assay as was done in the Detroit-562 model using these PCLS and found similar results for two of the commensal strains, *E. faecium* and *S. mitis. N. sicca* and *B. vulgatus* however lost their inhibitory activity. As with the Detroit-562 model, the phenotype could be observed within the first few hours of exposure. It was dependent on the presence of living bacteria, and was likely due to a secreted factor as the filtered supernatant of the PCLS exposed to *E. faecium* and *S. mitis* retained its inhibitory activity. The quantification of the cytokines and chemokines expressed by the PCLS in response to the bacteria revealed that *P. aeruginosa* created a pro-inflammatory response while *E. faecium* prevented the upregulation of pro-inflammatory cytokines and *S. mitis* led to the upregulation of neutrophil chemoattractants.

Overall, these results were similar to those obtained from the Detroit-562 model. The only notable difference had to do with the cytokines released by the cells exposed to *N. sicca* and *P. aeruginosa* as well as those exposed to *B. vulgatus* and *P. aeruginosa* which, in the PCLS model, clustered with the cytokines released in response to *P. aeruginosa* alone. Considering that these two commensals did not inhibit *P. aeruginosa* in this model, the cytokine response of the PCLS was driven by *P. aeruginosa.*

Our ultimate objective was to observe the effects of *E. faecium* and *S. mitis* in an *in vivo* model to determine whether these commensals could protect the mice from a respiratory tract infection with *P. aeruginosa.* However, our attempts to develop a *P. aeruginosa* model of infection were not encouraging. A lower respiratory tract infection model led to the development of sepsis and rapid death, making us feel it was unethical to submit the mice to such treatment. Then, I was unable to observe any protective effect of the commensals in the upper respiratory tract infection model because the mice did not become sick at all. The mouse model therefore failed to produce any data that would support our hypotheses. I had to look elsewhere to elucidate the potential mechanism of action of the observed inhibitory phenotype.

Besides the interaction of the bacteria with the host cells, the direct killing effect had to be mediated by either the bacteria themselves or a factor released by the host cells. I started by ruling out that the inhibitory activity could be the result of a direct action by the host cells composing the PCLS. By priming the PCLS, either *in*

vitro or *in vivo,* I examined the role of immune factors or any other factors released by the PCLS and found that there was little difference between PCLS, whether they had been primed or not. From this I concluded that the observed inhibitory phenotype was the result of a direct action from the commensal bacteria, potentially with the assistance of the host cells or in response to the host cells.

Our second step was to investigate the role of hydrogen peroxide in the phenotype exhibited by *S. mitis.* I used catalase to remove hydrogen peroxide from the medium and found a slight reduction in the inhibitory activity of this commensal, which helped us understand that the phenotype is not driven by the release of hydrogen peroxide. There was still the possibility, however, that this chemical played a role in inhibiting *P. aeruginosa*.

Finally, I used different bioinformatic tools to get a glimpse at the genes present in the genomes of the bacterial strains of interest. As a result, I was able to determine that *P. aeruginosa* possessed a variety of antimicrobial resistance genes and virulence genes. As a multidrug resistant pathogen, these results were not surprising. *N. sicca* and *B. vulgatus* were found to possess very few genes of interest. The genome of *E. faecium,* on the other hand, contained a number of antimicrobial resistance genes. Considering that *E. faecium* can be pathogenic in some circumstances, these results are concerning. If we were to move forward with any of these bacterial strains, *E. faecium* would be excluded as a probiotic. Of interest, *S. mitis* possessed a number of virulence genes. Considering that this commensal is

typically not pathogenic, these genes might be used to increase the commensalism, as they could be involved in immune evasion, colonization, and inhibition of other bacterial species. In these genes we might find the one responsible for the inhibition of *P. aeruginosa.*

Using these results as a starting point, a number of avenues could be explored. As I have determined that the main inhibitory effect is derived from the bacteria themselves, it would be of great interest to better define the exact mechanism behind this. This could be done through a number of microbiological or biochemical assays which would attempt to isolate the exact molecule(s) responsible for killing *P. aeruginosa.* If the molecule(s) of interest were identified, their potential as antimicrobial agents could be characterized, and they could be developed into effective new drugs. This would be of more interest than using probiotics as antimicrobial agents.

Another way of identifying the mechanism of action would be to use the genome assembly results. Accordingly, I used several tools to identify the genes present in the bacteria of interest as well as their potential roles. Combing through this data could reveal genes involved in microbe-host interactions as well as genes involved in microbe-microbe interactions. These results could potentially reveal a number of ways used notably by *E. faecium* and *S. mitis* to inhibit the growth of *P. aeruginosa.* These findings could, in turn, be tested using biochemical assays.

The other avenue to explore is the immunomodulatory potential of these commensal bacteria. By quantifying the cytokines and chemokines produced by the Detroit-562 cells and the PCLS I have scratched the surface of the interactions occurring between the bacteria and the immune system of the host. Immunomodulation would be a great way of increasing the natural resistance to infection. It would therefore be of significant interest to further characterize the effects of the commensal bacteria on the immune pathways targeted. It could be done by collecting bronchioalveolar lavages, nasal washes, and full tissues, then using different methods, such as multiplex cytokine assays or flow cytometry to identify the cytokines and chemokines released as well as immune cells recruited in response to these bacteria in the respiratory tract. Different cell types could be investigated, such as neutrophils, monocytes/macrophages, innate lymphoid cells, or T and B cells.

Overall, this project provides an experimental framework for screening and validating microbes capable of inhibiting specific pathogens in a host-dependent manner going from cell line screens to *ex vivo* tissue characterization and *in vivo* animal models. The results of these initial studies provide a better understanding of the immune response triggered by the presence of our specific commensals. They also provide information pertaining to the mechanism behind the inhibitory potential of the commensals as Ill as their potential as probiotics, which could be used in prevention of respiratory tract infections. This is an avenue of exploration

which holds real promise and could finally give us an advantage over increasingly resistant pathogens.

References

Al-Mulla NA, Taj-Aldeen SJ, El Shafie S, Janahi M, Al-Nasser AA, Chandra P. Bacterial bloodstream infections and antimicrobial susceptibility pattern in pediatric hematology/oncology patients after anticancer chemotherapy. *Infection and Drug Research.* 2014; **7**: 289.

Alekshun MN, Levy SB. Molecular mechanisms of antibacterial multidrug resistance. *Cell*. 2007; **128**(6): 1037–1050.

Altschul SF, Gish W, Miller W, Myers EW, Lipman DJ. Basic local alignment search tool. *Journal of Molecular Biology.* 1990; **215**: 403-410.

Andrews S. FastQC: a quality control tool for high throughput sequence data. 2010. Available online at: http://www.bioinformatics.babraham.ac.uk/projects/fastqc

Aziz RK, Bartels D, Best AA, DeJongh M, Disz T, Edwards RA, Formsma K, Gerdes S, Glass EM, Kubal M, *et al.* The RAST server: rapid annotations using subsystems technology. *BMC Genomics.* 2008; **9**: 75.

Arend WP. Interleukin-1 receptor antagonist: discovery, structure and properties. *Progress in Growth Factor Research.* 1990; **2**(4): 193-205.

Barton P, Riley RJ. A new paradigm for navigating compound property related drug attrition. *Drug Discovery Today.* 2016; **21**: 72–81.

Bassis CM, Erb-Downward JR, Dickson RP, Freeman CM, Schmidt TM, Young VB, Beck JM, Curtis JL, Huffnagle GB. Analysis of the upper respiratory tract microbiotas as the source of the lung and gastric microbiotas in healthy individuals. *mBio.* 2015; **6**: e00037-15.

Baulmer AJ, Sperandio V. Interactions between the microbiota and pathogenic bacteria in the gut. *Nature*. 2016; **535**: 85-93.

Bellamy WD, Klimek JW. Some properties of penicillin-resistant staphylococci. *Journal of Bacteriology.* 1948; **55**(2): 153–160.

Bergan T. Pathogenetic factors of *Pseudomonas aeruginosa. Scandinavian Journal of Infectious Diseases.* 1981; **29**: 7-12.

Biesbroek G, Tsivtsivadze E, Sanders EAM, Montjin R, Veenhoven RH, Keijser BJF, Bogaert D. Early respiratory microbiota composition determines bacterial succession patterns and respiratory health in children. *American Journal of Respiratory Critical Care Medicine.* 2014; **190**: 1283-1292.

Blanc DS, Petignat C, Janin B, Bille J, Francioli P. Frequency and molecular diversity of *Pseudomonas aeruginosa* upon admission and during hospitalization: a prospective epidemiologic study. *Clinical Microbioly and Infection.* 1998; **4**: 242-247.

Bosch ATM, Biesbroek G, Trzcinski K, Sanders EAM, Bogaert D. Viral and bacterial interactions in the upper respiratory tract. *PLoS Pathogens.* 2013; **9**(1): e1003057.

Bodey GP, Bolivar R, Fainstein V, Jadeja L. Infections caused by *Pseudomonas aeruginosa. Reviews of Infectious Diseases.* 1983; **5**(2): 279-313.

Bogaert D, De Grott R, Hermans PWM. *Streptococcus pneumoniae* colonization: the key to pneumococcal disease. *Lancet Infectious Diseases.* 2004; **4**: 144-154.

Bragonzi A. Murine models of acute and chronic lung infection with cystic fibrosis pathogens. *International Journal of Medical Microbiology.* 2010; **300**: 584-593.

Bush K, Courvalin P, Dantas G, Davies J, Eisenstein B, Huovinen P, Jacoby GA, Kishony R, Kreiswirth BN, Kutter E, Lerner SA, Levy S, Lewis K, Lomovskaya O, Miller JH, Mobashery S, Piddock LJ, Projan S, Thomas CM, Tomasz A, Tulkens PM, Walsh TR, Watson JD, Witkowski J, Witte W, Wright G, Yeh P, Zgurskaya HI. Tackling antibiotic resistance. *Nature Review Microbiology.* 2011; **9**(12): 894–896.

Campodonica VL, Gadjeva M, Paradis-Bleau C, Uluer A, Pier GB. Airway epithelial control of *Pseudomonas aeruginosa* infection in cystic fibrosis. *Trends in Molecular Medecine.* 2008; **14**: 120-133.

Chelikani P, Fita I, Loewen PC. Diversity of structures and properties among catalases. *Cellular and Molecular Life Sciences.* 2004; **61**(2): 192-208.

Cohen TS, Prince AS. Activation of inflammasome signaling mediates pathology of acute *P. aeruginosa* pneumonia. *Journal of Clinical Investigations.* 2013; **123**: 1630-1637.

Coil D, Jospin G, Darling AE. A5-miseq: an updated pipeline to assemble microbial genomes from Illumina Miseq data. *Bioinformatics.* 2015; **31**(4): 587-589.

Cole AM, Ganz T, Liese AM, Burdick MD, Lui L, Strieter RM. Cutting edge: IFN-inducible ELR-CXC chemokines display defensin-like antimicrobial activity. *Journal of Immunology.* 2001; **167**: 623-627.

Costello EK, Lauber CL, Hamady M, Fierer N, Gordon JI, Knight R. Bacterial community variation in human body habitats across space and time. *Science.* 2009; **326**(5960): 1694-7.

Dickson RP, Erb-Downward JR, Martinez FJ, Huffnagle GB. The microbiome and the respiratory tract. *Annual Reviews in Physiology.* 2016; **78**: 481-504.

DiGiandomenico A, Sellman BR. Antibacterial monoclonal antibodies: the next

generation? *Current Opinion in Microbiology*. 2015; **27**:78-85.

Dominguez-Bello MG, Costello EK, Contreras M, Magris M, Hidalgo G, Fierer N, Knight R. Delivery mode shapes the acquisition and structure of the initial microbiota across multiple body habitats in newborns. *Proceedings of the National Academy of Sciences.* 2010; **107**: 11971-11975.

El Zowalaty ME, Al Thani AA, Webster TJ, El Zowalaty AE, Schweizer HP, Nasrallah GK. *Pseudomonas aeruginosa:* arsenal of resistance mechanisms, decades of changing resistance profiles, and future antimicrobial therapies. *Future Microbiology.* 2015; **10**(10): 1683-1713.

Epelman S, Bruno TF, Neely GG, Woods DE, Mody CH. *Pseudomonas aeruginosa* exoenzyme S induces transcriptional expression of proinflammatory cytokines and chemokines. *Infection and Immunity.* 2000; **68**: 4811-4814.

Faure K, Sawa T, Ajayi T, Fujimoto J, Moriyama K, Shime N, Wiener-Kronish JP. TLR4 signaling is essential for survival in acute lung injury induced by virulent *Pseudomonas aeruginosa* secreting type III secretory toxins. *Respiratory Research.* 2004; **5**: 1.

Filkins LM, Hampton TH, Gifford AH, Gross MJ, Hogan DA, Sogin ML, Morrison HG, Paster BJ, O'Toole GA. Prevalence of streptococci and increased polymicrobial diversity associated with cystic fibrosis patient stability. *Journal of Bacteriology.* 2012; **194**: 4709-4717.

Fischbach MA, Walsh CT. Antibiotics for emerging pathogens. *Science.* 2009; **325**(5944): 1089–1093.

Fleming AG. Responsibilities and opportunities of the private practitioner in Preventive Medicine. *Canadian Medical Association Journal.* 1929; **20**(1): 11–13.

Fothergill JL, Neill DN, Loman N, Winstanley C, Kadioglu A. *Pseudomonas aeruginosa*

adaptation in the nasopharyngeal reservoir leads to migration and persistence in the lungs. *Nature Communications.* 2014; **5**: 4780.

France MM, Turner JR. The mucosal barrier at a glance. *Journal of Cell Science*. 2017; **0**: 1-8.

Franchi L, Kamada N, Nakamura Y, Burberry A, Kuffa P, Suzuki S, Shaw MH, Kim YG, Nunez G. NLRC4-driven production of IL-1beta discriminates between pathogenic and commensal bacteria and promotes host intestinal defense. *Nature Immunology.* 2012; **13**: 449-456.

Gurevich A, Saveliev V, Vyahhi N, Tesler G. QUAST: quality assessment tool for genome assemblies. *Bioinformatics.* 2013; **29**(8): 1072-1075.

Harder J, Meyer-Hoffert U, Teran LM, Schwichtenberg L, Bartels J, Maune S, Schroder JM. Mucoid *Pseudomonas aeruginosa,* TNF-alpha, and IL-1beta, but not IL-6, induce human beta-defensin-2 in respiratory epithelia. *American Journal of Respiratory Cell and Molecular Biology.* 2000; **22**: 714-721.

Hartl D, Gaggar A, Bruscia E, Hector A, Marcos V, Jung A, Greene C, McElvaney G, Mall M, Doring G. Innate immunity in cystic fibrosis lung disease. *Journal of Cystic Fibrosis.* 2012; **11**: 363-382.

Hasleton PS. The internal surface area of the adult human lung. *Journal of Anatomy.* 1972; **112**: 391-400.

Hatch TF. Distribution and deposition of inhaled particles in the respiratory tract. *Bacteriological Reviews.* 1961; **25**: 237-240.

Hlatky L, Hahnfeldt P, Tsionou C, Coleman CN. Vascular endothelial growth factor: environmental controls and effects in angiogenesis. *The British Journal of Cancer. Supplement.* 1996; **27**: S151-156.

Huxley EJ, Viroslav J, Gray WR, Pierce AK. Pharyngeal aspirations in normal adults and patients with depressed consciousness. *American Journal of Medecine*. 1978; **64**: 564-568.

Isolauri E, Sütas Y, Kankaanpää P, Arvilommi H, Salminen S. Probiotics: effects on immunity. *American Journal of Clinical Nutrition.* 2001; **73**(2): 444Se50S.

Iwasaki A, Foxman EF, Molony RD. Early local immune defences in the respiratory tract. *Nature Reviews Immunology.* 2017; **17**: 7-20.

Iwase T, Uehara Y, Shinji H, Tajima A, Seo H, Takada K, Agata T, Mizunoe Y. *Staphylococcus epidermidis* Esp inhibits *Staphylococcus aureus* biofilm formation and nasal colonization. *Nature Letters.* 2010; **465**: 346-349.

Jia *et al.* CARD 2017: expansion and model-centric curation of the Comprehensive Antibiotic Resistance Database. *Nucleic Acids Research.* 2017; **45**:D566-573.

Joseph T, Look D, Ferkol T. NF-kappaB activation and sustained IL-8 gene expression in primary cultures of cystic fibrosis airway epithelial cells stimulated with *Pseudomonas aeruginosa. American Journal of Physiology-Lung Cellular and Molecular Physiology.* 2005; **288**: L471-L479.

Kamada N, Chen GY, Inohara N, Nunez G. Control of pathogens and pathobionts by the gut microbiota. *Nature Immunology*. 2013; **14**: 685-690.

Kanmani P, Clua P, Vizoso-Pinto MG, Rodriguez C, Alvarez S, Melnikov V, Takahashi H, Kitazawa H, Villena J. Respiratory commensal bacteria *Corynebacterium pseudodiphtheriticum* improves resistance of infant mice to respiratory syncytial virus and *Streptococcus pneumoniae* superinfection. *Frontiers in Microbiology*. 2017; **8**: 1613.

Keene WE, Markum AC, Samadpour M. Outbreak of *Pseudomonas aeruginosa* infections caused by commercial piercing of upper ear cartilage. *JAMA.* 2004;

291(8): 981-985.

Kim YJ, Paek SH, Jin S, Park BS, Ha UH. A novel *Pseudomonas aeruginosa*-derived effector cooperates with flagella to mediate the upregulation of interleukin-8 in human epithelial cells. *Microbial Pathogenesis.* 2014; **66**: 24-28.

Kobayashi Y. Neutrophil infiltration and chemokines. *Critical Reviews in Immunology.* 2006; **26**(4): 307-16.

Kube D, Sontich U, Fletcher D, Davis PB. Proinflammatory cytokine responses to *P. aeruginosa* infection in human airway epithelial cell lines. *American Journal of Physiology-Lung Cellular and Molecular Physiology.* 2001; **280**: L493-L502.

Lau GW, Hassett DJ, Britigan BE. Modulation of lung epithelial functions by *Pseudomonas aeruginosa. Trends in Microbiology.* 2005; **13:** 389-397.

Lewis K. New approaches to antimicrobial discovery. *Biochemistry and Pharmacology*. 2016.

Lister PD, Wolter DJ, Hanson ND. Antibacterial-resistant *Pseudomonas aeruginosa:* clinical impact and complex regulation of chromosomally encoded resistance mechanisms. *Clinical Microbiology Reviews.* 2009; **22**(4): 582-610.

Lloyd CM, Marsland BJ. Lung homeostasis: influence of age, microbes, and the immune system. *Immunity Reviews.* 2017; **46**: 549-561.

Lovewell RR, Patankar YR, Berwin B. Mechanisms of phagocytosis and host clearance of *Pseudomonas aeruginosa. American Journal of Physiology-Lung Cellular and Molecular Physiology.* 2014; **306:** L591-L603.

Lysenko ES, Clarke TB, Shchepetov M, Ratner AJ, Roper DI, Dowson CG, Weiser JN. Nod1 signaling overcomes resistance of *S. pneumoniae* to opsonophagocytic killing. *PLoS Pathogens.* 2007; **3**: e118.

Mesaros N, Nordmann P, Plésiat P, Roussel-Delvallez M, Eldere J, Glupczynski Y, Van Laethem Y, Jacobs F, Lebesque P, *et al. Pseudomonas aeruginosa:* resistance and therapeutic options at the turn of the new millennium. *Clinical Microbiology and Infection.* 2007; **13**: 560-578.

Metcalf D. The granulocyte-macrophage colony-stimulating factors. *Science.* 1985; **229**(4708): 16-22.

Miao EA, Mao DP, Yudkovsky N, Bonneau R, Lorang CG, Warren SE, Leaf IA, Aderem A. Innate immune detection of the type II secretion apparatus through the NLRC4 inflammasome. *Proceedings of the National Academy of Science USA.* 2010; **107**: 3076-3080.

Morris AE, Liggitt HD, Hawn TR, Skerrett SJ. Role of Toll-like receptor 5 in the innate immune response to acute *P. aeruginosa* pneumonia. *American Journal of Physiology-Lung Cellular and Molecular Physiology.* 2009; **297**: L1112-L1119.

Morris A, Beck JM, Schloss PD, Campbell TB, Crothers K, Curtis JL, Flores SC, Fontenot AP, Ghedin E, Huang L, Jablonski K, Kleerup E, Lynch SV, Sodergren E, Twigg H, Young VB, Bassis CM, Venkataraman A, Schmidt TM, Weinstock GM. Comparison of the respiratory microbiome in healthy nonsmokers and smokers. *American Journal of Respiratory Critical Care Medicine.* 2013; **187**: 1067-1075.

Munyard P, Bush A. How much coughing is normal? *Archives of Disease in Childhood.* 1996; **74**: 531-534.

Murphy K, Travers P, Walport M. (2008) *Janeway's Immunobiology 7th edition*. New York, NY: Garland Science.

Nagata S. Gene structure and function of granulocyte colony-stimulating factor. *Bioessays.* 1989; **10**(4): 113-117.

Neish AS. Mucosal immunity and the microbiome. *Annals of the American Thoracic*

Society. 2014; **11**: S28-32.

Neyt K, Lambrecht BN. The role of lung dendritic cell subsets in immunity to respiratory viruses. *Immunology Reviews.* 2013; **255**: 57-67.

Ottomani S, Scherpbier R, Chaulet P, Pio A, Van Beneden C, Raviglione M. Respiratory care in primary care services – survey in 9 countries. *Geneva: World Health Organization*. 2004.

Parker D, Prince A. Innate immunity in the respiratory epithelium. *American Journal of Respiratory Cell and Molecular Biology* 2011; **45**: 189-201.

Payne DJ, Gwynn MN, Holmes DJ, Pompliano DL. Drugs for bad bugs: confronting the challenges of antibacterial discovery. *Nature Reviews Drug Discovery.* 2007; **6**(1): 29–40.

Pechere JC, Kohler T. Patterns and modes of b-lactam resistance in *Pseudomonas aeruginosa. Clinical Microbiology and Infection.* 1999; **5**(1):S15-S18.

Petrosyan V, Holder M, Ajami NJ, Petrosin JF, Sahasrabhojane P, Thompson EJ, Kalia A, Shelburne SA. Complete genome sequence of Streptococcus mitis strain SVGS_061 isolated from a neutropenic patient with Viridans group Streptococcal Shock Syndrome. *Genome Announcement.* 2016; **4**(2): e00259-16.

Pierrakos C, Karanikolas M, Scolletta S, Karamouzos K, Velissaris D. Acute respiratory distress syndrome: pathophysiology and therapeutic options. *Journal of Clinical Medecine Research.* 2012; **4**: 7-16.

R Development Core Team. R: A language and environment for statistical computing. *R Foundation for Statistical Computing,* Vienna, Austria. ISBN 3-900051-07-0. Can be found at http://www.R-project.org

Rahme LG, Stevens EJ, Wolfort SF, Shao J, Tompkins RG, Ausubel FM. Common

virulence factors for bacterial pathogenicity in plants and animals. *Science.* 1995; **268**: 1899-1902.

Rajan S, Saiman L. Pulmonary infections in patients with cystic fibrosis. *Seminars in Respiratory Infections.* 2002; **17**(1): 47-56.

Ramphal R, Balloy V, Jvot J, Verma A, Si-Tahar M, Chignard M. Control of *Pseudomonas aeruginosa* in the lung requires the recognition of either lipopolysaccharide or flagellin. *Journal of Immunology.* 2008; **181**: 586-592.

Saha S, Rajpal DK, Brown JR. Human microbial metabolites as a source of new drugs. *Drug Discovery Today.* 2016; **21**(4): 692-698.

Sawa T, Corry DB, Gropper MA, Ohara M, Kurahashi K, Wiener-Kronish JP. IL-10 improves lung injury and survival in *Pseudomonas aeruginosa* pneumonia. *Journal of Immunology.* 1997; **159**: 2858-2866.

Schatz A, Bugie E, Waksman SA. Streptomycin, a substance exhibiting antibiotic activity against gram-positive and gram-negative bacteria. *Proceedings of the Society for Experimental Biology and Medicine.* 1944; **55**: 66–69.

Schroeder M, Brooks BD, Brooks AE. The complex relationship between virulence and antibiotic resistance. *Genes*. 2017; **8**(1): 39.

Schultz MJ, Rijneveld AW, Florquin S, Edwards CK, Dinarello CA, van der Poll T. Role of interleukin-1 in the pulmonary immune response during *Pseudomonas aeruginosa* pneumonia. *American Journal of Physiology-Lung Cellular and Molecular Physiology.* 2002; **282**: L285-L290.

Scoffield JA, Wu H. Oral *Streptococci* and nitrite-mediated inferference of *Pseudomonas aeruginosa. Infection and Immunity.* 2015; **83**(1): 101-107.

Seemann T. Prokka: rapid prokaryotic genome annotation. *Bioinformatics.* 2014;

30(14):2068-9.

Segal LN, Alekseyenko AV, Clemente JC, Kulkarni R, Wu B, Gao Z, Chen H, Berger KI, Goldring RM, Rom WN, Blaser MJ, Weiden MD.. Enrichment of lung microbiome with supraglottic taxa is associated with increased pulmonary inflammation. *Microbiome.* 2013; **1**: 19.

Selva L, Viana D, Regev-Yochay G, Trzcinski K, Corpa JM, Lasa I, Novik RP, Penadés JR. Killing niche competitors by remote-control bacteriophage induction. *PNAS*. 2009; **106**(4): 1234-1238.

Sibley CD, Duan K, Fischer C, Parkins MD, Storey DG, Rabin HR, Surette MG. Discerning the complexity of community interactions using a Drosophila model of polymicrobial infections. *PLoS Pathogens.* 2008; **4**(10): e1000184.
Sibley CD, Parkins MD, Rabin HR, Duan K, Norgaard JC, Surette MG. A polymicrobial perspective of pulmonary infections exposes an enigmatic pathogen in cystic fibrosis patients. *Proceedings of the National Academy of Science USA.* 2008; **105**: 15070-15075. Skinnider MA, Merwin NJ, Johnston CW, Magarvey NA. Prism 3: expanded prediction of natural product chemical structures from microbial genomes. *Nucleic Acid Research.* 2017; **45**:W49-W54.
Skerrett SJ, Wilson CB, Liggitt HD, Haijar AM. Redundant Toll-like receptor signaling in the pulmonary host response to *Pseudomonas aeruginosa. American Journal of Physiology-Lung Cellular and Molecular Physiology.* 2007; **292**: L312-L322.
Song C, Li H, Zhang Y, Yu J. Effects of *Pseudomonas aeruginosa* and *Streptococcus mitis* mixed infection on TLR4-mediated immune response in acute pneumonia mouse model. *BMC Microbiology.* 2017; **17**: 82-89.
St Leger AJ, Desai JV, Drummond RA, Kugadas A, Almaghrabi F, Silver P Ravchaudhuri K, Gadjeva M, Iwakura Y, Lionakis MS, Caspi RR. An ocular commensal protects against corneal infection by driving an interleukin-17 response from mucosal γδ T cells. *Immunity.* 2017; **47**(1): 148-158.

Stearns JC, Davidson CJ, McKeon S, Whelan FJ, Fontes ME, Schryvers AB, Bowdish DM, Kellner JD, Surette MG. Culture and molecular-based profiles show shifts in bacterial communities of the upper respiratory tract that occur with age. *International Society for Microbial Ecology Journal.* 2015; **9**: 1246-1259.

Stressmann FA, Rogers GB, van der Gast CJ, Marsh P, Vermeer LS, Carroll MP, Hoffman L, Daniels TW, Patel N, Forbes B, Bruce KD. Lon-term cultivation-independent microbial diversity analysis demonstrates that bacterial communities infecting the adult cystic fibrosis lung show stability and resilience. *Thorax*. 2012; **67**: 867-873.

Strateva T, Yordanov D. *Pseudomonas aeruginosa* – a phenomenon of bacterial resistance. *Journal of Medical Microbiology.* 2009; **58**(9): 1133-48.

Tait Wojno ED, Artis D. Emerging concepts and future challenges in innate lymphoid cell biology. *Journal of Experimental Medicine.* 2016; **213**: 2229-2248.

Taylor SL, Wesselingh S, Rogers GB. Host-microbiome interactions in acute and chronic respiratory infections. *Cellular Microbiology.* 2016; **18**(5): 652-662.

Tenover FC. Mechanisms of antimicrobial resistance in bacteria. *American Journal of Medicine.* 2006; **119**: 3–10.

Teo SM, Mok D, Pham K, Kusel M, Serralha M, Troy N, Holt BJ, Hales BJ, Walker ML, Hollams E, Bochkov YA, Grindle K, Johnston SL, Gern JE, Sly PD, Holt PG, Holt KE, Inouyel M. The infant nasopharyngeal microbiome impacts severity of lower respiratory infection and risk of asthma development. *Cell Host Microbe.* 2015; **17**: 704-715.

Thomson SC, Hewlett RT. The fate of micro-organisms in inspired air. *Lancet.* 1896; **147**: 86-87.

Tredget EE, Shankowsky HA, Rennie R, Burrell RE, Logsetty S. *Pseudomonas* infections in the thermally injured patient. *Burns.* 2004; **30**(1): 3-26.

Vale PF, McNally L, Doeschl-Wilson A, King KC, Popat R, Domingo-Sananes MR, Allen JE, Soares MP, Kümmerli R. Beyond killing – Can we find new ways to manage infection? *Evolution, Medicine, and Public Health.* 2016; 148-157.

Veliz Rodriguez T, Moalli F, Polentarutti N, Paroni M, Bonavita E, Anselmo A, Nebuloni M, Mantero S, Jaillon S, Bragonzi A, Mantovani A, Riva F, Garlanda C. Role of Toll interleukin-1 receptor (IL-1R) 8, a negative regulator of IL-1R/Toll-like receptor signaling, in resistance to acute *Pseudomonas aeruginosa* lung infection. *Infection and Immunity.* 2012; **80:** 100-109.

Walker TS, Bais HP, Déziel E. *Pseudomonas aeruginosa*-plant root interactions. Pathogenicity, biofilm formation, and root exudation. *Plant Physiology.* 2004; **134**(1): 320-331.

Wang S, Zeng X, Yang Q, Qiao S. Antimicrobial peptides as potential alternatives to antibiotics in food animal industry. *International Journal of Molecular Sciences*. 2016; **17**(603).

Warnes G, Bolker B, Bonebakker L, Gentleman R, Huber W, Liaw A, Lumley T, Mächler M, Magnusson A, Möller S. gplots: various R programming tools for plotting data. R package version 2. 2005.

Wattam AR, Davis JJ, Assaf R, Boisvert S, Brettin T, Bun C, Conrad N, Dietrich EM, Disz T, Gabbard JL, Gerdes S, Henry CS, Kenyon RW, Machi D, Mao C, Nordberg EK, Olsen GJ, Murphy_olson DE, Olson R, Overbeek R, Parrello B, Pusch GD, Shulka M, Vonstein V, Warren A, Xia F, Yoo H, Stevens RL. Improvements to PATRIC, the all-bacterial Bioinformatics Database and Analysis Resource Center. *Nucleic Acids Research.* 2017; **45**(D1):D535-D542.

Whiley RA, Fleming EV, Makhija R, Waite RD. Environment and colonization sequence are key parameters driving cooperation and competition between *Pseudomonas aeruginosa* cystic fibrosis strains and oral commensal Streptococci. *PLoS ONE*. 2015; **10**(2): e0115513.

Wolbeling F, Munder A, Kerber-Momot T, Neumann D, Hennig G, Tummler B, Baumann U. Lung function and inflammation during murine *Pseudomonas aeruginosa* airway infection. *Immunobiology.* 2011; **216**: 901-908.

Wolpe SD, Cerami A. Macrophage inflammatory proteins 1 and 2: members of a novel superfamily of cytokines. *FASEB Journal.* 1989; **3**(14): 2565-73.

Wostmann BS. The germfree animal in nutritional studies. *Annual Review of Nutrition.* 1981; **1**: 257-279.

Wright GD. The antibiotic resistome: the nexus of chemical and genetic diversity. *Nature Reviews Microbiology.* 2007; **5**: 175-186.

Yoon GS, Dong C, Gao K, Kumar A, Standiford TJ, Yu FS. Interferon regulatory factor-1 in flagellin-induced reprogramming: potential protective role of CXCL10 in cornea innate defense against *Pseudomonas aeruginosa* infection. *Investigative Ophthalmology and Visual Science.* 2013; **54**(12): 7510-21

Yona S, Kim KW, Wolf Y, Mildner A, Varol D, Breker M, Strauss-Ayali D, Viukov S, Guilliams M, Misharin A, Hume DA, Perlman H, Malissen B, Zelzer E, Jung S. Fate mapping reveals origins and dynamics of monocytes and tissue macrophages under homeostasis. *Immunity.* 2013; **38**: 79-91.

Yun Y, Srinivas G, Kuenzel S, Linnenbrink M, Alnahas S, Bruce KD, Steinhoff U, Baines JF, Schaible UE. Environmental determined differences in the murine lung microbiota and their relation to alveolar architecture. *PLoS ONE.* 2014; **9**: e113466.

Yung SC, Murphy PM. Antimicrobial chemokines. *Frontiers in Immunology.* 2012;

3(276): 1-11.

Xu X, Shao B, Wang R, Zhou S, Tang Z, Lu W, Xiong S. Role of Interleukin-17 in defense against *Pseudomonas aeruginosa* infection in lungs. *International Journal of Clinical and Experimental Medecine.* 2014; **7**: 809-816.

Zhang H, Yeh C, Jin Z, Ding L, Liu BY, Zhang L, Dannelly HK. Prospective study of probiotic supplementation results in immune stimulation and improvement of upper respiratory infection rate. *Synthetic and Systems Biotechnologies.* 2018; **3**: 113-120.

Appendix

Table A.1 Strains capable of host-dependent *E. coli* inhibition. Bacteria from the human isolate library were incubated for 24 hours with Detroit-562 cells after which *E. coli* K12-*lux* was added and grown for an additional 24 hours. The bacteria capable of inhibiting the growth of *E. coli-lux* in a host-dependent manner were isolated and identified through 16S sequencing. (Data obtained from Dr. Steve Bernier)

Strain	Number of isolates
Pseudomonas aeruginosa	1
Staphylococcus epidermidis	2
Streptococcus mitis	5
Streptococcus parasanguinis	19
Streptococcus sanguinis	28
Staphylococcus aureus	13
Streptococcus oralis	10
Streptococcus agalactiae	2
Enterococcus faecium	17
Streptococcus massiliensis	1
Streptococcus cristatus	3
Streptococcus peroris	1
Escherichia coli	2
Streptococcus dentisani	1
Streptococcus salivarius	2
Enterobacter cloacae	2
Neisseria sicca	2

Total	111

Table A.2 Summary of the bacterial strains used in this study. Most bacterial strains were obtained from the Human isolates library composed of strains isolated from the airway of patients. The identity of the bacterial strains was verified by sequencing the 16S sequence.

Strain	**Origin**	**Identification number**	**Aerobic/Anaerobic**
Pseudomonas aeruginosa PA14	Obtained from Dr. Steve Bernier	N30F7	Aerobic
Neisseria sicca	Human isolates library	N33G1	Aerobic
Enterococcus faecium	Human isolates library	N17H11	Aerobic
Streptococcus mitis	Human isolates library	N2B6	Aerobic
Veillonella spp.	Human isolates library	N60H7	Anaerobic
Veillonella pervula	Human isolates library	GIL344	Anaerobic
Prevotella spp.	Human isolates library	N60H8	Anaerobic
Prevotella melanogenica	Human isolates library	C1009JK	Anaerobic
Bacteroides vulgatus	Human isolates library	HV08BH118	Anaerobic

Table A.3 Epithelial cells produced different cytokines in response to the bacteria they were exposed to. *Neisseria sicca*, *Enterococcus faecium*, *Streptococcus mitis*, and *Bacteroides vulgatus* were incubated for 24 hours with Detroit-562 cells after which *Pseudomonas aeruginosa* was added. After 24 hours of exposure, the cytokines and chemokines produced by the epithelial cells were measured using a Luminex multiplex assay (Eve technologies). The values of the different cytokines produced in response to the bacteria are indicated in pg/mL. A / represents values that were below the detection limit.

	Unstimulated	*N.sicca*	*E.faecium*	*S.mitis*	*B. vulgatus*	*N.sicca+ P.aeruginosa*	*E.faecium+ P.aeruginosa*	*S.mitis+ P.aeruginosa*	*B. vulgatus+ P.aeruginosa*	*P.aeruginosa*
FGF-2	52	137.6	14.3	0	70.7	148.3	0	8.2	107	1679
TGF-α	0	6	0.1	0	3.5	5.2	0	0.9	3.3	1.4
G-CSF	22.5	201.1	4.9	75.4	146.5	170	1.1	83.9	152	80.4
GM-CSF	33	1090.9	6.6	79.3	186.3	1247.1	10.1	204.8	181.1	87.2
GROα	8267.1	15937.7	4407.7	10550.8	10399.1	8397.4	4698.7	16723.6	8909.2	7259.3
PDGF-AA	831.8	66.3	43.7	65.4	104.4	65.8	36	113.8	93.9	354.6
PDGF-BB	170.5	610.4	151.7	182.6	296.2	505.4	159.9	218.1	267	229.8
IL-15	14.9	6.1	1.5	1	4.3	4.8	1.2	2.9	4.2	18.3
IL-1RA	3.3	27.8	95.1	26.2	91	20.3	76.1	35.2	82.5	68.4
IL-1α	18.5	42.1	12	19.6	40.3	42.1	12.3	29.7	78	365.1
IL-6	78.1	297.2	50.6	106.1	102.4	292.2	46.5	126.4	86.1	116.6
IL-7	5.4	2.8	0.4	0.5	1	2.3	0.3	1.4	1.1	3.5
IL-8	4691.3	5553.1	1476.3	5582.9	5510.5	5324.8	1110.1	6515.1	5496	6211.3
IP-10	194.2	30.9	10.7	14.2	2.6	10.5	8.1	24.2	2.3	5.6
MCP-1	1022.1	188.7	32.2	100	109	82.3	28.9	105.4	95.9	10.8
RANTES	30.1	10.4	7.7	9.4	9.5	5.8	6.8	10.4	9.3	3.4
TNFα	1.2	7.3	0.2	0.5	3.9	10.8	0.1	0.4	4.9	7.7
VEGF-A	447.6	447.6	170.7	447.6	437.2	358.4	169.1	447.6	307.9	65
IL-18	1.8	7.1	5.3	2.5	18.3	3.1	4.5	3.9	17.5	189.5
Flt-3F	/	/	/	/	/	/	/	/	/	/
Fractalkine	/	/	/	/	/	/	/	/	/	/
IFNα2	/	/	/	/	/	/	/	/	/	/
IFNγ	/	/	/	/	/	/	/	/	/	/
IL-10	/	/	/	/	/	/	/	/	/	/
MCP-3	/	/	/	/	/	/	/	/	/	/
IL-12p40	/	/	/	/	/	/	/	/	/	/
MDC	/	/	/	/	/	/	/	/	/	/
IL-1β	/	/	/	/	/	/	/	/	/	/
IL-4	/	/	/	/	/	/	/	/	/	/
MIP-1B	/	/	/	/	/	/	/	/	/	/

Table A.4 PCLS produced different cytokines in response to the bacteria they were exposed to. *Neisseria sicca*, *Enterococcus faecium*, *Streptococcus mitis*, and *Bacteroides vulgatus* were incubated for 24 hours with PCLS after which *Pseudomonas aeruginosa* was added. After 24 hours of exposure, the cytokines and chemokines produced by the PCLS were measured using a Luminex multiplex assay (Eve technologies). The values of the different cytokines produced in response to the bacteria are indicated in pg/mL. A / represents values that were below the detection limit.

Cytokine	*N. sicca*	*E. faecium*	*S. mitis*	*B. vulgatus*	*N. sicca* + *P. aeruginosa*	*E. faecium* + *P. aeruginosa*	*S. mitis* + *P. aeruginosa*	*B. vulgatus* + *P. aeruginosa*	*P. aeruginosa*	anaerobic *P. aeruginosa*	unstimulated	anaerobic unstimulated
G-CSF	168.9	199.6	412.5	1072.2	46.3	81.8	416.5	423	226	378.1	8.9	111.1
GM-CSF	299.1	37.1	329.2	265.6	104.4	28.1	267.3	487	274.2	555	7	26.6
IL-1α	66.7	6.4	43.9	16.9	42.2	2.9	42	84.7	60.7	65.5	1.2	2.3
IL-5	2.4	1.2	2.1	4.3	0.9	0.9	2.3	1	0.7	1.2	2.4	3
IL-6	681.1	703.2	905	2086	108.9	387.7	1177.2	11	11.1	6.5	68.6	147.8
IL-12p40	0.8	0.4	2.1	0.4	5.3	0	0.9	23.1	14.3	16.5	0.4	0
IL-17	0.6	1.8	0.5	11.3	0	0.3	0.9	0.1	0	0.1	0.1	0
IP-10	410.4	149.3	132.3	28	0.1	73.3	158	0	0	0.1	290.4	195.2
KC	1508.5	692.7	3506.9	9841.2	0.4	459.6	2641.7	0.9	0	0	764.6	1716.9
LIF	43.8	25.4	139.7	67.4	13.5	19.8	113	145.8	78.5	173	22.4	39.1
LIX	42.7	30.3	43.6	163.8	33	35.8	27.9	41	32.7	37.5	25.7	37.4
MCP-1	544.2	256.7	1085.3	3959.6	89	198.6	770.5	13	48.1	33.5	1853.8	1684.7
MIP-1α	176.7	72.8	159.5	542.7	26.4	59	182.4	24.9	21	19.8	31.6	42
MIP-1β	303	67.5	71.7	209	4.8	70.3	105.5	3.7	0	4.3	35.8	55.2
MIP-2	3825.7	1397.7	3558.9	11511.2	592.4	971.2	3524.4	311.9	394.7	673.5	56.1	283.2
RANTES	4.9	3.1	6.4	23.6	0.8	2.5	5.1	0.3	0.4	1.1	8.6	9.5
TNFα	15.9	3.2	5.5	100.6	12.6	3	6.2	2.9	2.3	1.9	4.6	4.9
VEGF	1	2.6	16.4	18.5	0.2	2	9.3	0.8	0.8	1.2	0.9	17.8
Eotaxin	/	/	/	/	/	/	/	/	/	/	/	/
IFNγ	/	/	/	/	/	/	/	/	/	/	/	/
IL-1β	/	/	/	/	/	/	/	/	/	/	/	/
IL-2	/	/	/	/	/	/	/	/	/	/	/	/
IL-3	/	/	/	/	/	/	/	/	/	/	/	/
IL-4	/	/	/	/	/	/	/	/	/	/	/	/
IL-7	/	/	/	/	/	/	/	/	/	/	/	/
IL-9	/	/	/	/	/	/	/	/	/	/	/	/
IL-10	/	/	/	/	/	/	/	/	/	/	/	/
IL-12p70	/	/	/	/	/	/	/	/	/	/	/	/
IL-13	/	/	/	/	/	/	/	/	/	/	/	/
IL-15	/	/	/	/	/	/	/	/	/	/	/	/
M-CSF	/	/	/	/	/	/	/	/	/	/	/	/
MIG	/	/	/	/	/	/	/	/	/	/	/	/

Table A.5 Summary of CARD data. Whole genome sequencing data was obtained for the different bacterial strains used in the study. These genomes were assembled with a5_MiSeq and annotated with prokka. CARD was then used to identify antibiotic resistance genes.

Neisseria sicca

RGI criteria	ARO term	SNP	Detection criteria	AMR gene family	Drug class	Resistance mechanism	% Identity of matching region	% length of reference sequence
Perfect	TEM-1	n/a	protein homolog model	TEM beta-lactamase	cephalosporin, monobactam, penam, penem	antibiotic inactivation	100	100
Perfect	sul2	n/a	protein homolog model	sulfonamide resistant sul	sulfonamide antibiotic, sulfone antibiotic	antibiotic target replacement	100	100
Strict	APH(6)-Id	n/a	protein homolog model	APH(6)	aminoglycoside antibiotic	antibiotic inactivation	100	42.09
Strict	APH(3'')-Ib	n/a	protein homolog model	APH(3'')	aminoglycoside antibiotic	antibiotic inactivation	99.63	100

Enterococcus faecium

RGI criteria	ARO term	SNP	Detection criteria	AMR gene family	Drug class	Resistance mechanism	% Identity of matching region	% length of reference sequence

Perfect	efmA	n/a	protein homolog model	major facilitator superfamily (MFS) antibiotic efflux pump	fluoroquinolone antibiotic, macrolide antibiotic	antibiotic efflux	100	100
Perfect	vanRA	n/a	protein homolog model	glycopeptide resistance gene cluster, vanR	glycopeptide antibiotic	antibiotic target alteration	100	100
Perfect	vanHA	n/a	protein homolog model	vanH, glycopeptide resistance gene cluster	glycopeptide antibiotic	antibiotic target alteration	100	100
Perfect	APH(3')-IIIa	n/a	protein homolog model	APH(3')	aminoglycoside antibiotic	antibiotic inactivation	100	100
Perfect	dfrG	n/a	protein homolog model	trimethoprim resistant dihydrofolate reductase dfr	diaminopyrimidine antibiotic	antibiotic target replacement	100	100
Strict	ANT(6)-Ia	n/a	protein homolog model	ANT(6)	aminoglycoside antibiotic	antibiotic inactivation	100	20.56
Strict	vanSA	n/a	protein homolog model	vanS, glycopeptide resistance gene cluster	glycopeptide antibiotic	antibiotic target alteration	99.74	98.96
Strict	vanA	n/a	protein homolog model	glycopeptide resistance gene cluster, van ligase	glycopeptide antibiotic	antibiotic target alteration	99.71	100
Strict	vanZA	n/a	protein homolog model	glycopeptide resistance gene cluster, vanZ	glycopeptide antibiotic	antibiotic target alteration	100	100
Strict	tet(L)	n/a	protein homolog model	major facilitator superfamily (MFS) antibiotic efflux pump	tetracycline antibiotic	antibiotic efflux	98.23	99.78
Strict	Enterococcus faecium liaR mutant conferring daptomycin	W73C	protein variant model	daptomycin resistant liaR	peptide antibiotic	antibiotic target alteration	98.1	100

	resistance							
Strict	vanXA	n/a	protein homolog model	glycopeptide resistance gene cluster, vanX	glycopeptide antibiotic	antibiotic target alteration	99.5	100
Strict	tetM	n/a	protein homolog model	tetracycline-resistant ribosomal protection protein	tetracycline antibiotic	antibiotic target protection	96.48	35.52
Strict	msrC	n/a	protein homolog model	ATP-binding cassette (ABC) antibiotic efflux pump	macrolide antibiotic, streptogramin antibiotic	antibiotic efflux	95.12	100
Strict	aad(6)	n/a	protein homolog model	ANT(6)	aminoglycoside antibiotic	antibiotic inactivation	100	84.42
Strict	SAT-4	n/a	protein homolog model	streptothricin acetyltransferase (SAT)	nucleoside antibiotic	antibiotic inactivation	99.44	100
Strict	ErmB	n/a	protein homolog model	Erm 23S ribosomal RNA methyltransferase	streptogramin antibiotic, macrolide antibiotic, lincosamide antibiotic	antibiotic target alteration	98.37	98.79
Strict	Enterococcus faecium liaS mutant conferring daptomycin resistance	T120A	protein variant model	daptomycin resistant liaS	peptide antibiotic	antibiotic target alteration	97.18	100
Strict	AAC(6')-Ii	n/a	protein homolog model	AAC(6')	aminoglycoside antibiotic	antibiotic inactivation	98.9	100
Strict	tet(W/N/W)	n/a	protein homolog model	tetracycline-resistant ribosomal protection protein	tetracycline antibiotic	antibiotic target protection	65.03	73.4
Strict	vanYA	n/a	protein homolog model	vanY, glycopeptide resistance	glycopeptide antibiotic	antibiotic target alteration	99.67	100

				gene cluster				
Strict	ErmT	n/a	protein homolog model	Erm 23S ribosomal RNA methyltransferase	streptogramin antibiotic, macrolide antibiotic, lincosamide antibiotic	antibiotic target alteration	99.18	100

Streptococcus mitis

RGI criteria	ARO term	SNP	Detection criteria	AMR gene family	Drug class	Resistance mechanism	% Identity of matching region	% length of reference sequence
Perfect	mel	n/a	protein homolog model	ATP-binding cassette (ABC) antibiotic efflux pump	streptogramin antibiotic, macrolide antibiotc	antibiotic efflux	100	100
Strict	mefA	n/a	protein homolog model	major facilitator superfamily (MFS) antibiotic efflux pump	macrolide antibiotic	antibiotic efflux	96.3	100

Bacteroides vulgatus

RGI criteria	ARO term	SNP	Detection criteria	AMR gene family	Drug class	Resistance mechanism	% Identity of matching region	% length of reference sequence
Perfect	CfxA3	n/a	protein homolog model	CfxA beta-lactamase	cephamycin	antibiotic inactivation	100	100
Strict	adeF	n/a	protein homolog model	resistance-nodulation-cell division	fluoroquinolone antibiotic, tetracycline antibiotic	antibiotic efflux	42.9	98.02

				(RND) antibiotic efflux pump				
Strict	tetQ	n/a	protein homolog model	tetracycline-resistant ribosomal protection protein	tetracycline antibiotic	antibiotic target protection	96.41	97.56
Strict	adeF	n/a	protein homolog model	resistance-nodulation-cell division (RND) antibiotic efflux pump	fluoroquinolone antibiotic, tetracycline antibiotic	antibiotic efflux	41.87	97.54

Pseudomonas aeruginosa

RGI criteria	ARO term	SNP	Detection criteria	AMR gene family	Drug class	Resistance mechanism	% Identity of matching region	% length of reference sequence
Perfect	FosA	n/a	protein homolog model	fosfomycin thiol transferase	fosfomycin	antibiotic inactivation	100	100
Strict	catB7	n/a	protein homolog model	chloramphenicol acetyltransferase (CAT)	phenicol antibiotic	antibiotic inactivation	98.11	100
Strict	PDC-3	n/a	protein homolog model	PDC beta-lactamase	cephalosporin, monobactam, carbapenem	antibiotic inactivation	99.24	100
Strict	basS	n/a	protein homolog model	pmr phosphoethanolamine transferase	peptide antibiotic	antibiotic target alteration	98.95	100
Strict	APH(3')-IIb	n/a	protein homolog model	APH(3')	aminoglycoside antibiotic	antibiotic inactivation	98.88	100
Strict	OXA-50	n/a	protein homolog model	OXA beta-lactamase	penam, cephalosporin	antibiotic inactivation	99.24	100

Strict	arnA	n/a	protein homolog model	pmr phosphoethanolamine transferase	peptide antibiotic	antibiotic target alteration	99.4	100

Table A.6 Summary of PATRIC data. Whole genome sequencing data was obtained for the different bacterial strains used in the study. These genomes were assembled with a5_MiSeq and annotated with RAST on PATRIC. PATRIC was then used to identify virulence genes.

Neisseria sicca

Source	Source ID	Product	Classification	Subject Coverage	Query Coverage	Identity	E-value
Victors	15676067	Translation elongation factor Tu		43	100	97	1e-91
Victors	254804371	3-dehydroquinate synthase (EC 4.2.3.4)		100	100	82	1e-174
Victors	254804701	D-glycero-beta-D-manno-heptose 1-phosphate adenylyltransferase (EC 2.7.7.70) / D-glycero-beta-D-manno-heptose-7-phosphate kinase (EC 2.7.1.167)		99	99	95	1e-172
VFDB	VFG037082	Zinc ABC transporter, substrate-binding protein ZnuA	Stress protein	99	99	85	1e-146
Victors	15676067	Translation elongation factor Tu		25	100	98	4e-53
Victors	15676837	5-methyltetrahydropteroyltriglutamate--homocysteine methyltransferase (EC 2.1.1.14)		100	100	97	0.0
Victors	161869147	Phosphotransferase system, phosphocarrier protein HPr		100	100	92	2e-39
VFDB	VFG036992	RND efflux system, inner membrane transporter	Efflux pump	99	98	90	0.0
Victors	161870678	Quinolinate synthetase (EC 2.5.1.72)		100	100	98	1e-212
Victors	56707643	Succinyl-CoA ligase [ADP-forming] beta chain (EC 6.2.1.5)		98	98	80	1e-173
Victors	15677630	Glutaredoxin 3		100	100	81	2e-34

Victors	121635346	NADP-specific glutamate dehydrogenase (EC 1.4.1.4)		99	99	93	1e-243
Victors	121634746	5,10-methylenetetrahydrofolate reductase (EC 1.5.1.20)		100	100	98	1e-167
VFDB	VFG037028	Catalase KatE (EC 1.11.1.6)	Stress protein	100	100	97	1e-304
Victors	15676067	Translation elongation factor Tu		91	99	98	1e-207
Victors	15676646	RNA-binding protein Hfq		83	84	96	1e-37
Victors	121634484	Ribonuclease III (EC 3.1.26.3)		89	100	85	1e-114
VFDB	VFG036956	Multidrug efflux system EmrAB-OMF, inner-membrane proton/drug antiporter EmrB (MFS type)	Efflux pump	86	86	84	1e-223
VFDB	VFG037100	Thiol:disulfide oxidoreductase associated with MetSO reductase / Peptide-methionine (S)-S-oxide reductase MsrA (EC 1.8.4.11) / Peptide-methionine (R)-S-oxide reductase MsrB (EC 1.8.4.12)	Stress protein	100	100	95	1e-302
Victors	15677021	UDP-N-acetylmuramate:L-alanyl-gamma-D-glutamyl-meso-diaminopimelate ligase (EC 6.3.2.-)		99	99	93	1e-257
Victors	121634217	Fructose-bisphosphate aldolase class II (EC 4.1.2.13)		100	100	97	1e-201
Victors	15676105	Acyl-[acyl-carrier-protein]--UDP-N-acetylglucosamine O-acyltransferase (EC 2.3.1.129)		100	100	94	1e-145
Victors	16272865	Catalase KatE (EC 1.11.1.6)		97	98	93	1e-287
Victors	126207906	Argininosuccinate synthase (EC 6.3.4.5)		96	95	89	1e-227
Victors	15677796	Phospholipid ABC transporter ATP-binding protein MlaF		100	100	97	1e-145
Victors	161869702	Polyribonucleotide nucleotidyltransferase (EC 2.7.7.8)		100	100	96	0.0
Victors	15676688	Phosphoglucomutase (EC 5.4.2.2) @ Phosphomannomutase (EC 5.4.2.8)		100	100	90	1e-244

Victors	15676225	2-keto-3-deoxy-D-arabino-heptulosonate-7-phosphate synthase I alpha (EC 2.5.1.54)		99	99	88	1e-181
Victors	15676538	UTP--glucose-1-phosphate uridylyltransferase (EC 2.7.7.9)		97	98	89	1e-146
VFDB	VFG037118	DNA repair protein RecN	Stress protein	98	99	90	1e-283
Victors	161870537	DedA protein		98	98	86	1e-112
VFDB	VFG006199	Type IV pilus assembly ATPase component PilU		99	97	84	1e-182
VFDB	VFG036974	RND efflux system, membrane fusion protein	Efflux pump	83	80	86	1e-167
Victors	15676725	ADP-L-glycero-D-manno-heptose-6-epimerase (EC 5.1.3.20)		100	100	96	1e-192
Victors	147675137	Na(+)-translocating NADH-quinone reductase subunit F (EC 1.6.5.8)		87	88	82	1e-181
VFDB	VFG018241	S-ribosylhomocysteine lyase (EC 4.4.1.21) @ Autoinducer-2 production protein LuxS	Regulation,Quorum sensing system	84	86	81	7e-65
VFDB	VFG037064	Zinc ABC transporter, permease protein ZnuB	Stress protein	97	97	84	1e-136
Victors	161870942	16S rRNA (cytosine(967)-C(5))-methyltransferase (EC 2.1.1.176)		99	99	92	1e-230
Victors	121635702	Phosphoenolpyruvate-protein phosphotransferase of PTS system (EC 2.7.3.9)		98	98	85	1e-295
VFDB	VFG000232	Twitching motility protein PilT	Adherence,Phase variation	99	99	88	1e-173

Enterococcus faecium

Source	Source ID	Product	Classification	Subject Coverage	Query Coverage	Identity	E-value
VFDB	VFG000077	ATP-dependent Clp protease proteolytic subunit ClpP (EC 3.4.21.92)	Stress protein	94	94	83	2e-85

Victors	29376708	Methionine aminopeptidase (EC 3.4.11.18)		100	100	87	1e-134
Victors	67043736	Peroxide stress regulator PerR, FUR family		86	85	87	2e-63
Victors	116516623	Adenylosuccinate lyase (EC 4.3.2.2) @ SAICAR lyase (EC 4.3.2.2)		93	94	85	1e-207
Victors	29375537	Maltose operon transcriptional repressor MalR, LacI family		99	98	87	1e-167
VFDB	VFG002197	Maltose operon transcriptional repressor MalR, LacI family	Biofilm formation	99	98	87	1e-167
Victors	29376139	Thymidylate synthase (EC 2.1.1.45)		100	100	82	1e-159
VFDB	VFG043511	hypothetical protein	Adherence,Biofilm formation	100	100	100	1e-178
Victors	16804506	ATP-dependent Clp protease proteolytic subunit ClpP (EC 3.4.21.92)		94	94	83	2e-85
Victors	76788416	Translation elongation factor LepA		98	98	83	1e-300
VFDB	VFG043518	Alcohol dehydrogenase (EC 1.1.1.1)	Adherence,MSCRAMM	100	100	100	0.0

Streptococcus mitis

Source	Source ID	Product	Classification	Subject Coverage	Query Coverage	Identity	E-value
Victors	15901608	hypothetical protein		80	57	84	2e-72
Victors	15901716	Oligopeptide transport system permease protein OppC (TC 3.A.1.5.1)		100	100	88	1e-158
Victors	15900716	Phosphopentomutase (EC 5.4.2.7)		100	100	93	1e-224
Victors	15899995	IMP cyclohydrolase (EC 3.5.4.10) / Phosphoribosylaminoimidazolecarboxamide formyltransferase (EC 2.1.2.3)		100	100	97	1e-291
Victors	15675920	tRNA-5-carboxymethylaminomethyl-2-thiouridine(34) synthesis protein MnmG		98	97	85	0.0

Victors	15675705	Fructose-bisphosphate aldolase class II (EC 4.1.2.13)		100	100	87	1e-147
Victors	15901021	Ribonuclease HII (EC 3.1.26.4)		96	96	82	1e-115
Victors	15901374	Probable cell division protein YtgP		100	97	87	1e-272
Victors	15901985	D-alanyl transfer protein DltB		100	99	87	1e-225
Victors	15900988	1,4-alpha-glucan (glycogen) branching enzyme, GH-13-type (EC 2.4.1.18)		99	99	91	0.0
Victors	225855490	Catabolite control protein A		99	99	90	1e-172
Victors	15901793	Aspartate--ammonia ligase (EC 6.3.1.1)		100	100	94	1e-186
Victors	15900088	N-acyl-L-amino acid amidohydrolase (EC 3.5.1.14)		100	100	94	1e-257
Victors	15901058	Galactose-6-phosphate isomerase, LacA subunit (EC 5.3.1.26)		99	99	97	2e-71
Victors	15900308	Membrane protein LiaF(VraT), specific inhibitor of LiaRS(VraRS) signaling pathway		100	100	87	1e-116
Victors	15900008	PTS system, galactosamine-specific IID component		100	99	97	1e-151
Victors	15900690	Lysyl aminopeptidase (EC 3.4.11.15)		99	99	92	0.0
Victors	15901469	Two-component transcriptional response regulator, OmpR family		100	100	93	1e-120
Victors	194397931	Phosphoribosylformylglycinamidine synthase, synthetase subunit (EC 6.3.5.3) / Phosphoribosylformylglycinamidine synthase, glutamine amidotransferase subunit (EC 6.3.5.3)		100	100	92	0.0
Victors	15900530	Oxygen-insensitive NAD(P)H nitroreductase (EC 1.-.-.-) / Dihydropteridine reductase (EC 1.5.1.34)		100	100	96	1e-106
Victors	15901825	Efflux ABC transporter, permease protein		100	100	90	1e-12

							6
Victors	15901689	Glycine betaine ABC transport system, ATP-binding protein OpuAA (EC 3.6.3.32)		99	99	89	1e-122
Victors	15901146	Uracil permease @ Uracil:proton symporter UraA		97	100	96	1e-234
Victors	15900979	DegV family protein		100	100	84	1e-130
Victors	15901422	Maltodextrin ABC transporter, ATP-binding protein MsmX		100	100	96	1e-208
Victors	15900035	ABC transporter, substrate-binding protein (cluster 1, maltose/g3p/polyamine/iron)		100	99	90	1e-266
Victors	15900889	Thymidine kinase (EC 2.7.1.21)		100	100	95	1e-108
Victors	15901609	Oligoendopeptidase F-like protein		100	100	97	0.0
Victors	15901065	DNA repair protein RecN		100	100	88	1e-283
Victors	15900982	Positive transcriptional regulator, MutR family		99	99	87	1e-147
Victors	15901821	L-asparaginase (EC 3.5.1.1)		100	100	87	1e-163
Victors	194396773	Response regulator CsrR		100	100	89	1e-114
Victors	15901787	DNA-entry nuclease (Competence-specific nuclease) (EC 3.1.30.-)		85	84	88	1e-117
Victors	15900269	ClpE-like protein		90	90	92	0.0
Victors	15900362	Acetolactate synthase large subunit (EC 2.2.1.6)		100	100	94	0.0
Victors	116515636	Undecaprenyl-diphosphatase (EC 3.6.1.27)		100	100	89	1e-142
Victors	116516623	Adenylosuccinate lyase (EC 4.3.2.2) @ SAICAR lyase (EC 4.3.2.2)		100	100	96	1e-246
Victors	15900957	Glutamine amidotransferase, class I		100	100	91	1e-122

Victors	116515895	Manganese ABC transporter, ATP-binding protein SitB		100	100	96	1e-130
Victors	159000796	Arginine decarboxylase (EC 4.1.1.19)		98	99	94	1e-269
Victors	159000394	Trk potassium uptake system protein TrkH		100	100	88	1e-246
Victors	159001980	Zinc ABC transporter, permease protein AdcB		98	98	94	1e-132
Victors	159001254	Phosphate ABC transporter, periplasmic phosphate-binding protein PstS (TC 3.A.1.7.1)		100	100	81	1e-136
Victors	159000508	ABC transporter, ATP-binding protein Vex2		98	98	94	1e-109
Victors	159001009	Toxin HigB		82	95	86	3e-45
Victors	116516913	Aminopeptidase C (EC 3.4.22.40)		100	100	97	1e-254
Victors	159001252	Phosphate transport system permease protein PstA (TC 3.A.1.7.1)		93	100	95	1e-147
Victors	159001333	ATP-dependent RNA helicase YfmL		100	100	93	1e-193
Victors	159002668	ABC transporter, permease protein (cluster 3, basic aa/glutamine/opines)		100	100	94	1e-118
Victors	159001923	Maltodextrin ABC transporter, substrate-binding protein MdxE		99	99	86	1e-216
Victors	159001763	MATE efflux family protein DinF		100	100	83	1e-219
Victors	159000043	FIG014387: Transcriptional regulator, PadR family		100	100	85	6e-47
Victors	116516216	ATP-dependent Clp protease proteolytic subunit ClpP (EC 3.4.21.92)		100	100	95	1e-102
Victors	159000856	Oligoendopeptidase F		100	100	90	0.0
Victors	159002667	ABC transporter, permease protein (cluster 3, basic aa/glutamine/opines)		100	100	97	1e-120
Victors	76788416	Translation elongation factor LepA		99	99	94	0.0

Victors	118090028	Na+/H+ antiporter		100	100	82	0.0
Victors	15901254	Phosphate ABC transporter, periplasmic phosphate-binding protein PstS (TC 3.A.1.7.1)		32	100	83	6e-38
Victors	15901956	alpha-mannosidase (EC 3.2.1.24)		99	100	88	0.0
Victors	15901682	Galactose operon repressor, GalR-LacI family of transcriptional regulators		99	99	84	1e-161
Victors	15901707	FIG009886: phosphoesterase		100	100	89	5e-91
Victors	15900083	Uncharacterized MFS-type transporter		100	100	95	1e-211
Victors	15900916	Transcription regulator [contains diacylglycerol kinase catalytic domain]		99	99	84	1e-141
Victors	116515802	Phosphoribosylglycinamide formyltransferase (EC 2.1.2.2)		95	94	89	2e-87
Victors	15900084	Branched-chain amino acid transport protein azlC		99	78	94	1e-114
Victors	15901236	Glucan 1,4-alpha-maltohexaosidase (EC 3.2.1.98)		98	99	86	1e-261
Victors	221232937	Serine protease, DegP/HtrA, do-like (EC 3.4.21.-)		86	86	81	1e-157
Victors	15903398	ABC transporter, permease protein (cluster 3, basic aa/glutamine/opines)		91	100	89	1e-105
Victors	15900199	6-phospho-beta-glucosidase (EC 3.2.1.86)		100	100	92	1e-266
Victors	15900564	UPF0340 protein YwlG		96	96	82	6e-81
Victors	15901765	ADP-ribose pyrophosphatase of COG1058 family (EC 3.6.1.13) / Nicotinamide-nucleotide amidase (EC 3.5.1.42)		99	98	85	1e-199
Victors	15900700	Septation ring formation regulator EzrA		100	100	80	1e-269
Victors	15900208	DNA polymerase III polC-type (EC 2.7.7.7)		100	100	92	0.0
Victors	116516669	NADH peroxidase (EC 1.11.1.1)		100	100	97	1e-260

Victors	15900729	Pyrimidine-nucleoside phosphorylase (EC 2.4.2.2)		96	96	89	1e-206
Victors	15901551	Efflux ABC transporter, ATP-binding protein		100	100	94	1e-159
Victors	15900843	Fibronectin/fibrinogen-binding protein		99	99	89	1e-287
Victors	15900807	Cysteine and methionine metabolism regulator CmbR, LysR family		100	100	94	1e-163
Victors	15900822	Methylenetetrahydrofolate--tRNA-(uracil-5-)-methyltransferase TrmFO (EC 2.1.1.74)		97	99	95	1e-248
VFDB	VFG000964	UTP--glucose-1-phosphate uridylyltransferase (EC 2.7.7.9)	Antiphagocytosis,Adherence,Tissue invasion	96	98	87	1e-145
Victors	15901481	Guanosine-3',5'-bis(diphosphate) 3'-pyrophosphohydrolase (EC 3.1.7.2) / GTP pyrophosphokinase (EC 2.7.6.5), (p)ppGpp synthetase II		88	88	94	0.0
Victors	15900566	Para-aminobenzoate synthase, aminase component (EC 2.6.1.85) / Aminodeoxychorismate lyase (EC 4.1.3.38)		100	100	86	1e-298
Victors	15901018	hypothetical protein		98	98	84	1e-197
Victors	15902771	ABC transporter, permease protein (cluster 3, basic aa/glutamine/opines)		99	100	91	1e-118
Victors	15901382	Streptococcal lipoprotein rotamase A; Peptidyl-prolyl cis-trans isomerase (EC 5.2.1.8)		100	100	89	1e-249
Victors	15901718	Oligopeptide ABC transporter, periplasmic oligopeptide-binding protein OppA (TC 3.A.1.5.1)		100	100	81	0.0
Victors	116515749	GTP-sensing transcriptional pleiotropic repressor CodY		100	100	92	1e-135
Victors	15901916	Lead, cadmium, zinc and mercury transporting ATPase (EC 3.6.3.3) (EC 3.6.3.5); Copper-translocating P-type ATPase (EC 3.6.3.4)		100	100	97	0.0

Victors	15900548	PTS system, galactose-specific IIA component (EC 2.7.1.204)		95	100	87	1e-74
Victors	15900038	Rhodanese domain protein UPF0176, Firmicutes subgroup		98	98	94	1e-187
VFDB	VFG001359	Manganese ABC transporter, periplasmic-binding protein SitA	Manganese uptake,ABC transporter	100	100	92	1e-168
Victors	116516199	S-ribosylhomocysteine lyase (EC 4.4.1.21) @ Autoinducer-2 production protein LuxS		100	100	98	8e-89
Victors	116516771	Manganese ABC transporter, inner membrane permease protein SitD		100	100	99	1e-151
Victors	15901250	Phosphate transport ATP-binding protein PstB (TC 3.A.1.7.1)		100	100	95	1e-134
Victors	15901549	Efflux ABC transporter, ATP-binding protein		45	97	91	1e-113
Victors	15900985	Predicted glycogen debranching enzyme (pullulanase-like, but lacking signal peptide)		91	91	82	0.0
Victors	15901646	Anthranilate synthase, aminase component (EC 4.1.3.27)		100	100	92	1e-247
Victors	15900978	Uncharacterized UPF0750 membrane protein YpjC		95	93	81	1e-127
Victors	116516276	Spermidine/putrescine import ABC transporter substrate-binding protein PotD (TC 3.A.1.11.1)		100	100	92	1e-196
Victors	15901609	Oligoendopeptidase F-like protein		39	92	94	1e-130
Victors	15901675	Xanthine phosphoribosyltransferase (EC 2.4.2.22)		99	99	84	5e-87
Victors	15903537	Manganese ABC transporter, periplasmic-binding protein SitA		100	100	93	1e-168
Victors	15900070	Ribosomal-protein-S18p-alanine acetyltransferase (EC 2.3.1.128)		100	100	92	4e-70
Victors	15900760	PTS system, fructose-specific IIA component (EC 2.7.1.202) / PTS system, fructose-specific IIB component (EC 2.7.1.202) / PTS system, fructose-specific IIC component		99	99	94	0.0

Victors	15901231	3-dehydroquinate dehydratase I (EC 4.2.1.10)		99	99	87	1e-110
Victors	15900894	Acetyltransferase, GNAT family		99	99	83	3e-63
VFDB	VFG005197	Fibronectin/fibrinogen-binding protein	Adherence	98	99	89	1e-285
Victors	15901145	16S rRNA (guanine(527)-N(7))-methyltransferase (EC 2.1.1.170)		100	100	89	1e-119
Victors	15900263	hypothetical protein		100	100	83	9e-82
Victors	15901644	Anthranilate phosphoribosyltransferase (EC 2.4.2.18)		99	99	91	1e-171
Victors	15901387	Aspartate aminotransferase (EC 2.6.1.1)		98	99	85	1e-194
Victors	15900874	Cationic amino acid transporter - APC Superfamily		99	98	84	1e-231
Victors	15901232	Putative ribosomal RNA large subunit methyltransferase YwbD		91	91	85	1e-179
Victors	116515547	Superoxide dismutase [Mn] (EC 1.15.1.1)		100	100	96	1e-112
Victors	169832534	Pyruvate oxidase (EC 1.2.3.3)		100	100	97	0.0
Victors	15900495	5,10-methylenetetrahydrofolate reductase (EC 1.5.1.20)		100	100	96	1e-161
Victors	15900063	Ribonuclease J1 (endonuclease and 5' exonuclease)		100	100	97	0.0
Victors	15900176	Phosphoglycerate mutase family protein		97	96	91	1e-119
Victors	169832640	Glutamine synthetase type I (EC 6.3.1.2)		100	100	97	1e-263
Victors	15900408	CTP synthase (EC 6.3.4.2)		99	99	96	1e-305
Victors	15900189	Leucyl-tRNA synthetase (EC 6.1.1.4)		100	100	96	0.0
Victors	15900741	Branched-chain amino acid aminotransferase (EC 2.6.1.42)		100	100	96	1e-196

Victors	15901645	Anthranilate synthase, amidotransferase component (EC 4.1.3.27) @ Para-aminobenzoate synthase, amidotransferase component (EC 2.6.1.85)		100	100	91	1e-96
Victors	15900177	Ferric iron ABC transporter, ATP-binding protein		99	99	92	1e-193
Victors	221232257	hypothetical protein		100	100	85	9e-84
Victors	15901717	Oligopeptide transport system permease protein OppB (TC 3.A.1.5.1)		100	100	92	1e-274
Victors	15900079	Positive transcriptional regulator, MutR family		100	100	90	1e-147
Victors	15901955	N-acetylmannosamine kinase (EC 2.7.1.60)		100	100	88	1e-152
Victors	15901482	MBL-fold metallo-hydrolase superfamily		100	100	93	1e-117
Victors	15901433	Xaa-Pro dipeptidase (EC 3.4.13.9)		100	100	95	1e-200
Victors	15900900	23S rRNA (uracil(1939)-C(5))-methyltransferase (EC 2.1.1.190)		82	99	93	1e-247
Victors	182684099	Mutator MutT protein (7,8-dihydro-8-oxoguanine-triphosphatase) (EC 3.6.1.-)		100	100	99	3e-90
Victors	15901683	Alcohol dehydrogenase (EC 1.1.1.1)		99	99	90	1e-182
Victors	15901472	Rrf2 family transcriptional regulator, group III		97	97	85	2e-62
Victors	116515465	Two component system response regulator CiaR		90	100	93	1e-116
Victors	15901138	Pyrimidine operon regulatory protein PyrR		100	100	97	2e-89
Victors	15901799	Pyruvate formate-lyase activating enzyme (EC 1.97.1.4)		100	100	95	1e-149
Victors	15900522	Tributyrin esterase		99	99	89	1e-138

Victors	15902017	Cysteine synthase (EC 2.5.1.47)		99	99	94	1e-159
Victors	15901253	Phosphate transport system permease protein PstC (TC 3.A.1.7.1)		100	100	94	1e-159

Bacteroides vulgatus

Source	Source ID	Product	Classification	Subject coverage	Query Coverage	Identity	E-value
Victors	15900252	2-dehydro-3-deoxy-D-gluconate 5-dehydrogenase (EC 1.1.1.127) @ 2-deoxy-D-gluconate 3-dehydrogenase (EC 1.1.1.125)		95	97	81	1e-121

Pseudomonas aeruginosa

Source	Source ID	Product	Classification	Subject Coverage	Query Coverage	Identity	E-value
Victors	116054099	hypothetical protein		98	50	100	2e-52
VFDB	VFG002066	T6SS secretion lipoprotein TssJ (VasD)	Secretion system,Type VI secretion system	100	100	100	2e-83
Victors	116050053	Outer membrane low permeability porin, OprD family => OccK3/OpdO pyroglutamate, cefotaxime uptake		100	100	99	1e-238
VFDB	VFG002062	T6SS associated component TagF (ImpM)	Secretion system,Type VI secretion system	100	100	99	1e-131
VFDB	VFG001231	still frameshift probable component of chemotactic signal transduction system	Adherence,Twitching motility	100	100	99	0.0
Victors	15596793	Chaperone protein HtpG		100	100	100	0.0
VFDB	VFG000172	Phenazine-specific methyltransferase PhzM	Pigment,Antimicrobial activity	100	100	100	1e-190

Victors	15599886	Protein-methionine-sulfoxide reductase catalytic subunit MsrP		100	100	98	1e-198
Victors	116053966	Transcriptional regulator, MarR family		97	100	100	4e-81
VFDB	VFG001223	Twitching motility protein PilT	Adherence,Twitching motility	100	100	100	1e-194
VFDB	VFG000213	Type III secretion protein (YscE)	Secretion system,Type III secretion system	100	100	97	6e-28
Victors	15600047	IMP cyclohydrolase (EC 3.5.4.10) / Phosphoribosylaminoimidazolecarboxamide formyltransferase (EC 2.1.2.3)		100	100	100	1e-309
VFDB	VFG000123	Alginate polymerase/glycosyltransferase Alg8	Antiphagocytosis,Serum resistance	99	100	100	1e-291
VFDB	VFG000114	Leader peptidase (Prepilin peptidase) (EC 3.4.23.43) / N-methyltransferase (EC 2.1.1.-)	Adherence,Twitching motility	100	100	98	1e-169
VFDB	VFG001226	twitching motility protein PilH	Adherence,Twitching motility	100	100	100	7e-63
VFDB	VFG014694	Flagellar motor rotation protein MotA		100	100	98	1e-155
VFDB	VFG016038	Pyoverdine sidechain non-ribosomal peptide synthetase PvdJ @ Siderophore biosynthesis non-ribosomal peptide synthetase modules		82	98	99	0.0
VFDB	VFG000149	EXOU	Toxin,Type III translocated protein,Phospholipase	100	100	99	0.0
VFDB	VFG014681	Flagellar motor rotation protein MotB		100	100	100	1e-200
VFDB	VFG000133	Mannose-1-phosphate guanylyltransferase (EC 2.7.7.13) / Mannose-6-phosphate isomerase (EC 5.3.1.8)	Antiphagocytosis,Serum resistance	100	100	99	1e-284
VFDB	VFG002059	ABC transporter, ATP-binding protein	Secretion system,Type VI secretion system	100	100	98	1e-131

VFDB	VFG000174	General secretion pathway protein M	Secretion system,Type II secretion system	100	100	100	3e-93
Victors	15598197	NADPH-dependent glyceraldehyde-3-phosphate dehydrogenase (EC 1.2.1.13)		100	94	99	1e-266
Victors	116049764	FIG005121: SAM-dependent methyltransferase (EC 2.1.1.-)		100	100	100	1e-151
VFDB	VFG000182	General secretion pathway protein E	Secretion system,Type II secretion system	100	100	100	1e-287
VFDB	VFG016058	Pyoverdine chromophore precursor synthetase PvdL @ Siderophore biosynthesis non-ribosomal peptide synthetase modules		100	100	99	0.0
VFDB	VFG000209	Type III secretion negative regulator (LscZ)	Secretion system,Type III secretion system	100	100	99	1e-160
VFDB	VFG001208	Type IV fimbrial biogenesis protein PilW	Adherence,Twitching motility	100	100	99	1e-155
VFDB	VFG000165	Pyochelin synthetase PchF, non-ribosomal peptide synthetase module @ Siderophore biosynthesis non-ribosomal peptide synthetase modules	Iron uptake,Siderophore	100	100	98	0.0
VFDB	VFG000126	Alginate export system Algk/AlgE, outer membrane porin AlgE	Antiphagocytosis,Serum resistance	100	100	100	1e-299
VFDB	VFG000180	General secretion pathway protein G	Secretion system,Type II secretion system	100	100	99	2e-82
VFDB	VFG000135	Sigma factor RpoE negative regulatory protein RseB precursor	Antiphagocytosis,Serum resistance	100	100	99	1e-181
VFDB	VFG000111	Type IV pilin PilA	Adherence,Twitching motility	100	100	91	2e-71
VFDB	VFG000183	General secretion pathway protein C	Secretion system,Type II secretion system	100	100	100	1e-129
VFDB	VFG002058	ABC-type antimicrobial peptide transport system, permease component	Secretion system,Type VI secretion	100	100	99	1e-220

			system				
VFDB	VFG014997	hypothetical protein		100	100	98	2e-44
VFDB	VFG001258	Flagellar biosynthesis protein FliO	Adherence,Motility	100	100	100	2e-79
VFDB	VFG000185	Type III secretion inner membrane protein (YscU,SpaS,EscU,HrcU,SsaU, homologous to flagellar export components)	Secretion system,Type III secretion system	100	100	99	1e-192
VFDB	VFG000193	Type III secretion outermembrane contact sensing protein (YopN,Yop4b,LcrE)	Secretion system,Type III secretion system	100	100	100	1e-155
VFDB	VFG000160	PvdE, pyoverdine ABC export system, fused ATPase and permease components	Iron uptake,Siderophore,Pigment	100	100	100	1e-314
VFDB	VFG000197	Chaperone protein YscY (Yop proteins translocation protein Y)	Secretion system,Type III secretion system	100	100	100	7e-56
VFDB	VFG001244	Flagellar hook-associated protein FlgK	Adherence,Motility	100	100	87	0.0
VFDB	VFG000161	Pyoverdine sidechain non-ribosomal peptide synthetase PvdD @ Siderophore biosynthesis non-ribosomal peptide synthetase modules	Iron uptake,Siderophore,Pigment	46	100	99	0.0
VFDB	VFG001250	Flagellar hook-basal body complex protein FliE	Adherence,Motility	100	100	100	5e-53
VFDB	VFG001207	Type IV fimbrial biogenesis protein PilV	Adherence,Twitching motility	100	100	98	1e-101
VFDB	VFG001225	twitching motility protein PilG	Adherence,Twitching motility	100	100	100	4e-71
Victors	15600137	RNA-binding protein Hfq		100	100	100	4e-40
VFDB	VFG000220	Type III secretion cytoplasmic protein (YscL)	Secretion system,Type III secretion system	100	100	99	1e-114
VFDB	VFG000173	FAD-dependent monooxygenase PhzS	Pigment,Antimicrobial activity	100	100	99	1e-232
Victors	15595239	Putative large exoprotein involved in heme utilization or adhesion of ShlA/HecA/FhaA family		3	94	96	3e-61

Victors	116050342	Pyoverdine sidechain non-ribosomal peptide synthetase PvdI @ Siderophore biosynthesis non-ribosomal peptide synthetase modules		14	99	99	0.0
Victors	15595781	CCA tRNA nucleotidyltransferase (EC 2.7.7.72)		100	100	99	1e-238
Victors	15600271	Glucans biosynthesis protein G precursor		100	100	100	0.0
Victors	15595962	Sigma factor RpoE regulatory protein RseC		100	100	100	5e-79
VFDB	VFG001212	Type IV pilus biogenesis protein PilE	Adherence,Twitching motility	100	100	100	9e-76
VFDB	VFG002075	T6SS component TssG (ImpH/VasB)	Secretion system,Type VI secretion system	100	100	100	1e-211
VFDB	VFG041011	VgrG protein		100	100	98	0.0
VFDB	VFG001253	Flagellar assembly protein FliH	Adherence,Motility	100	100	100	1e-151
Victors	15598091	hypothetical protein		100	100	98	1e-136
Victors	15600505	Aldehyde dehydrogenase (EC 1.2.1.3)		100	100	100	1e-289
VFDB	VFG000169	Pyochelin biosynthetic protein PchC, predicted thioesterase @ Thioesterase in siderophore biosynthesis gene cluster	Iron uptake,Siderophore	100	100	99	1e-142
VFDB	VFG001251	Flagellar M-ring protein FliF	Adherence,Motility	100	100	100	0.0
VFDB	VFG001267	ABC efflux pump, fused inner membrane and ATPase subunits in pyochelin gene cluster @ Putative ABC iron siderophore transporter, fused permease and ATPase domains	Iron uptake,Siderophore	100	100	99	0.0
VFDB	VFG000146	Vibriolysin, extracellular zinc protease (EC 3.4.24.25) @ Pseudolysin, extracellular zinc protease (EC 3.4.24.26)	Protease,Zinc metalloproteinase	100	100	98	1e-294
VFDB	VFG014629	RNA polymerase sigma factor for flagellar operon		96	100	100	1e-132

VFDB	VFG016038	Pyoverdine sidechain non-ribosomal peptide synthetase PvdJ @ Siderophore biosynthesis non-ribosomal peptide synthetase modules		12	100	99	1e-147
VFDB	VFG000159	L-ornithine 5-monooxygenase (EC 1.13.12.-), PvdA of pyoverdin biosynthesis @ Siderophore biosynthesis protein, monooxygenase	Iron uptake,Siderophore,Pigment	100	100	100	1e-258
Victors	15600630	LysR family transcriptional regulator PA5437		100	98	100	1e-173
VFDB	VFG000115	hypothetical protein	Toxin,Intracellular toxin,ADP-ribosyltransferase,A-B type,Molecular mimicry	100	100	99	0.0
VFDB	VFG000161	Pyoverdine sidechain non-ribosomal peptide synthetase PvdD @ Siderophore biosynthesis non-ribosomal peptide synthetase modules	Iron uptake,Siderophore,Pigment	21	100	99	1e-313
VFDB	VFG002060	T6SS Serine/threonine protein kinase (EC 2.7.11.1) PpkA	Secretion system,Type VI secretion system	100	100	99	0.0
Victors	15599958	Ferric uptake regulation protein FUR		100	100	100	6e-71
VFDB	VFG015506	Phenazine biosynthesis protein PhzB		96	96	93	5e-87
VFDB	VFG015045	RhlC, TDP-rhamnosyltransferase 2 (EC 2.4.1.-)		100	100	96	1e-181
VFDB	VFG000211	Type III secretion outermembrane pore forming protein (YscC,MxiD,HrcC, InvG)	Secretion system,Type III secretion system	100	100	99	0.0
Victors	15595239	Putative large exoprotein involved in heme utilization or adhesion of ShlA/HecA/FhaA family		14	100	99	1e-281
Victors	15596206	Glycine cleavage system transcriptional antiactivator GcvR		100	100	100	1e-104
VFDB	VFG001243	Flagellar protein FlgJ [peptidoglycan hydrolase]	Adherence,Motility	100	100	99	1e-228
Victors	15595239	Putative large exoprotein involved in heme utilization or		19	93	99	0.0

		adhesion of ShlA/HecA/FhaA family					
VFDB	VFG000208	Type III secretion thermoregulatory protein (LcrF,VirF,transcription regulation of virulence plasmid)	Secretion system,Type III secretion system	100	100	100	1e-161
Victors	116049673	Type III secretion bridge between inner and outermembrane lipoprotein (YscJ,HrcJ,EscJ, PscJ)		97	99	100	1e-131
Victors	15596445	Type I secretion outer membrane protein, TolC family @ ABC-type protease exporter, outer membrane component PrtF/AprF		100	100	99	1e-275
VFDB	VFG000206	FIG00962212: hypothetical protein	Secretion system,Type III secretion system	100	100	96	2e-37
Victors	15599684	Uncharacterized protein YfaQ		100	100	98	0.0
VFDB	VFG041046	hypothetical protein		100	100	98	6e-88
VFDB	VFG000207	Type III secretion transporter lipoprotein (YscW,VirG)	Secretion system,Type III secretion system	100	100	98	3e-71
VFDB	VFG000116	Alginate biosynthesis two-component system response regulator AlgB	Antiphagocytosis,Serum resistance	100	100	99	1e-253
VFDB	VFG001235	probable chemotaxis protein	Adherence,Twitching motility	100	100	99	1e-114
VFDB	VFG000145	LasA protease precursor	Protease,Serine protease	100	100	98	1e-245
VFDB	VFG000194	Type III secretion outermembrane negative regulator of secretion (TyeA)	Secretion system,Type III secretion system	100	100	100	7e-46
Victors	15598951	L,D-transpeptidase		100	100	100	3e-95
VFDB	VFG014473	Flagellar hook-length control protein FliK		100	100	97	1e-238
VFDB	VFG015994	Pyoverdin biosynthesis protein PvdN, putative aminotransferase, class V		100	100	99	1e-251
VFDB	VFG000130	Probable poly(beta-D-mannuronate) O-acetylase (EC	Antiphagocytosis,Serum	100	100	99	1e-31

		2.3.1.-)	resistance				0
VFDB	VFG000198	Type III secretion inner membrane channel protein (LcrD,HrcV,EscV,SsaV)	Secretion system,Type III secretion system	100	100	99	0.0
VFDB	VFG044080	PvcB protein, related to amino acid oxidizing enzymes		100	100	99	1e-175
Victors	15597622	Sigma factor PvdS, controling pyoverdin biosynthesis		100	100	100	1e-102
VFDB	VFG000155	RhlB, TDP-rhamnosyltransferase 1 (EC 2.4.1.-)	Biosurfactant	100	100	100	1e-257
VFDB	VFG002077	VgrG protein	Secretion system,Type VI secretion system	100	99	99	0.0
VFDB	VFG000177	General secretion pathway protein J	Secretion system,Type II secretion system	100	100	100	1e-137
Victors	15595242	hypothetical protein		100	100	99	1e-256
Victors	116052272	Catalase KatE (EC 1.11.1.6)		100	100	100	1e-296
VFDB	VFG000190	Type III secretion protein (YscP)	Secretion system,Type III secretion system	36	99	99	5e-70
Victors	15598482	beta-ketodecanoyl-[acyl-carrier-protein] synthase (EC 2.3.1.207)		99	93	99	1e-198
Victors	116048767	Phospholipase C (EC 3.1.4.3) => hemolytic PlcH		100	100	99	0.0
Victors	15676067	Translation elongation factor Tu		27	100	87	3e-51
VFDB	VFG000153	N-butanoyl-L-homoserine lactone synthase @ N-acyl-L-homoserine lactone synthase, LuxI family (EC 2.3.1.184)	Regulation,Quorum sensing system	100	100	99	1e-112
VFDB	VFG014984	Outer membrane stress sensor protease DegS		100	100	99	1e-220
Victors	15595959	RNA polymerase sigma factor RpoE		100	100	100	1e-106

VFDB	VFG002074	T6SS component TssF (ImpG/VasA)	Secretion system,Type VI secretion system	100	100	99	0.0
VFDB	VFG001238	Flagellar hook protein FlgE	Adherence,Motility	100	100	99	1e-270
VFDB	VFG002063	T6SS component TssM (IcmF/VasK)	Secretion system,Type VI secretion system	100	93	99	0.0
VFDB	VFG002076	T6SS AAA+ chaperone ClpV (TssH)	Secretion system,Type VI secretion system	100	100	99	0.0
Victors	116048914	EXOU		100	100	99	0.0
VFDB	VFG016046	Pyoverdin biosynthesis protein PvdH, L-2,4-diaminobutyrate:2-oxoglutarate aminotransferase (EC 2.6.1.76)		100	100	100	1e-273
VFDB	VFG000118	Alginate regulatory protein AlgQ, positive transcriptional regulator of AlgD	Antiphagocytosis,Serum resistance	100	100	100	6e-90
VFDB	VFG000201	Type III secretion cytoplasmic LcrG inhibitor (LcrV,secretion and targeting control protein, V antigen)	Secretion system,Type III secretion system	100	100	98	1e-161
VFDB	VFG001241	Flagellar L-ring protein FlgH	Adherence,Motility	100	100	100	1e-131
Victors	15600324	2,3-bisphosphoglycerate-independent phosphoglycerate mutase (EC 5.4.2.12)		100	100	99	1e-300
VFDB	VFG000124	Alginate polymerisation protein Alg44, membrane fusion protein	Antiphagocytosis,Serum resistance	100	100	100	1e-222
VFDB	VFG001233	probable chemotaxis protein	Adherence,Twitching motility	100	100	98	2e-87
VFDB	VFG000144	Secreted alkaline metalloproteinase (EC 3.4.24.-), PrtA/B/C/G homolog	Protease	100	100	99	1e-281
VFDB	VFG001237	Flagellar basal-body rod modification protein FlgD	Adherence,Motility	100	100	100	1e-129
VFDB	VFG000139	UDP-glucose:(heptosyl) LPS alpha1,3-glucosyltransferase WaaG	Adherence,Endotoxin	100	100	99	1e-216

VFDB	VFG015521	Pyridoxamine 5'-phosphate oxidase PhzG (EC 1.4.3.5)		100	100	100	1e-124
VFDB	VFG000122	GDP-mannose 6-dehydrogenase (EC 1.1.1.132)	Antiphagocytosis,Serum resistance	100	100	100	1e-254
TCDB	Q7BFA7	Type III secretion inner membrane protein (YscS,homologous to flagellar export components)	3.A.6.1.1	86	86	81	2e-28
Victors	15597387	Adenylate cyclase ExoY (EC 4.6.1.1)		31	100	99	2e-67
Victors	116050154	Sigma-54 dependent DNA-binding transcriptional regulator		99	72	99	1e-270
Victors	116053639	Periplasmic thiol:disulfide interchange protein DsbA		100	100	100	1e-120
VFDB	VFG001265	Flagellar synthesis regulator FleN	Adherence,Motility	100	100	100	1e-155
Victors	116054141	type IV pili signal transduction protein PilI		100	100	100	1e-101
Victors	15598674	RhlB, TDP-rhamnosyltransferase 1 (EC 2.4.1.-)		100	100	100	1e-257
VFDB	VFG015506	Phenazine biosynthesis protein PhzB		100	100	99	2e-97
VFDB	VFG000192	Type III secretion cytoplasmic ATP synthase (EC 3.6.3.14, YscN,SpaL,MxiB,HrcN,EscN)	Secretion system,Type III secretion system	100	100	99	1e-252
PATRIC_VF	S4595	RNA-binding protein Hfq	Regulation of gene expression	66	82	92	2e-28
VFDB	VFG041030	hypothetical protein		100	100	100	4e-87
VFDB	VFG044083	HTH-type transcriptional regulator PtxR		100	100	99	1e-176
VFDB	VFG001230	Probable type IV pilus assembly FimV-related transmembrane protein	Adherence,Twitching motility	100	100	98	0.0
VFDB	VFG002071	T6SS component Hcp	Secretion system,Type VI secretion system	100	100	100	3e-90
VFDB	VFG001217	Type IV pilus biogenesis protein PilF	Adherence,Twitching motility	100	100	99	1e-139

VFDB	VFG015973	Pyoverdine biosynthesis related protein PvdP		100	100	99	0.0
VFDB	VFG015551	Phenazine modifying protein PhzH / Asparagine synthetase [glutamine-hydrolyzing] (EC 6.3.5.4)		100	100	99	0.0
VFDB	VFG015521	Pyridoxamine 5'-phosphate oxidase PhzG (EC 1.4.3.5)		100	100	100	1e-124
VFDB	VFG014950	HtrA protease/chaperone protein		100	100	99	1e-268
VFDB	VFG015509	2-keto-3-deoxy-D-arabino-heptulosonate-7-phosphate synthase II PhzC (EC 2.5.1.54)		62	100	100	1e-146
VFDB	VFG015503	Phenazine biosynthesis protein PhzA		90	90	97	8e-85
VFDB	VFG000121	RNA polymerase sigma factor RpoE	Antiphagocytosis,Serum resistance	100	100	100	1e-106
VFDB	VFG000218	Type III secretion bridge between inner and outermembrane lipoprotein (YscJ,HrcJ,EscJ, PscJ)	Secretion system,Type III secretion system	97	99	100	1e-131
VFDB	VFG000217	Type III secretion cytoplasmic protein (YscI)	Secretion system,Type III secretion system	100	100	98	2e-55
Victors	15595288	T6SS AAA+ chaperone ClpV (TssH)		100	100	99	0.0
VFDB	VFG002070	T6SS component TssC (ImpC/VipB)	Secretion system,Type VI secretion system	100	100	99	1e-296
VFDB	VFG001248	Flagellar regulatory protein FleQ	Adherence,Motility	100	100	100	1e-283
VFDB	VFG002072	T6SS associated component TagJ (ImpE)	Secretion system,Type VI secretion system	92	100	99	1e-146
VFDB	VFG014486	Flagellar basal body-associated protein FliL		100	100	100	7e-91
Victors	15600454	Alginate biosynthesis two-component system response regulator AlgR		100	100	100	1e-137
VFDB	VFG001262	Flagellar biosynthesis protein FlhB	Adherence,Motility	100	100	100	1e-212
Victors	116050024	hypothetical protein		100	100	99	0.0

VFDB	VFG002064	T6SS outer membrane component TssL (ImpK/VasF) / OmpA/MotB domain	Secretion system,Type VI secretion system	100	100	99	1e-262
VFDB	VFG001211	Type IV fimbrial biogenesis protein PilY2	Adherence,Twitching motility	100	100	95	2e-58
Victors	15676067	Translation elongation factor Tu		27	100	87	3e-51
VFDB	VFG001263	Flagellar biosynthesis protein FlhA	Adherence,Motility	100	100	99	0.0
VFDB	VFG000136	Sigma factor RpoE regulatory protein RseC	Antiphagocytosis,Serum resistance	100	100	100	5e-79
VFDB	VFG000181	General secretion pathway protein F	Secretion system,Type II secretion system	100	100	100	1e-222
Victors	15600305	Phospholipase/lecithinase/hemolysin		100	100	100	0.0
VFDB	VFG001242	Flagellar P-ring protein FlgI	Adherence,Motility	100	100	100	1e-206
VFDB	VFG000178	General secretion pathway protein I	Secretion system,Type II secretion system	100	100	99	5e-66
VFDB	VFG001257	Flagellar motor switch protein FliN	Adherence,Motility	100	100	100	1e-82
VFDB	VFG000187	Type III secretion inner membrane protein (YscS,homologous to flagellar export components)	Secretion system,Type III secretion system	100	100	98	1e-40
VFDB	VFG001219	Type IV pilus biogenesis protein PilP	Adherence,Twitching motility	100	100	99	2e-94
VFDB	VFG044079	PvcA protein, related to known isonitrile synthases		100	100	99	1e-188
VFDB	VFG015983	Putative dipeptidase, pyoverdin biosynthesis PvdM		100	100	100	1e-266
VFDB	VFG001227	type IV pili signal transduction protein PilI	Adherence,Twitching motility	100	100	100	1e-101
VFDB	VFG000215	Type III secretion spans bacterial envelope protein (YscG)	Secretion system,Type III secretion system	100	100	99	1e-61
VFDB	VFG001232	Chemotaxis response regulator protein-glutamate methylesterase CheB (EC 3.1.1.61)	Adherence,Twitching motility	100	100	99	1e-202

Victors	15598930	Threonine synthase (EC 4.2.3.1)		100	100	99	1e-275
VFDB	VFG000140	Lipopolysaccharide core heptose(I) kinase RfaP	Adherence,Endotoxin	100	100	99	1e-155
VFDB	VFG001214	Type IV fimbriae expression regulatory protein PilR	Adherence,Twitching motility	100	100	100	1e-254
VFDB	VFG000179	General secretion pathway protein H	Secretion system,Type II secretion system	100	100	99	3e-90
Victors	116051700	Chemotaxis response regulator protein-glutamate methylesterase CheB (EC 3.1.1.61)		100	100	100	1e-189
Victors	15595239	Putative large exoprotein involved in heme utilization or adhesion of ShlA/HecA/FhaA family		9	99	99	1e-190
VFDB	VFG044082	hypothetical protein		100	100	99	1e-122
Victors	15597123	5-methyltetrahydropteroyltriglutamate--homocysteine methyltransferase (EC 2.1.1.14)		100	100	99	0.0
VFDB	VFG001256	Flagellar motor switch protein FliM	Adherence,Motility	100	100	100	1e-183
Victors	116053999	Transcriptional regulator		100	100	99	1e-177
VFDB	VFG000205	Unknown, probably involved in type III secretion	Secretion system,Type III secretion system	100	100	100	4e-77
VFDB	VFG000142	Lipopolysaccharide core heptosyltransferase I	Adherence,Endotoxin	100	100	99	1e-212
Victors	116050342	Pyoverdine sidechain non-ribosomal peptide synthetase PvdI @ Siderophore biosynthesis non-ribosomal peptide synthetase modules		37	99	99	0.0
VFDB	VFG000219	Type III secretion cytoplasmic protein (YscK)	Secretion system,Type III secretion system	80	81	99	5e-96

VFDB	VFG000191	Type III secretion spans bacterial envelope protein (YscO)	Secretion system,Type III secretion system	100	100	99	1e-84
Victors	15600048	Phosphoribosylamine--glycine ligase (EC 6.3.4.13)		100	100	99	1e-246
VFDB	VFG001228	twitching motility protein PilJ	Adherence,Twitching motility	100	100	99	0.0
VFDB	VFG014655	Negative regulator of flagellin synthesis FlgM (anti-sigma28)		100	100	100	2e-53
VFDB	VFG016041	Pyoverdine sidechain non-ribosomal peptide synthetase PvdI @ Siderophore biosynthesis non-ribosomal peptide synthetase modules		47	94	99	0.0
Victors	15597060	Molybdenum ABC transporter, substrate-binding protein ModA		100	100	98	1e-137
VFDB	VFG000120	Alginate biosynthesis two-component system sensor histidine kinase AlgZ/FimS	Antiphagocytosis,Serum resistance	100	100	100	1e-204
VFDB	VFG002065	T6SS component TssK (ImpJ/VasE)	Secretion system,Type VI secretion system	100	100	100	1e-258
Victors	15600634	hypothetical protein		100	100	99	0.0
VFDB	VFG001268	Pyochelin biosynthetic protein PchG, oxidoreductase (NAD-binding) @ Thiazolinyl imide reductase in siderophore biosynthesis gene cluster	Iron uptake,Siderophore	100	100	99	1e-198
Victors	15598168	Maf-like protein YceF		100	100	97	1e-101
VFDB	VFG001260	Flagellar biosynthesis protein FliQ	Adherence,Motility	100	100	100	4e-42
Victors	15595239	Putative large exoprotein involved in heme utilization or adhesion of ShlA/HecA/FhaA family		11	100	97	1e-215
VFDB	VFG000132	Alginate O-acetyltransferase AlgF, periplasmic	Antiphagocytosis,Serum resistance	100	100	100	1e-122
VFDB	VFG001236	Flagellar basal-body rod protein FlgC	Adherence,Motility	100	100	100	2e-76
VFDB	VFG001264	Flagellar biosynthesis protein FlhF	Adherence,Motility	100	100	99	1e-239

Victors	15597835	NADH-ubiquinone oxidoreductase chain C (EC 1.6.5.3) / NADH-ubiquinone oxidoreductase chain D (EC 1.6.5.3)		100	100	100	0.0
VFDB	VFG001213	Two-component sensor PilS	Adherence,Twitching motility	100	100	99	1e-303
VFDB	VFG000113	Type IV fimbrial assembly protein PilC	Adherence,Twitching motility	100	92	99	1e-208
VFDB	VFG001254	Flagellum-specific ATP synthase FliI	Adherence,Motility	100	100	100	1e-257
VFDB	VFG000154	N-(3-oxododecanoyl)-L-homoserine lactone synthase @ N-acyl-L-homoserine lactone synthase, LuxI family (EC 2.3.1.184)	Regulation,Quorum sensing system	100	100	100	1e-112
Victors	116049394	Flagellar biosynthesis protein FlhB		100	100	100	1e-212
VFDB	VFG001215	Type IV fimbrial biogenesis protein FimT	Adherence,Twitching motility	100	100	95	3e-90
Victors	116051830	Type IV pilus biogenesis protein PilF		100	100	100	1e-140
VFDB	VFG015950	Acyl-homoserine lactone acylase PvdQ (EC 3.5.1.-), quorum-quenching		100	100	99	0.0
Victors	15595239	Putative large exoprotein involved in heme utilization or adhesion of ShlA/HecA/FhaA family		5	99	99	1e-108
Victors	116054461	Adenylate cyclase ExoY (EC 4.6.1.1)		58	97	99	1e-135
VFDB	VFG000196	Type III secretion protein SctX	Secretion system,Type III secretion system	100	100	99	3e-64
Victors	116048931	Multiple virulence factor regulator MvfR/PqsR		100	100	99	1e-188
VFDB	VFG015503	Phenazine biosynthesis protein PhzA		100	100	100	2e-96
VFDB	VFG001222	Type IV pilus biogenesis protein PilM	Adherence,Twitching motility	100	100	100	1e-194

VFDB	VFG000166	Dihydroaeruginoate synthetase PchE, non-ribosomal peptide synthetase modules @ Siderophore biosynthesis non-ribosomal peptide synthetase modules	Iron uptake,Siderophore	100	100	98	0.0
VFDB	VFG000176	General secretion pathway protein K	Secretion system,Type II secretion system	100	100	96	1e-182
Victors	15598194	Na(+)-translocating NADH-quinone reductase subunit B (EC 1.6.5.8)		100	100	100	1e-240
VFDB	VFG015518	Trans-2,3-dihydro-3-hydroxyanthranilate isomerase (EC 5.3.3.17)		100	100	98	1e-158
VFDB	VFG002067	T6SS forkhead associated domain protein ImpI/VasC	Secretion system,Type VI secretion system	100	100	99	1e-296
VFDB	VFG000210	Type III secretion chaperone protein for YopN (SycN,YscB)	Secretion system,Type III secretion system	100	100	99	2e-74
VFDB	VFG016069	Thioesterase PvdG involved in non-ribosomal peptide biosynthesis		100	100	98	1e-143
VFDB	VFG000170	Isochorismate pyruvate-lyase (EC 4.2.99.21) [pyochelin] siderophore @ Isochorismate pyruvate-lyase (EC 4.2.99.21) of siderophore biosynthesis	Iron uptake,Siderophore	100	100	100	1e-52
Victors	116052217	Lysyl endopeptidase (EC 3.4.21.50)		100	100	100	1e-273
VFDB	VFG015515	2-Amino-2-deoxy-isochorismate synthase (EC 2.6.1.86) PhzE		100	100	97	0.0
Victors	116050967	3-oxoacyl-[acyl-carrier-protein] synthase, KASII (EC 2.3.1.179)		100	100	100	1e-240
Victors	15598958	Phosphoribosylformylglycinamidine synthase, synthetase subunit (EC 6.3.5.3) / Phosphoribosylformylglycinamidine synthase, glutamine amidotransferase subunit (EC 6.3.5.3)		100	100	99	0.0
VFDB	VFG001240	Flagellar basal-body rod protein FlgG	Adherence,Motility	100	100	100	1e-146

VFDB	VFG000143	ADP-heptose--lipooligosaccharide heptosyltransferase II	Adherence,Endotoxin	100	100	100	1e-205
VFDB	VFG001229	Chemotaxis protein methyltransferase CheR (EC 2.1.1.80)	Adherence,Twitching motility	100	100	99	1e-170
VFDB	VFG001261	Flagellar biosynthesis protein FliR	Adherence,Motility	99	99	99	1e-138
VFDB	VFG000214	Type III secretion cytoplasmic protein (YscF)	Secretion system,Type III secretion system	100	100	100	1e-41
VFDB	VFG001216	type 4 fimbrial biogenesis protein FimU	Adherence,Twitching motility	100	100	98	1e-87
Victors	15595239	Putative large exoprotein involved in heme utilization or adhesion of ShlA/HecA/FhaA family		6	100	98	1e-117
TCDB	P40290	Type III secretion cytoplasmic ATP synthase (EC 3.6.3.14, YscN,SpaL,MxiB,HrcN,EscN)	3.A.6.1.1	94	94	85	1e-202
Victors	15599413	FAD-dependent monooxygenase PhzS		100	100	99	1e-232
VFDB	VFG001218	Type IV pilus biogenesis protein PilQ	Adherence,Twitching motility	100	100	100	0.0
VFDB	VFG000195	Type III secretion chaperone SycN	Secretion system,Type III secretion system	100	100	99	2e-65
VFDB	VFG000189	Type III secretion inner membrane protein (YscQ,homologous to flagellar export components)	Secretion system,Type III secretion system	100	100	99	1e-176
VFDB	VFG014148	Flagellar basal-body rod protein FlgB		100	100	99	4e-70
VFDB	VFG000171	Isochorismate synthase (EC 5.4.4.2) [pyochelin] siderophore @ Isochorismate synthase (EC 5.4.4.2) of siderophore biosynthesis	Iron uptake,Siderophore	93	99	100	1e-265
Victors	15599310	Pyrimidine/purine nucleotide 5'-monophosphate nucleosidase PpnN (EC 3.2.2.4) (EC 3.2.2.10)		100	100	100	1e-271
VFDB	VFG000150	Adenylate cyclase ExoY (EC 4.6.1.1)	Toxin,Type III translocated protein,Intracellular toxin,Adenylate	31	100	99	2e-67

			cyclase				
VFDB	VFG014707	Flagellar motor rotation protein MotA		100	100	100	1e-134
Victors	15595239	Putative large exoprotein involved in heme utilization or adhesion of ShlA/HecA/FhaA family		6	100	99	1e-128
Victors	15599021	FIG018175: Predicted transmembrane protein		100	100	98	7e-93
VFDB	VFG000112	Type IV fimbrial assembly, ATPase PilB	Adherence,Twitching motility	100	100	99	0.0
Victors	15595960	Sigma factor RpoE negative regulatory protein RseA		100	100	100	1e-105
VFDB	VFG015000	Intramembrane protease RasP/YluC, implicated in cell division based on FtsL cleavage		100	100	99	1e-258
VFDB	VFG000161	Pyoverdine sidechain non-ribosomal peptide synthetase PvdD @ Siderophore biosynthesis non-ribosomal peptide synthetase modules	Iron uptake,Siderophore,Pigment	8	100	100	1e-115
Victors	15596131	Inactive (p)ppGpp 3'-pyrophosphohydrolase domain / GTP pyrophosphokinase (EC 2.7.6.5), (p)ppGpp synthetase I		100	100	100	0.0
VFDB	VFG014893	Phosphoglucomutase (EC 5.4.2.2) @ Phosphomannomutase (EC 5.4.2.8)		100	53	99	1e-272
VFDB	VFG000127	Poly (beta-D-mannuronate) C5 epimerase AlgG (EC 5.1.3.-)	Antiphagocytosis,Serum resistance	100	100	99	0.0
Victors	15595349	Ferrichrome-iron receptor @ Iron siderophore receptor protein		100	100	99	0.0
Victors	15597219	UTP--glucose-1-phosphate uridylyltransferase (EC 2.7.7.9)		100	100	100	1e-161
VFDB	VFG015509	2-keto-3-deoxy-D-arabino-heptulosonate-7-phosphate synthase II PhzC (EC 2.5.1.54)		100	100	98	1e-233
Victors	15595280	T6SS component TssA (ImpA)		100	100	98	1e-19

							0
VFDB	VFG001221	Type IV pilus biogenesis protein PilN	Adherence,Twitching motility	100	100	100	1e-106
Victors	15599685	UPF0192 protein YfaS		100	99	99	0.0
VFDB	VFG001252	Flagellar motor switch protein FliG	Adherence,Motility	100	100	100	1e-185
VFDB	VFG041047	Bacterial lysozyme Tse3, effector of type VI secretion system		100	100	100	1e-236
Victors	15596345	hypothetical protein		100	100	99	0.0
VFDB	VFG002068	T6SS component TssA (ImpA)	Secretion system,Type VI secretion system	100	100	98	1e-190
Victors	15595356	Multidrug efflux system, inner membrane proton/drug antiporter (RND type) => TriC of TriABC-OpmH system		100	100	99	0.0
VFDB	VFG000141	3-deoxy-D-manno-octulosonic acid transferase (EC 2.4.99.12)(EC 2.4.99.13)	Adherence,Endotoxin	100	100	99	1e-247
VFDB	VFG002061	T6SS protein serine/threonine phosphatase PppA	Secretion system,Type VI secretion system	100	100	99	1e-133
VFDB	VFG000186	Type III secretion inner membrane protein (YscT,HrcT,SpaR,EscT,EpaR1, homologous to flagellar export components)	Secretion system,Type III secretion system	100	100	98	1e-141
Victors	15595271	ABC transporter, ATP-binding protein		100	100	98	1e-131
VFDB	VFG000202	Type III secretion chaperone protein for YopD (SycD)	Secretion system,Type III secretion system	98	98	98	3e-90
VFDB	VFG001255	Flagellar protein FliJ	Adherence,Motility	100	100	99	2e-78
VFDB	VFG000148	hypothetical protein	Toxin,Type III translocated protein,Intracellular toxin,ADP-ribosyltransferase and GTPase activating	100	100	99	1e-256
Victors	11605017	Tn4652, transposase		87	87	97	0.0

	7						
Victors	15599642	Outer membrane stress sensor protease DegS		100	100	99	1e-220
Victors	15600642	Mannosyltransferase		100	100	99	1e-274
VFDB	VFG014733	Putative outer membrane protein		100	100	99	1e-182
VFDB	VFG002057	hypothetical protein	Secretion system,Type VI secretion system	100	100	99	0.0
VFDB	VFG000161	Pyoverdine sidechain non-ribosomal peptide synthetase PvdD @ Siderophore biosynthesis non-ribosomal peptide synthetase modules	Iron uptake,Siderophore,Pigment	31	100	99	0.0
VFDB	VFG000128	Alginate O-acetyltransferase AlgX, periplasmic	Antiphagocytosis,Serum resistance	100	100	99	1e-280
Victors	15676067	Translation elongation factor Tu		24	95	83	5e-40
VFDB	VFG015518	Trans-2,3-dihydro-3-hydroxyanthranilate isomerase (EC 5.3.3.17)		11	100	100	5e-09
VFDB	VFG002069	T6SS component TssB (ImpB/VipA)	Secretion system,Type VI secretion system	100	100	100	1e-91
Victors	116049375	N-(3-oxododecanoyl)-L-homoserine lactone-binding transcriptional activator @ Acyl-homoserine lactone-binding transcriptional activator, LuxR family @ Transcriptional regulator LasR		98	99	100	1e-135
VFDB	VFG014369	Flagellar sensor histidine kinase FleS		100	100	100	1e-227
VFDB	VFG000188	Type III secretion inner membrane protein (YscR,SpaR,HrcR,EscR,homologous to flagellar export components)	Secretion system,Type III secretion system	100	99	100	1e-118
VFDB	VFG000131	Alginate O-acetyltransferase AlgJ, inner membrane	Antiphagocytosis,Serum resistance	100	100	99	1e-230

VFDB	VFG001234	Transcriptional regulator, AraC family	Adherence,Twitching motility	100	100	100	1e-148
VFDB	VFG044088	MbtH-like NRPS chaperone		100	100	100	4e-37
VFDB	VFG016005	PvdO, pyoverdine responsive serine/threonine kinase (predicted by OlgaV)		100	100	98	1e-172
VFDB	VFG001239	Flagellar basal-body rod protein FlgF	Adherence,Motility	100	100	100	1e-138
VFDB	VFG000134	Sigma factor RpoE negative regulatory protein RseA	Antiphagocytosis,Serum resistance	100	100	100	1e-105
Victors	15596354	Two-component transcriptional response regulator, OmpR family		100	100	100	1e-131
VFDB	VFG016016	Pyoverdine synthetase PvdF, N5-hydroxyornithine formyltransferase		100	100	99	1e-160
VFDB	VFG014668	Flagellar biosynthesis protein FlgN		100	100	99	6e-81
VFDB	VFG000204	Type III secretion host injection and negative regulator protein (YopD)	Secretion system,Type III secretion system	100	100	98	1e-156
VFDB	VFG000200	Type III secretion cytoplasmic plug protein (LcrG)	Secretion system,Type III secretion system	100	100	98	9e-48
VFDB	VFG000203	Type III secretion host injection protein (YopB)	Secretion system,Type III secretion system	100	100	98	1e-207
Victors	15600520	Oxidoreductase, FAD-binding		100	95	99	1e-262
Victors	15599404	Phenazine-specific methyltransferase PhzM		100	100	100	1e-190
VFDB	VFG016041	Pyoverdine sidechain non-ribosomal peptide synthetase PvdI @ Siderophore biosynthesis non-ribosomal peptide synthetase modules		14	99	99	0.0
VFDB	VFG002073	T6SS lysozyme-like component TssE	Secretion system,Type VI secretion system	100	100	99	3e-90
Victors	15598072	Orotidine 5'-phosphate decarboxylase (EC 4.1.1.23)		100	100	100	1e-12

							8
VFDB	VFG000168	2,3-dihydroxybenzoate-AMP ligase (EC 2.7.7.58) [pyochelin] siderophore @ 2,3-dihydroxybenzoate-AMP ligase (EC 2.7.7.58) of siderophore biosynthesis	Iron uptake,Siderophore	100	100	99	0.0
VFDB	VFG000125	Alginate export system AlgK/AlgE, periplasmic component AlgK	Antiphagocytosis,Serum resistance	100	100	99	1e-275
VFDB	VFG016041	Pyoverdine sidechain non-ribosomal peptide synthetase PvdI @ Siderophore biosynthesis non-ribosomal peptide synthetase modules		37	99	99	0.0
VFDB	VFG000164	Outer membrane receptor for ferric-pyochelin FptA @ Outer membrane receptor for ferric siderophore	Iron uptake,Siderophore	100	100	100	0.0
Victors	15599026	Cytosol aminopeptidase PepA (EC 3.4.11.1)		100	100	99	1e-283
Victors	15598369	Putative short-chain dehydrogenase		100	100	99	1e-137
VFDB	VFG000156	RhlA, 3-(3-hydroxyalkanoyloxy)alkanoic acids (HAAs) synthase	Biosurfactant	100	100	99	1e-168
Victors	15599724	Leader peptidase (Prepilin peptidase) (EC 3.4.23.43) / N-methyltransferase (EC 2.1.1.-)		100	100	98	1e-169
Victors	15600080	Uncharacterized MFS-type transporter		100	100	99	1e-258
VFDB	VFG015512	2-amino-2-deoxy-isochorismate hydrolase PhzD (EC 3.-.-.-)		100	100	99	1e-117
Victors	116050573	BarA-associated response regulator UvrY (= GacA = SirA)		100	100	100	1e-117
VFDB	VFG000175	General secretion pathway protein L	Secretion system,Type II secretion system	100	100	99	1e-223
VFDB	VFG044081	4-hydroxyphenylacetate 3-monooxygenase (EC 1.14.14.9)		100	100	99	1e-295
Victors	15599687	Uncharacterized protein YfaA		100	100	98	0.0
VFDB	VFG041010	Autotransporter adhesin		100	100	98	1e-16

							8
VFDB	VFG001209	Type IV fimbrial biogenesis protein PilX	Adherence,Twitching motility	100	100	98	1e-106
VFDB	VFG000216	Type III secretion effector protein (YopR, encoded by YscH)	Secretion system,Type III secretion system	100	100	99	2e-74
VFDB	VFG000163	Outer membrane ferripyoverdine receptor FpvA, TonB-dependent @ Ferric siderophore receptor, TonB dependent	Iron uptake,Siderophore,Pigment	98	100	99	0.0
Victors	116050342	Pyoverdine sidechain non-ribosomal peptide synthetase PvdI @ Siderophore biosynthesis non-ribosomal peptide synthetase modules		50	99	98	0.0
VFDB	VFG000117	Alginate regulatory protein AlgP, positive transcriptional regulator of AlgD	Antiphagocytosis,Serum resistance	100	100	96	1e-184
Victors	15595749	Phosphoglycerate kinase (EC 2.7.2.3)		100	100	100	1e-215
VFDB	VFG000212	Type III secretion inner membrane protein (YscD,homologous to flagellar export components)	Secretion system,Type III secretion system	100	100	98	1e-245
VFDB	VFG001224	Type IV pilus assembly ATPase component PilU	Adherence,Twitching motility	100	100	99	1e-218
VFDB	VFG000167	Transcriptional regulator PchR	Iron uptake,Siderophore	100	100	99	1e-171
VFDB	VFG001249	Flagellar two-component response regulator FleR	Adherence,Motility	100	100	99	1e-266
VFDB	VFG000119	Alginate biosynthesis two-component system response regulator AlgR	Antiphagocytosis,Serum resistance	100	100	100	1e-137
VFDB	VFG001220	Type IV pilus biogenesis protein PilO	Adherence,Twitching motility	100	100	100	1e-111
VFDB	VFG000157	Phospholipase C (EC 3.1.4.3) => hemolytic PlcH	Toxin,Membrane-damaging,Phospholipase	100	100	99	0.0
VFDB	VFG014720	Flagellar motor rotation protein MotB		100	100	100	1e-168

VFDB	VFG000162	Sigma factor PvdS, controling pyoverdin biosynthesis	Iron uptake,Siderophore,Pigment	100	100	100	1e-102
VFDB	VFG014642	Flagellar basal-body P-ring formation protein FlgA		100	100	99	1e-127
VFDB	VFG001266	ABC efflux pump, fused inner membrane and ATPase subunits in pyochelin gene cluster @ Putative ABC iron siderophore transporter, fused permease and ATPase domains	Iron uptake,Siderophore	100	100	99	0.0
VFDB	VFG000150	Adenylate cyclase ExoY (EC 4.6.1.1)	Toxin,Type III translocated protein,Intracellular toxin,Adenylate cyclase	64	97	98	1e-134
VFDB	VFG000199	Type III secretion low calcium response protein (LcrR)	Secretion system,Type III secretion system	100	100	100	5e-81
Victors	116049953	Short-chain fatty acids transporter		100	100	100	1e-274
VFDB	VFG000129	Alginate lyase AlgL (EC 4.2.2.3)	Antiphagocytosis,Serum resistance	100	100	100	1e-216
Victors	15599760	Conserved uncharacterized protein CreA		100	100	100	4e-83
VFDB	VFG001259	Flagellar biosynthesis protein FliP	Adherence,Motility	100	100	100	1e-136

Table A.7 Summary of PRISM data. Whole genome sequencing data was obtained for the different bacterial strains used in the study. These genomes were assembled

with a5_MiSeq and annotated with prokka. PRISM was then used to identify secondary metabolite pathways.

Bacterium	Cluster identified	Open reading frame
Neisseria sicca	No clusters identified	
Enterococcus faecium	Polyketide	orf_32
Streptococcus mitis	Polyketide	orf_86
Bacteroides vulgatus	No clusters identified	
Pseudomonas aeruginosa	Non-ribosomal peptide	orf_38, orf_40, orf_41
	Polyketide	orf_244
	Non-ribosomal peptide	orf_47
	Non-ribosomal peptide	orf_98
	Non-ribosomal peptide	orf_89
	Non-ribosomal peptide	orf_10, orf_13
	Non-ribosomal peptide	orf_1, orf_2
	Non-ribosomal peptide	orf_1
	Unknown thiotemplated cluster type	

Neisseria sicca

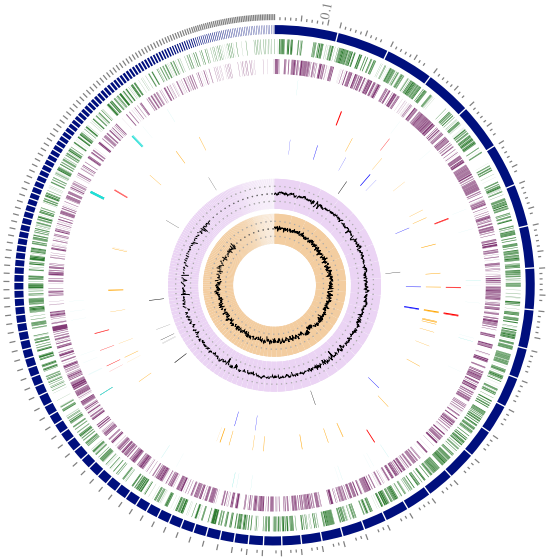

Enterococcus faecium

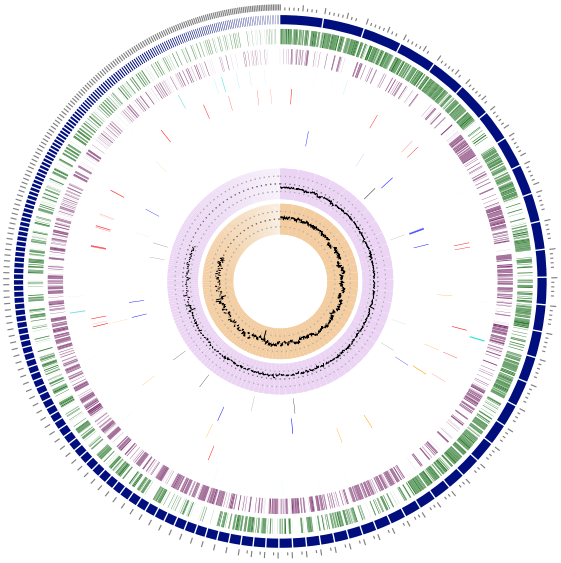

Streptococcus mitis

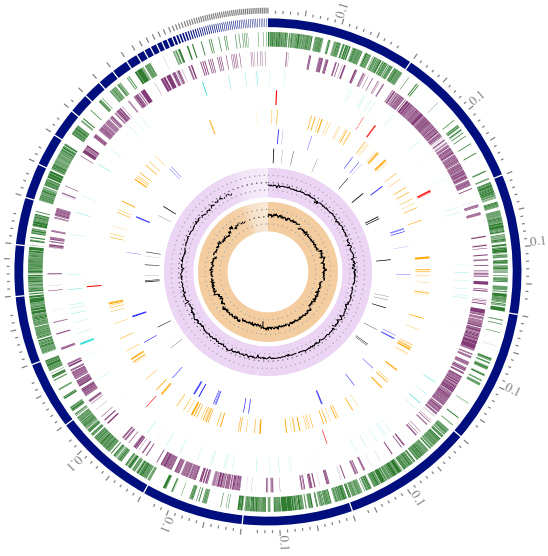

Bacteroides vulgatus

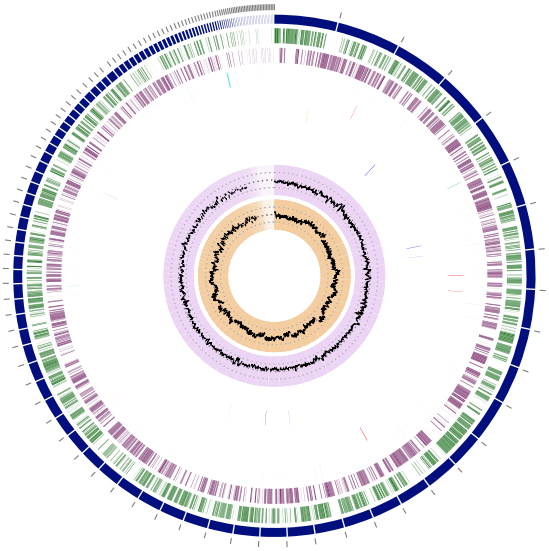

Pseudomonas aeruginosa

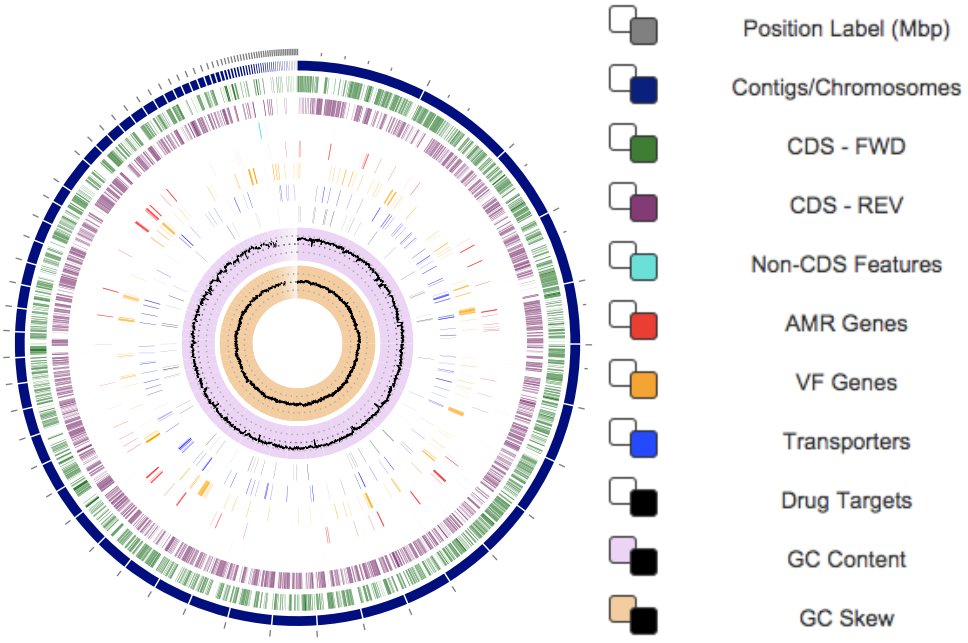

Figure A.1 Circular representation of the bacterial genomes. Whole genome sequencing data was obtained for the different bacterial strains used in the study. These genomes were assembled with a5_MiSeq and annotated using RAST on PATRIC. The "Circular Viewer" tool on PATRIC was then used to generate a visual representation of the draft genomes produced from Illumina sequencing. CDS = coding region, FWD = forward, REV = reverse, AMR = antimicrobial resistance, VF = virulence factors.